Spectrophotometric determination of pH and its influence in soils

Sima Bargrizan

Thesis submitted to The University of Adelaide in fulfilment of the requirements for the degree of Doctor of Philosophy

Faculty of Sciences

School of Agriculture, Food and Wine

The University of Adelaide

February, 2019

Dedicated to my family

Table of Contents

CHAPTER 3

CHAPTER 4

CHAPTER 5

CHAPTER 6

ABSTRACT

It would be beneficial to develop an alternative pH measurement technique for soils, since the standard glass electrode method suffers deficiencies with unpredictability in liquid junction potential, high drift and the necessity for electrode calibration with variable ionic strength solutions if high accuracy is required. Other problems with the electrode method for use in soils include clogging of the porous fiber of electrodes, and the "suspension effect", which can result in a negative bias when there is substantial H^+ present on exchange sites.

Spectrophotometric methods using indicators offer an alternative to eliminate several inherent issues with potentiometric pH measurement. This approach has been widely used in for pH determination of marine waters due to the high reproducibility achievable (≥ 0.001 pH units) but has not previously been developed for soils.

The aims of this thesis were i) to develop a spectrophotometric method for measuring soil pH in the circumneutral (5-8) and acidic (< 5) pH range; ii) to develop a mixed dye spectrophotometric method that can be used for any the soil in the pH range 3-9; and iii) to use these techniques for evaluating the consistency of the thermodynamics of the soil carbonate system.

In the first experiment, spectrophotometric determination of the concentrations of the acid and base forms of phenol red and bromocresol purple were used for soil pH measurement in the pH range of 5.0-8.5. This spectrophotometric method showed a strong relationship ($r^2 > 0.95$) with values determined using a glass electrode in both water and $CaCl_2$ soil extracts. Similar precision of ±0.02-0.08 pH unit was obtained

for measurement on replicate soil extracts for both spectrophotometric and glass electrode methods. The application of the spectrophotometric method was then extended to use with acidic soils by employing an indicator, bromocresol green, with a lower pK_a; again, a strong correlation ($r^2 > 0.99$) was achieved between spectrophotometric and glass electrode pH measurements.

In the next experiment, a mixed dye (bromophenol blue, bromocresol purple, m-cresol purple, and thymol blue) method was developed that has a much wider working pH range of 3-9; in comparison the working pH range of single dye methods is approx. ±1 pH unit from their pK_a. In the mixed-dye method, pH was calculated based on ratio of absorbance at selected two wavelengths and individual dye properties using fundamental equations derived from Beer's law. The accuracy of the method was found to be within ±0.00-0.06 pH units against certified pH buffers.

In the last experiment, measurements and modelling was conducted to evaluate the consistency of the thermodynamics of the soil carbonate system. pH was calculated from a known concentration of pCO_2 applied for soil solution equilibration and alkalinity titration and then comparing the results with pH measured using spectrophotometer and glass electrode. The internal consistency of the soil carbonate system was shown with a precision of ±0.03 pH units. Difference of calculated pH from measured pH was within 0.00-0.1 pH units in soil solutions with alkalinity > 0.5 meq L^{-1}.

In conclusion, the application of novel spectrophotometric pH measurement methods for soils has been developed. The indicators which have been calibrated allow wider soil pH measurement between 3-9 which is also useful for other application such as oceanic pH. This study will provide a better understanding of the role of pH in

illuminating acid-base reactions in soils, especially including the geochemically significant carbon dioxide system.

DECLARATION

I certify that this work contains no material which has been accepted for the award of any other degree or diploma in my name, in any university or other tertiary institution and, to the best of my knowledge and belief, contains no material previously published or written by another person, except where due reference has been made in the text. In addition, I certify that no part of this work will, in the future, be used in a submission in my name, for any other degree or diploma in any university or other tertiary institution without the prior approval of the University of Adelaide and where applicable, any partner institution responsible for the joint-award of this degree.

I acknowledge that copyright of published works contained within this thesis resides with the copyright holders of those works.

I also give permission for the digital version of my thesis to be made available on the web, via the University's digital research repository, the Library Search and also through web search engines, unless permission has been granted by the University to restrict access for a period of time.

I acknowledge the support I have received for my research through the provision of an Australian Government Research Training Program Scholarship.

Author:

Sima Bargrizan

28/02/2019

ACKNOWLEDGEMENTS

First and foremost, I would like to express my sincere gratitude and appreciation to my principal supervisor Associate Prof. Luke Mosley for the long-term and kind support he has provided throughout the rough road to finish this thesis. His precious supervision, guidance and profound insights enabled me to grow as a research scientist in an outstanding environment. I am particularly indebted to Luke for his exceptional character and great patience at different stages of my research work. Once more, a big thank you to Dr Luke Mosley, as conducting this PhD would have not been possible without his support.

I would particularly like to acknowledge my co-supervisor Associate Prof. Ron Smernik for not only his sound pieces of advice, insightful comments and support but also for the key questions he would put to me in numerous supervisory meetings to view things from different perspectives. I would also like to thank him for allowing me the opportunity to participate in his writing group lectures throughout my studies which were indeed informative and fruitful.

Besides my supervisors, my sincere thanks go to my advisor Prof. Rob Fitzpatrick for his instructive advice and supervision for selecting soil material during field work for several parts of my research.

I am grateful to the prestigious University of Adelaide, for awarding me PhD scholarship and the Australian Commonwealth Government for their financial support during my studies.

I would like to acknowledge Mr Colin Rivers for his help whenever needed and Dr. Cameron Grant who provided assistance with soil texture measurements and also for his kind support at hardships. I am grateful to my friends and colleagues in the Soil Chemistry and Biology research groups, Ashlea, Xuan, Tan and Flynn, particularly Bogumila Tomczak and John Gouzos at CSIRO for ions measurements using ICP-OES. I also acknowledge Zhoubin Maneshi of Heidelberg University, Germany for his assistance with the justifications of the theoretical equations for a mixed dye solution.

I wish to thank my previous supervisor Associate Prof. Mohammad Matinizadeh in Tehran, Iran for encouraging me to embark on the soil path, and for providing me with an excellent lab training during my Master's and most importantly for becoming a lifelong friend.

Hooman Maneshi, undoubtedly without your love, support and encouragement I could not have come this far on the research path. I will always remember how excited you would get to help me with my chemistry questions. I will always appreciate this statement from you upon applying for my PhD which was "always dream big, aim high and do your best to achieve so".

Last but not the least, I was not able to accomplish my life dreams without all of the sacrifices and the love from my perfect family: both my parents and my sister back home. Their support has been unconditional during all years of my life.

LIST OF PUBLICATIONS

1. Bargrizan S, Smernik RJ, Mosley LM (2017) Development of a Spectrophotometric Method for Determining pH of Soil Extracts and Comparison with Glass Electrode Measurements. Soil Science Society of America Journal 81, 1350-1358.
2. Bargrizan S, Smernik RJ, Fitzpatrick RW, Mosley LM (2018) The application of a spectrophotometric method to determine pH in acidic (pH < 5) soils. Talanta 186, 421-426.
3. Bargrizan S, Smernik RJ, Mosley LM (2018) Spectrophotometric measurement of the pH of soil extracts using a multiple indicator dye mixture. European Journal of Soil Science https://doi.org/10.1111/ejss.12745.

CHAPTER 1

INTRODUCTION AND REVIEW OF LITERATURE

1.1 Introduction

Measurement of pH is conducted routinely in various scientific areas due to its significance in biological and chemical reactions. In soil studies, pH is utilized to understand and predict metal speciation (Sauve et al. 2000; Wiesner et al. 2006), inorganic carbon speciation (Bond-Lamberty and Thomson 2010) and nutrient availability and microbial activity (Miller and Kissel 2010). Accurate and precise measurement of pH is vital in all of these applications.

Soil pH is also widely used in soil classification (Isbell and National Committee on Soils and Terrain 2016; Soil Survey Staff 2017) and assessment of environmental hazard related to acidification (Brennan et al. 2004) especially for acid sulfate soil materials which are categorized as sulfuric, hypersulfidic, hyposulfidic or monosulfidic depending of their current and potential pH (Fitzpatrick et al. 2010; Creeper et al. 2012).

The established method for determining soil pH involves the use of a potentiometric glass electrode (Skoog et al. 2007). However, even when used carefully, errors of 0.1 pH units or greater may occur due to inherent issues such as residual liquid junction potential (Millero 1986), high electrode drift (Yuan and DeGrandpre 2008), and clogging of electrode porous fibres (Skoog et al. 2007).

Spectrophotometric pH determination using indicators offers an alternative to potentiometric pH measurement that obviates many of the above-mentioned problems with glass electrodes. Spectrophotometric pH determination has been extensively applied in the marine chemistry field because of the high accuracy (> 0.01 pH units) obtained by instant indicator equilibrium (Yao and Byrne 2001). In addition, this method does not require the use of calibrating buffers so long as dye characteristics have been determined (Clayton and Byrne 1993).

There is therefore potential to develop spectrophotometric pH determination as a more accurate pH measurement technique for soils that can circumvent many of the potential inaccuracies associated with the conventional glass electrode method. This chapter reviews potential problems related to pH determination using the glass electrode method and the potential advantages of the spectrophotometric method, along with the theory behind it.

1.2 Soil pH

Soil pH is the negative logarithm of the activity of protons (H^+) in the soil solution (Essington 2005), and is an indicator of the relative degree of acidity or alkalinity (Strawn et al. 2015). Accurate soil pH measurement is necessary in assessing acid-base equilibria (Stumm and Morgan 1996), including equilibria involving soil carbon dioxide and carbonate (Suarez 1977), the weathering of soil minerals and the cascade of reaction that occur as a result of human-induced soil acidification (Andrews and Schlesinger 2001; King et al. 2001; Berner 1997; Bormann et al. 1998).

The speciation and consequent plant availability of numerous soil trace metals are also pH sensitive (Lindsay 1979; Sauve et al. 1997; Strawn et al. 2015). Sauvé et al. (2000) showed that there is a significant difference in Zn partition coefficients (the ratio of

sorbed metal concentration to the dissolved metal concentration (K_d)) through narrow pH ranges (K_d = 562 at pH 6, 488 at pH 5.9 and 648 at pH 6.1). Therefore, it is vital to develop an accurate pH measurement technique for soils as even a +/- 0.1 pH unit errors can induce significant changes in the bio- chemical processes in soil, especially near toxicity thresholds (Lindsay 1979; Kiseel et al. 2009). As an example, figure 1 shows the activity of Al^{3+} in equilibrium with amorphous Al^{3+} hydroxide (Lindsay, 1979), dropping approximately 60% for each 0.1 unit rise in pH.

The other main use of soil pH determination is in informing farm management practices, especially liming, but also fertilizer application (Kissel et al. 2009), since soil pH influences microorganism activity (Miller and Kissel 2010) which governs the soil organic matter decomposition resulting in release of plant-available nutrients (Jones and Benton 2012). Soil pH is also used extensively in soil classification (Isbell and National Committee on Soils and Terrain 2016 and Soil Survey Staff 2017) which provides comprehensive information on soil physicochemical properties, including degree of weathering, soil moisture and metal oxide content (Hewitt 1992).

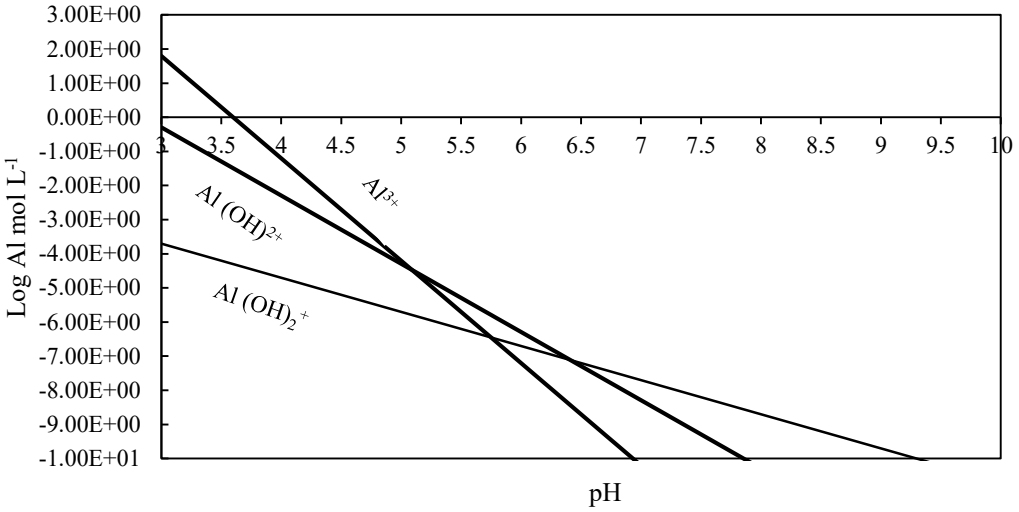

Figure 1: Theoretical lines for hydrolysis species of Al^{3+} in equilibrium with amorphous Al^{3+} hydroxide against pH (3-10, at 0.1 pH units intervals).

1.3 Soil pH measurement methods

1.3.1 Glass electrode method

Soil solution pH (prepared at a particular soil/solution (often water or dilute $CaCl_2$) ratio (e.g.,1:1, 1:2 or 1:5 w/v)) measurements are traditionally made electrometrically using a glass electrode, consisting of a glass membrane electrode paired with a reference electrode (McLean 1982; Essington 2015; Rayment and Lyons 2011).

The glass electrode is surrounded by a buffer solution of known pH that is encompassed in a glass membrane which is proton sensitive. The reference electrode consists of an Ag(s)/AgCl(aq) couple in a saturated reference electrolyte (KCl) solution. The corresponding reaction is expressed by:

Ag(s) / AgCl(aq) / Cl^- (aq) $\qquad\qquad$ $AgCl(s) + e^- \rightleftharpoons Ag(s) + Cl^-$

These two electrodes are connected to each other through a salt bridge which balances the internal positive and negative charges of ions produced or consumed as well as producing an electrical connection via diffusion of KCl into the soil solution (Essington 2015) (Figure 2).

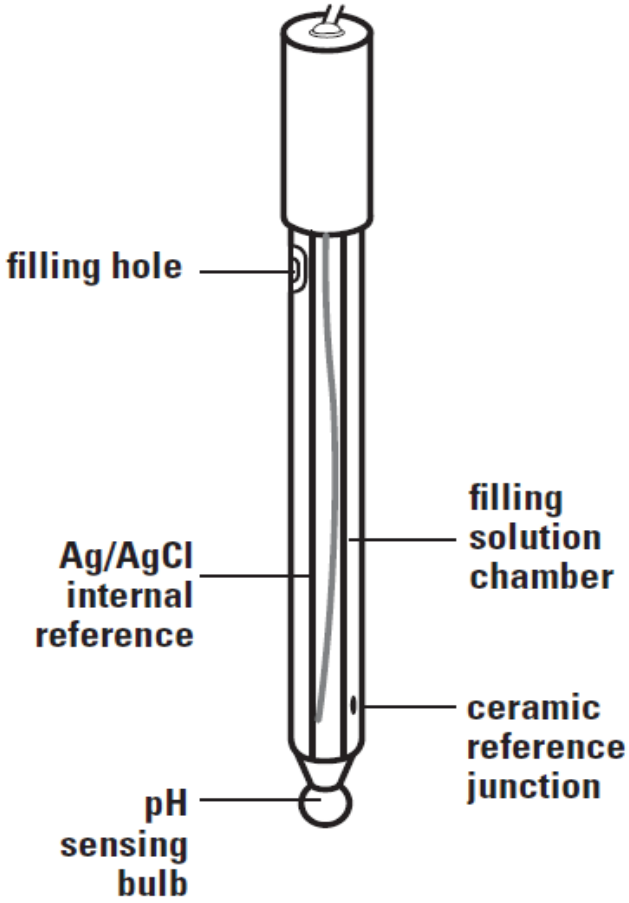

Figure 2: A typical pH electrode is a combination of glass membrane electrode and reference electrode.

There are potential problems in gaining an accurate measurement of pH in soils using the glass electrode. First, an inherent and unmeasurable liquid junction potential exists between the two internal solutions in the two neighbouring electrodes (Manov et al.

1944; Skoog et al. 2007); this can cause errors of the order of 0.1 pH units (Millero 1986).

Also, another potential issue with the glass electrode is the effect of soil cation exchange capacity on the electrode performance; this is referred to as the suspension effect (Essington 2015). This causes a potential difference between the soil sample solution and the KCl solution in the reference electrode (Coleman et al. 1951; Peech et al. 1953; Deshpande and Marshall 1961) leading to inaccurate pH measurements. According to Essington (2015) and Wiesner et al. (2006), such errors can be eliminated through electrode calibration using buffers with the same electrolyte composition as the samples. This in fact is quite difficult and time consuming to perform in practice due to the range of ionic strengths found in different soils.

A third potential problem is alteration in electrode response over time (Whitfield et al. 1985). This is especially true for samples with low ionic strength (Millero 1986). Using a dilute salt solution such as $CaCl_2$ rather than water as an extractant has been widely adopted by soil scientists to avoid this problem; this also improves stabilization of electrodes during calibration (Rayment and Lyons 2011). However, this practice has been found to lead to lower pH readings (Miller and Kissel 2010) due to the replacing of protons by Ca^{2+} on soil cation exchange sites (Conyers and Davey 1988). Hence, the measurement of true pH in the soil solution is not obtained via this method.

Finally, there is the potential for clogging of the porous fibres of pH electrodes over time, which limits the flow of liquid from the salt bridge into the solution resulting in slow equilibration and ultimately an inaccurate pH measurement (Skoog et al. 2007).

pH can be explained through the NBS, free hydrogen ion concentration (pH_{free}) and total hydrogen concentration (pH_T) scales. The NBS pH scale is described by electrode

measurements of NBS certified buffers. However, liquid junction potential restricts the effectiveness of this scale. The free hydrogen ion concentration scale (applied for freshwater, Yao and Byrne 2001) is regarded as the free hydrogen ion concentration which is defined by spectrophotometric pH measurements. The total hydrogen concentration which has been used for seawater include free hydrogen ion concentration and the total sulfate concentration. (Dickson and Goyet 1994; Seidel 2001).

1.3.2 Colorimetric methods

Methods that use indicator chemicals whose colour varies with pH have been used for determining the soil pH in a number of different ways (Snyder 1935; Raupach and Tucker 1959; Mclean 1982;). Snyder (1935) used addition of individual indicator (pH range of 3-9) to determine the pH of centrifuged soil solution through the comparison of solution colour change with colour standards. In the approach of Raupach and Tucker (1959), soil was compounded with a mixed dye and dusted with barium sulfate powder to provide a white background to better observe the indicator colour. The pH determined this way agreed well with the glass electrode method. However, the colour chart used is less accurate (within ±0.5 pH units) and the method slower than use of a glass electrode. Colorimetric methods have also been used as embedded dyes in the form of pH test paper in fields for rough pH determination (Mclean 1982).

1.4 The introduction of spectrophotometric pH measurement method

The colorimetric methods for pH determination all use the human eye to detect colour. From an analytical chemistry point of view, a spectrophotometer should be able to achieve this with better sensitivity as it can measure the absorbance at the particular wavelength appropriate to a given molecule or part of a molecule (chromophore).

Beer-Lambert's Law (eqn.1) describes the reduction in the intensity of light caused by absorbed of a solution in spectrophotometer cell (Sarkar 2005).

$$_{\lambda}A = \left(_{\lambda}\varepsilon[x]\right)l \qquad [1]$$

Where $_{\lambda}A$ is the absorbance at wavelength λ, $_{\lambda}\varepsilon$ is the molar absorptivity of a molecule at specific wavelength λ, [x] is the concentration of the molecule and *l* is the optical (spectrophotometer cell) pathlength.

Sulfonephthalein indicators are a group of chemicals well suited to spectrophotometric water pH measurement due to 1) their relatively high solubility in aqueous solution (Yuan et al. 2006); 2) different absorption maxima in the visible range for deprotonated (I^{2-}) and protonated (HL^{-}) species (Byrne et al. 1988) (Figure 3 shows the absorbance spectra of acid and base forms of bromocresol purple (BCP) as an example); and 3) dependency of first and second dissociation constants of indicator (H_2I) on pH offering a primary basis for relating absorbance to $[H^+]$ (equations 2a and 2b) (Clayton and Byrne 1993).

$$H_2I \rightleftharpoons HI^- + H^+ \qquad K_{1=}\frac{[HI^-]\,[H^+]}{[H_2\,I]} \qquad [2a]$$

$$HI^- \rightleftharpoons I^{2-} + H^+ \qquad K_2 = \frac{[I^{2-}][H^+]}{[HI^-]} \qquad [2b]$$

Table 1 shows the working pH range of several sulfonephthalein indicators, covering the pH range of 3-9.6. The working pH range of individual indicator dyes is restricted approximately ±1 pH unit from their pK_a (King and Kester 1990; Yao and Byrne 2001). This is a particular problem for soils with a wide pH range. Although previous studies have indicated a universal mixed dye is theoretically achievable for accurate pH determination in a wide pH range (Raghuraman et al. 2006), it has not yet been

entirely trialed. Furthermore, less attention has been given to the dissociation constant and molar absorptivities of some indicators at lower ionic strength; these are vital parameters needed for spectrophotometric pH measurement specifically in acidic soils.

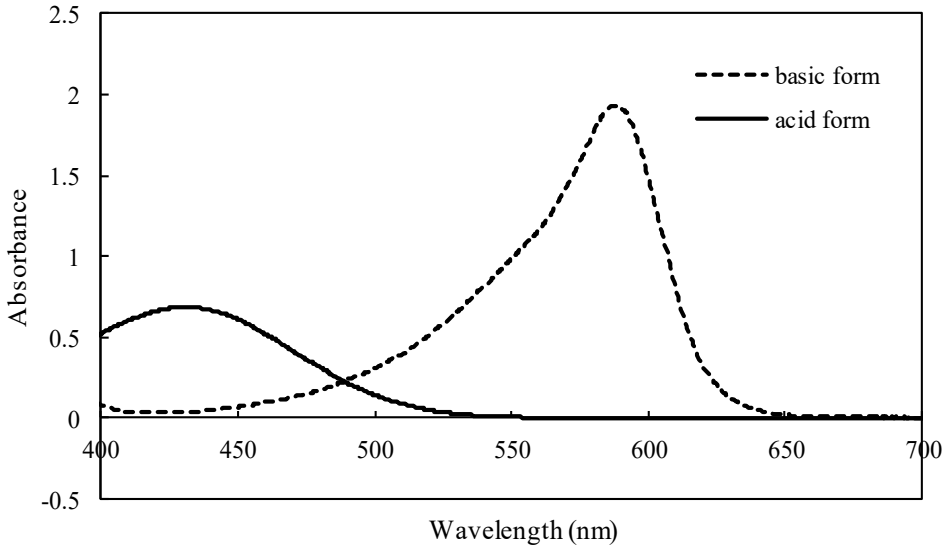

Figure 3: The absorbance spectra of acid (solid line) and base (dotted line) forms of bromocresol purple (BCP, $2*10^{-5}$ mol L^{-1}).

Table 1: Sulfonephthalein indicators at pH range 3-9.6

Indicator	pH range
Bromocresol green	3.5 - 5.3
Bromocresol purple	5.3 - 6.8
Phenol red	6.8 - 8.3
m-Cresol purple	7.4 - 9
Thymol blue	8 - 9.6

1.4.1 Theory of spectrophotometric method

The principles of the spectrophotometric method have been previously discussed by Bates (1973), Robert-Baldo (1985), and Clayton and Byrne (1993). The measurement is built upon the second dissociation of a sulfonephthalein pH indicator as a weak acid added to sample solution:

$$HI^- \rightleftharpoons I^{2-} + H^+ \qquad K_2 = \left[\frac{[I^{2-}][H^+]}{[HI^-]}\right] \qquad [3]$$

Where the brackets [ ] signify the concentration of ions.

The negative logarithmic form of equation [3] (Henderson–Hasselbalch equation) can be used for determination of pH of the conjugate acid-base system:

$$\mathrm{pH} = \mathrm{pK_a} + \log\left[\frac{[\mathrm{I^{2-}}]}{[\mathrm{HI^-}]}\right] \quad [4]$$

Based on equation 1 (Beer-Lambert law), the absorbance of an indicator dye at wavelength λ in solution is given by:

$$_{\lambda}\mathrm{A} = (\,_{\lambda}\varepsilon_{\mathrm{HI}}\,[\mathrm{HI^-}] + \,\,_{\lambda}\varepsilon_{\mathrm{I}}[\mathrm{I^{2-}}])l \quad [5]$$

Where $_{\lambda}\varepsilon_x$ is the molar absorptivity of each individual dye species (x = I^{2-} or HI^-), and *l* is the optical (spectrophotometer cell) path length.

Combining equations 4 and 5 gives equation 6, which provides pH on the free hydrogen ion concentration scale (pH_{free}) (Yao and Byrne 2001):

$$\mathrm{pH} = -\log[\mathrm{H^+}] = \mathrm{pK_a} + \log\frac{(\mathrm{R}-\mathrm{e_1})}{(\mathrm{e_2}-\mathrm{Re_3})} \quad [6]$$

Where R is the absorbance ratio of base to acid indicator species (A_2 / A_1) at wavelength λ_2 and λ_1, and e_1-e_3 are the ratios of indicator molar absorptivities (ε) which depend on each indicator's absorbance properties.

Equations [6] must be modified to account for the effect of ionic strength on ion activity. Therefore, Equation [4] is explained in terms of the individual ion activity coefficient terms (γ_I, γ_H, γ_{HI}) for the dye dissociation:

$$\mathrm{pH} = \mathrm{pK_a} + \log\left[\frac{[\mathrm{I^{2-}}]}{[\mathrm{HI^-}]}\right] + \log\left[\frac{\gamma_{\mathrm{H^+}}\,\gamma_{\mathrm{I^{2-}}}}{\gamma_{\mathrm{HI^-}}}\right] \quad [7]$$

Where γ_i are the ion activity coefficients of each ion which can be determined via the Davies equation (Stumm and Morgan 1996):

$$\log\gamma = -Az^2\left(\frac{\mu^{1/2}}{1+\mu^{1/2}} - 0.3\mu\right) \quad [8]$$

Where A= 0.5092 + (T-298.15) x 8.5 x 10^{-4} (T is temperature in kelvin), z is the charge on the ion, and μ is ionic strength (M). (these values for the Davies equation are appropriate for < 0.5 M solutions, Stumm and Morgan 1996). Debye–Hückel equation is only acceptable to very dilute solution, with the ionic strength of < 0.01 (Murray 2004) which signifies is not suitable for soil solutions used in this study.

By combining equation (6) with the Davies equation (8), pH can now be calculated for a solution with indicator dye added through:

$$\mathrm{pH} = -\log[\mathrm{H}^+] = \mathrm{pK_a} + \log\frac{(\mathrm{R}-\mathrm{e_1})}{(\mathrm{e_2}-\mathrm{Re_3})} - 4\mathrm{A}\left(\frac{\mu^{1/2}}{1+\mu^{1/2}} - 0.3\mu\right) \quad [9]$$

Full justification of equation [9] will be discussed in the following chapter.

1.4.2 The application of spectrophotometric methods for pH measurement in water

The spectrophotometric method using a pH sensitive indicator has been found to be straightforward, swift and precise (Chierici et al. 1999) in monitoring the effect of human-induced increases in atmospheric carbon dioxide concentration on the marine carbonate system (consisting of total alkalinity, total inorganic carbon, pH and pCO_2) and subsequently water acidification (Ohline et al. 2007). The spectrophotometric method has been used for pH measurements in seawater (Robert-Baldo et al. 1985; Byrne and Breland 1989; King and Kester 1989; Bellerby et al. 1995; DeGrandpre et al. 2014), freshwater (Yao and Byrne 2001; French et al. 2002; Lai et al. 2016) and estuarine water (Millero, 1986; Mosley et al. 2004; Gabriel et al. 2005; Gallego-Urrea and Turner 2017).

Spectrophotometric equipment has been designed by marine chemists for monitoring *in situ* pH of seawater (Seidel et al. 2006; Liu et al. 2006; Ohline et al. 2007) with high spatial and temporal resolution. This can provide more reliable calculated pCO_2 values in comparison with directly measured pCO_2 (Tapp et al. 2000; Nakano et al. 2006) due to its the high accuracy of 0.004-0.005 pH units and precision of 0.001 pH units (Bellerby et al. 1995, 2002; Tapp et al. 2000).

The higher precision (within ±0.0004-0.001 pH units) and accuracy (0.001-0.005 pH units) (Clayton and Byrne 1993; McElligott et al. 1998; Tapp et al. 2000; Bellerby et al. 2002; Martz et al. 2003) of spectrophotometric pH measurements relative to glass electrode measurement is governed by the knowledge of indicator dye characteristics such as the equilibrium constant (pK_a) which is temperature, salinity and pressure dependent and the absorbances of acid and base indicator dye species which are measured so as to determine pH (Bates and Vijh 1973; Yao and Byrne 2001).

Additionally, this method does not require calibration with standard materials (Chierici et al. 1999) as it is dependent only pK_a and e_i values (Seidel 2006). (However, DeGrandpre et al. (2014) recommended tris buffer for checking the performance of spectrophotometer). Therefore, in the marine field, spectrophotometric pH measurement has long been used in preference to the potentiometric glass electrode method (Shao et al. 2013) since it obviates many potential problems related to glass electrode outlined above (Yao and Byrne 2001).

Soil inorganic carbonate is a significant potential global carbon sink (Schlesinger 1977) and it also needs to be characterized accurately so as to better understand the response of soil's carbon cycle to climate change. However, first, the internal consistency of soil carbonate system parameters needs to be evaluated. The internal

consistency of marine carbonate system has previously been documented as mentioned above (Clayton et al. 1995, Wanninkhof et al. 1999; Lueker et al. 2000; Patsavas et al. 2015).

1.5 The aims of this study

As described above, the higher precision and accuracy of spectrophotometric pH measurement has led to it being preferred over the glass electrode method in the field of marine chemistry (Robert-Baldo et al. 1985; Byrne et al. 1988; Ohlin et al. 2007). On the other hand, in the field of soil chemistry, the glass electrode method has remained the standard technique to determine soil pH despite the deficiencies outlined above. The main goal of this research was to develop and apply novel spectrophotometric techniques for soil pH measurement.

The following experiments/chapters follow as:

i. The first experiment involved development of a spectrophotometric method for determining pH of soil extracts and comparison with glass electrode measurements (chapter 2). Based on the typical pH range found in soils (5-8.5), two sulfonephthalein indicators, bromocresol purple and phenol red, were deployed for this study. The precision of spectrophotometric soil pH values was evaluated against those obtained with the glass electrode.

ii. The second experiment extended the application of the spectrophotometric method to acidic soils (chapter 3). This required the identification of a suitable indicator dye and determination of its characteristics (pK_a, molar absorbances) for accurate pH determination in the acidic range (pH < 5). The method was tested during the incubation of acid sulfate soils which undergo a wide range of pH variations during oxidation.

iii. The third experiment was aimed at further optimizing and testing a mixed indicator dye for soil solution pH measurements across the wide pH range (pH, 3-9) found in soils circumventing problems associated with single dye measurement in soils (chapter 4).

iv. The fourth experiment was to develop a model to evaluate the consistency of thermodynamics of the soil carbonate system by calculation of one parameter from the other two inputs. In the laboratory, we investigated the probability that persistent and true soil solution pH could be achieved indirectly from carbon dioxide equilibria using the carbonate model suggested by Stumm and Morgan (1996). This will be conducted through calculating pH from known concentration of pCO_2 applied for soil solution equilibration and alkalinity titration and then comparing the results with pH measured using spectrophotometer and glass electrode (Chapter 5).

v. A summary and identification of potential future work (Chapter 6).

References

Andrews, J.A., Schlesinger, W.H., 2001. Soil CO_2 dynamics, acidification, and chemical weathering in a temperate forest with experimental CO_2 enrichment. Global Biogeochemical Cycles 15, 149-162.

Bates, R.G., 1973. Determination of pH: Theory and Practice 2nd Edition. Wiley-Interscience, New York.

Bates, R.G., Vijh, A.K., 1973. Determination of pH: theory and practice, Journal of The Electrochemical Society 120, 263C-263C.

Bellerby, R.G.J., Turner, D.R., Millward, G.E., Worsfold, P.J., 1995. Shipboard flow injection determination of seawater pH with spectrophotometric detection. Analytica Chimica Acta 309, 259-270.

Bellerby, R.G.J., Olsen, A.; Johannessen, T., Croot, P.A., 2002. A high precision spectrophotometric method for on-line shipboard seawater pH measurements: the automated marine pH sensor (AMpS). Talanta 56, 61-69.

Berner, R.A., 1997. The rise of plants and their effect on weathering and atmospheric CO_2. Science 276, 544-546.

Bond-Lamberty, B., and Thomson, A., 2010. Temperature-associated increases in the global soil respiration record. Nature 464, 79-582.

Bormann, B.T., Wang, D., Bormann, F.H., Benoit, G., April, R., Snyder, R., 1998. Rapid, plant-induced weathering in an aggrading experimental ecosystem. Biogeochemistry 43, 129-155.

Brennan, R.F., Bolland, M.D.A., Bowden, J.W., 2004. Potassium deficiency, and molybdenum deficiency and aluminium toxicity due to soil acidification, have become problems for cropping sandy soils in south-western Australia. Australian Journal of Experimental Agriculture 44, 1031-1039.

Byrne, R.H., Robert-Baldo, G., Thompson, S.W., Chen, C.T.A., 1988. Seawater pH measurements: an at-sea comparison of spectrometric and potentiometric methods. Deep-Sea Research Part A 35, 1405-1410.

Byrne, R.H., Breland, J.A., 1989. High precision multiwavelength pH determinations in seawater using cresol red. Deep-Sea Research 36(5), 803-810.

Chierici, M., Fransson, A., Anderson, L.G., 1999. Influence of m-cresol purple indicator additions on the pH of seawater samples: corrections factors evaluated from a chemical speciation model. Marine Chemistry 65, 281-290.

Clayton, T.D., Byrne, R.H., 1993. Spectrophotometric seawater pH measurements: total hydrogen ion concentration scale calibration of m-cresol purple and at-sea results. Deep-Sea Resarch., Part I: Oceanographic Research Papers 40, 2115-2129.

Clayton, T.D., Byrne, R.H., Breland, J.A., Feely, R.A., Millero, F.J., Campbell, D.M., Murphy,P.P., Lamb, M.F., 1995. The role of pH measurements in modern oceanic CO_2-system characterizations: Precision and thermodynamic consistency. Deep-Sea Research II, Vol. 42, No. 2-3. pp. 41 l-429.

Coleman, N.T., Williams, D.E., Nielson, J.R., Jenny, H., 1951. On the validity of interpretations of potentiometrically measured soil pH. Soil Science Society of American journal 15, 106-114.

Conyers, M.K., Davey, B.G., 1988. Observations on some routine methods for soil pH determination. Soil Science 145, 29-36.

Creeper, N., Fitzpatrick, R., Shand, P., 2012. A simplified incubation method using chip trays as incubation vessels to identify sulphidic materials in acid sulphate soils. Soil Use and Management 28, 401-408.

DeGrandpre, M.D., Spaulding, R.S., Newton, J.O., Jaqueth, E.J., Hamblock, S.E., Umansky, A.A., Harris, K.E., 2014. Considerations for the measurement of spectrophotometric pH for ocean acidification and other studies. Limonology and Oceanography 12, 830-839.

Deshpande, K. B., Marshall, C. E., 1961. Comparisons of electrometric measurements in clay systems. The Journal of Physical Chemistry 65, 33-36.

Dickson, A.G., Goyet, C., 1994. Handbook of Methods for the Analysis of the Various Parameters of the Carbon Dioxide System in Sea Water, Prepared for the U.S. Department of Energy, Special Research Grant Program 89-7A: Global survey of carbon dioxide in the oceans, p. 189.

Essington, M.E., 2015. Soil and water chemistry: An integrative approach 2nd Edition. CRC Press, New York.

Fitzpatrick, R.W., Grealish, G., Shand, P., Merry, R., Creeper, N., Thomas, M., Baker, A., Thomas, B., Hicks, W., Jayalath, N., 2010. Chip-tray incubation, A new field and laboratory method to support Acid Sulfate Soil Hazard Assessment, Classification and Communication. In: Gilkes, R.J., Prakongkep N. (Eds.), Proceedings of the 19th World Congress of Soil Science; Soil Solutions for a Changing World, ISBN 987-0-

646-53783-2; published on DVD. ⟨http://www.iuss.org; Symposium WG 3.1 Processes in acid sulfate soil materials⟩ Brisbane, Australia, IUSS, pp. 28-31.

French, C.R., Carr, J.J., Dougherty, E.M., Eidson, L.A., Reynolds, J.C., DeGrandpre, M.D., 2002. Spectrophotometric pH measurements of freshwater Analytica Chimica Acta 453, 13-20.

Gabriel, M.D., Forja, J.M., Rubio, J.A., Gomez-Parra, A., 2005. Temperature and salinity dependence of molar absorptivities of thymol blue: Application to the spectrophotometric determination of pH in estuarine waters. Ciencia Marinas 31(1B), 309-318.

Gallego-Urrea, J.A., Turner, D. R., 2017. Determination of pH in estuarine and brackish waters: Pitzer parameters for Tris buffers and dissociation constants for m-cresol purple at 298.15 K. Marine Chemistry 195, 84-89.

Hewitt, A.E., 1992. Soil classification in New Zealand-Legacy and lessons. Australian Journal of Soil Research 30, 843-854.

Isbell, R., National Committee on Soils and Terrain, 2016. The Australian soil classification 2nd Edition. CSIRO Publishing.

Jones, J.R., Benton, J., 2012. Plant Nutrition and Soil Fertility Manual 2nd Edition. CRC Press, Taylor & Francis Group, Boca Raton.

King, D.W., Kester, D.R., 1989. Determination of seawater pH from 1.5 to 8.5 using colorimetric indicators, Marine Chemistry 26, 5-20.

King, D.W., Kester, D.R., 1990. Spectral modeling of sulfonephthalein indicators: application to pH measurements using multiple indicators. Applied Spectroscopy 44, 722-727.

King, J.S., Pregitzer, K.S., Zak, D.R., Sober, J., Isebrands, J.G., Dickson, R.E., Hendrey, G.R., Karnsoky, D.F., 2001. Fine-root biomass and fluxes of carbon in young stands of paper birch and trembling aspen as affected by elevated atmospheric CO_2 and tropospheric O_3. Oecologia 128, 237-250.

Kissel, D.E., Sonon, L., Vendrell, P.F., Isaac, R.A., 2009. Salt concentration and measurement of soil pH. Communications in Soil Science Plant Analysis 40, 179-187.

Lai, C.Z., DeGrandpre, M.D., Wasser, B.D., Brandon, T.A., Clucas, D.S., Jaqueth, E.J., Benson, Z.D., Beatty, C.M., Spaulding, R.S., 2016. Spectrophotometric measurement of freshwater pH with purified meta- cresol purple and phenol red. Limnology and Oceanography: Methods 14, 864-873.

Lindsay, W.L., 1979. Chemical Equilibria in Soils. John Wiley & Sons Ltd, UK.

Liu, X., Wang, Z. A., Byrne, R.H., Kaltenbacher, E.A., Bernstein, R.E., 2006. Spectrophotometric measurements of pH in-situ: Laboratory and field evaluations of instrumental performance. Environmental science and technology 40, 5036-5044.

Lueker, T.J., Dickson, A.G., Keeling, C.D., 2000. Ocean pCO_2 calculated from dissolved inorganic carbon, alkalinity, and equations for K_1 and K_2: validation based on laboratory measurements of CO_2 in gas and seawater at equilibrium. Marine Chemistry 70, 105-119.

Manov, G.G., DeLollis, N.J., Acree, S.F., 1944. Liquid junction potentials and relative activity coefficients of chloride ions, in concentrated mixed chlorides and nitrates at 25°C. Journal of Research of the National Bureau of Standards 33, 273-285.

Martz, T.R., Carr, J.J., French, C.R., DeGrandpre, M.D., 2003. A submersible autonomous sensor for spectrophotometric pH measurements of natural waters. Analytical Chemistry 75, 1844-1850.

McElligott, S., Byrne, R.H., Lee, K., Wanninkhof, R., Millero, F.J., Feely, R.A., 1998. Discrete water column measurements of CO_2 fugacity and pHT in seawater: A comparison of direct measurements and thermodynamic calculations. Marine Chemistry 60, 63-73.

Mclean, 1982. Soil pH and Lime Requirement. Methods of soil analysis. Part 2. Chemical and microbiological properties 199-224.

Miller, R.O., Kissel, D.E., 2010. Comparison of soil pH methods on soils of North America. Soil Science Society of American Journal 74, 310-316.

Millero, F.J., 1986. The pH of estuarine waters. Limnology and Oceanography 31, 839-847.

Mosley, L.M., Husheer, S.L., Hunter, K.A., 2004. Spectrophotometric pH measurement in estuaries using thymol blue and m-cresol purple. Marine Chemistry 91, 175-186.

Murray, J.W., 2004. Activity Scales and Activity Corrections. Retrieved November 6, 2010, from: http://www.ocean.washington.edu/courses/oc400/Lecture_Notes/CHPT6.pdf.

Nakano, Y., Kimoto, H., Watanabe, S., Harada, K., Watanabe, Y.W., 2006. Simultaneous vertical measurements of in situ pH and CO_2 in the sea using spectrophotometric profilers. Journal of Oceanography 62, 71-81.

Ohline, S. M., Reid, M. R., Husheer, S.L.G., Currie, K. I., Hunter, K. A., 2007. Spectrophotometric determination of pH in seawater off Taiaroa Head, Otago, New

Zealand: full-spectrum modelling and prediction of pCO_2 levels. Marine Chemistry 107, 143-155.

Patsavas, M.C., Byrne, R.H., Yang, B., Easley, R.A., Wanninkhof, R., Liu, X., 2015. Procedures for direct spectrophotometric determination of carbonate ion concentrations: measurements in the US Gulf of Mexico and East Coast Waters. Marine Chemistry 168, 80-85.

Peech, M., Olsen, R. A., Bolt, G. H., 1953. The significance of potentiometric measurements involving liquid junction in clay and soil suspensions. Soil Science Society of American Journal 17, 214-218.

Raghuraman, B., Gustavson, G., Van Hal, R.E.G., Dressaire, E. and Zhdaneev, O., 2006. Extended-range spectroscopic pH measurement using optimized mixtures of dyes. Applied pectroscopy 60, 1461-1468.

Raupach, M., Tucker, B., 1959. The field determination of soil reaction. Journal of the Australian Institute of Agricultural Science 25, 129-133.

Rayment, G.E., Lyons, D.J., 2011. Soil chemical methods. CSIRO publishing, Victoria, Australia.

Robert-Baldo, G.L., Morris, M.J., Byrne, R.H., 1985. Spectrophotometric determination of seawater pH using phenol red. Analytical Chemistry 57, 2564-2567.

Sarkar, D., 2005. Physical and chemical methods in soil analysis. New Age International.

Sauvé, S., McBride, M.B., Norvell, W.A., Hendershot, W.H., 1997. Copper Solubility and Speciation of In Situ Contaminated Soils: Effects of Copper Level, pH and Organic Matter. Water, Air, and Soil Pollution, Vol.100. pp.133-149.

Sauve, S., Hendershot, W., Allen, H.E., 2000. Solid-solution partitioning of metals in contaminated soils. Environmental Science & Technology 34, 1125-1131.

Schlesinger, W. H., 1977. Carbon balance in terrestrial detritus. Annual Review of Ecology and Systematics 8, 51-81.

Seidel, M.P., 2001. A sensor for in situ spectrophotometric measurements of seawater pH.

Seidel, M.P., 2006. A sensor for in situ spectrophotometric measurements of seawater pH.

Shao, H., Thompson, C. J., Cantrell, k. J., 2013. Evaluation of experimentally measured and model-calculated pH for rock-brine-CO_2 systems under geologic CO_2 sequestration conditions. Chemical Geology 359, 116-124.

Skoog, D.A., Holler, F.J., Crouch, S.R., 2007. Principles of instrumental analysis. Cengage Learning (Inc.), Belmont, CA.

Snyder, E.F., 1935. Methods for determining the hydrogen ion concentration of soils. USDA Circular, No. 56. US Department of Agriculture Washington, DC.

Soil Science Division Staff, 2017. Soil Survey Manual: Handbook of Department of Agriculture, No. 18. USDA-NRCS, U.S. Gov. Print. Office, Washington, D.C. USA.

Strawn, D.G., Bohn, H.L., O'Connor, G.A., 2015. Soil chemistry. John Wiley & Sons.

Stumm, W., Morgan. J., 1996. Aquatic chemistry: Chemical equilibria and rates in natural waters 3rd Edition.Wiley-Interscience, New York.

Suarez, D.L., 1977. Ion activity products of calcium carbonate in waters below the root zone. Soil Science Society of American Journal 41, 310-315.

Tapp, M., Hunter, K., Currie, K., Macaskill, J., 2000. Apparatus for continuous-flow underway spectrophotometric measurement of surface water pH. Marine Chemistry 72, 193-202.

Wanninkhof, R., Lewis, E., Feely, R. A., and Millero, F. J., 1999. The optimal carbonate dissociation constants for determining surface water pCO_2 from alkalinity and total inorganic carbon, Marine Chemistry 65, 291-301.

Whitfield, M., Butler, R.A., Covington, A.K., 1985. The determination of pH in estuarine waters: I. Definition of pH scales and the selection of buffers. Oceanologica Acta 8, 423-432.

Wiesner, A.D., Katz, L.E., Chen, C.C., 2006. The impact of ionic strength and background electrolyte on pH measurements in metal ion adsorption experiments. Journal of colloid and interface science 301, 329-332.

Yao, W., Byrne, R.H., 2001. Spectrophotometric determination of freshwater pH using bromocresol purple and phenol red. Environmental Science and Technology 35, 1197-1201.

Yuan, S., 2006. Optimization of a submersible autonomous spectrophotometric sensor for pH measurements in low ionic strength freshwater.

Yuan, S., DeGrandpre, M.D., 2008. Evaluation of indicator-based pH measurements for freshwater over a wide range of buffer intensities. Environmental Science and Technology 42, 6092-6099.

CHAPTER 2

Development of a spectrophotometric method for determining pH of soil extracts and comparison with glass electrode measurements

Sima Bargrizan[a], Ronald J. Smernik[a], and Luke M. Mosley[b]

[a] The School of Agriculture, Food and Wine, The University of Adelaide, South Australia

[b] Acid Sulfate Soils Centre, School of Biological Sciences, The University of Adelaide, South Australia

Bargrizan S, Smernik RJ, & Mosley LM (2017). Development of a Spectrophotometric Method for Determining pH of Soil Extracts and Comparison with Glass Electrode Measurements. *Soil Science Society of America Journal* **81**, 1350-1358.

Statement of Authorship

Title of Paper	Development of a spectrophotometric method for determining pH of soil extracts and comparison with glass electrode measurements.
Publication Status	☑ Published ☐ Accepted for Publication ☐ Submitted for Publication ☐ Unpublished and Unsubmitted w ork w ritten in manuscript style
Publication Details	2017, Soil Science Society of America Journal **81**, 1350–1358.

Principal Author

Name of Principal Author (Candidate)	Sima Bargrizan		
Contribution to the Paper	Accomplished experiment, data collection, data analysis and interpretation, wrote manuscript.		
Overall percentage (%)	70%		
Certification:	This paper reports on original research I conducted during the period of my Higher Degree by Research candidature and is not subject to any obligations or contractual agreements with a third party that would constrain its inclusion in this thesis. I am the primary author of this paper.		
Signature		Date	21.01.2019

Co-Author Contributions

By signing the Statement of Authorship, each author certifies that:

i. the candidate's stated contribution to the publication is accurate (as detailed above);

ii. permission is granted for the candidate in include the publication in the thesis; and

iii. the sum of all co-author contributions is equal to 100% less the candidate's stated contribution.

Name of Co-Author	Luke Mosley		
Contribution to the Paper	Supervised development of work, data interpretation and manuscript evaluation and correction, and acted as corresponding author.		
Signature		Date	21.01.2019

Name of Co-Author	Ron Smernik		
Contribution to the Paper	Supervised development of work, data interpretation, manuscript evaluation and correction.		
Signature		Date	21.01.2019

Please cut and paste additional co-author panels here as required.

Published online January 4, 2018

Development of a Spectrophotometric Method for Determining pH of Soil Extracts and Comparison with Glass Electrode Measurements

Sima Bargrizan
Ronald J. Smernik
School of Agriculture, Food and Wine
Univ. of Adelaide
South Australia, 5005
Australia

Luke M. Mosley*
Acid Sulfate Soils Centre
School of Biological Sciences
Univ. of Adelaide
South Australia, 5005
Australia

Soil pH measurement using conventional glass electrodes has several limitations. A spectrophotometric method was developed for determining soil pH involving indicator dye (bromocresol purple or phenol red) addition to soil extracts. Results were compared against values determined using a glass electrode for a range of soils (n = 13) with varying properties using different extraction conditions (1:1 w/v soil/water, 1:1 soil/0.01 mol L^{-1} $CaCl_2$, 1:5 soil/water and 1:5 soil/0.01 mol L^{-1} $CaCl_2$) and high and low ionic strength buffer calibrations of the electrode. For all extraction conditions, there was a strong relationship (r^2 > 0.95, slope ≈ 1) between values of the spectrophotometric (pH_{spec}) and glass electrode (pH_{elec}) methods. The precision of pH_{spec} was similar to pH_{elec} measurements across the different extraction conditions (±0.02–0.08 average standard deviation of triplicate measurements, n = 39). Large and variable differences were observed between pH_{elec} measured following calibration with high (μ = 0.1 mol L^{-1}) and low (μ = 0.005 mol L^{-1}) ionic strength buffers. In contrast, ionic strength effects on the indicator dye and resulting pH_{spec} calculation are implicitly accounted for. A spectrophotometric reflectance probe in situ method was also successfully trialed. The spectrophotometric pH method circumvents many of the problems associated with the use of glass electrodes in soil solutions.

Core Ideas

- **Soil pH is a critical parameter in soils as it influences many biogeochemical processes.**
- **There are problems in pH measurements in soils using glass electrodes.**
- **A new spectrophotometric method was developed to measure pH in soils.**
- **The method compared well to measurements using glass electrodes in a range of soils.**
- **A reflectance probe technique was also successfully trialed for in situ measurement.**

Soil pH is a very important controller of chemical and biological processes in soils. Accurate measurement of pH is needed for prediction of metal ion binding to oxide minerals, which occurs in relatively narrow pH ranges (Sauve et al., 2000; Wiesner et al., 2006). Equilibria among inorganic carbon species are also controlled by pH in soils (Suarez, 1977), and there is currently a need for better quantifying inorganic carbon fluxes to and from soils in the context of global climate change (Bond-Lamberty and Thomson, 2010). Nutrient availability and microbial activity in the soil are also influenced by pH, and many farm management practices (e.g., liming, fertilizer application) are dependent on, and/or influence, pH measurements (Miller and Kissel, 2010).

Historically, soil pH determination has typically involved extraction of the soil in a simple solution (e.g., water, dilute $CaCl_2$) at a particular soil/solution ratio (e.g., 1:1, 1:2 or 1:5 w/v) followed by measurement using a glass electrode calibrated with buffer solutions (Heintze, 1934; Rayment and Lyons, 2011). However there are several potential issues associated with using glass electrodes to measure pH in soil extracts. First, the two main components of the glass electrode, namely the reference and the membrane glass electrode, are connected by a salt bridge of saturated KCl solution. An inherent but unquantifiable source of measurement error arises from the potential at the liquid junction between the two internal solutions surrounding the two electrodes (Manov et al., 1944; Skoog et al., 2007). This can cause errors of the order of 0.1 pH units, and is generally greatest when the solution used to cali-

Supplemental material is available for this article.
Soil Sci. Soc. Am. J. 81:1350–1358
doi:10.2136/sssaj2017.04.0119
Received 17 Apr. 2017.
Accepted 26 July 2017.
*Corresponding author (luke.mosley@adelaide.edu.au).
© Soil Science Society of America, 5585 Guilford Rd., Madison WI 53711 USA. All Rights reserved.

brate the electrode has a different ionic composition to that of the sample solution, especially for samples with low (<0.003 mol L^{-1} or approximately <0.24 mS cm^{-1} electrical conductivity in extract) ionic strength (Millero, 1986). Wiesner et al. (2006) found that to eliminate errors in soil pH measurement, and associated metal adsoprtion prediction errors, electrodes needed to be calibrated with buffers prepared with the same electrolyte and ionic strength as samples. This is often impractical due to the range of ionic strengths and electrolyte compositions found in different soils and hence is not usually performed. Second, K^+ and Cl^- mobility across the salt bridge may be different between soils with high and low cation exchange capacity (CEC) and this can lead to a lower or higher pH readings, respectively (Essington, 2015). To stabilize electrodes, $CaCl_2$ is commonly used as an extractant solution for soil pH measurements (Rayment and Lyons, 2011). The addition of $CaCl_2$ commonly reduces the soil pH relative to when water is used as an extractant (Miller and Kissel, 2010), which has been proposed to be due to the added Ca^{2+} displacing protons from soil cation exchange sites (Conyers and Davey, 1988). Hence in stabilizing electrodes, an error is introduced relative to the true soil pH and the magnitude of this error is variable between different soil types. Third, the porous fiber of pH electrodes can become clogged, limiting the flow of liquid from the salt bridge into the solution, resulting in slow equilibration and ultimately an inaccurate pH measurement (Skoog et al., 2007). Fourthly, electrode pH measurements can suffer problems with drift (e.g., on order of –0.01 to –0.03 pH units per day, Yuan and DeGrandpre, 2008).

Substantial progress has been made in developing spectrophotometric methods for measuring the pH of seawater (Robert-Baldo et al., 1985; Clayton and Byrne, 1993), estuarine water (Mosley et al., 2004) and freshwater (Yao and Byrne, 2001; French et al., 2002; Lai et al., 2016). In the spectrophotometric method, an acid-base indicator dye is added to the sample, and the absorbance readings of conjugate acidic and basic dye species at different wavelengths are measured and used to calculate pH. Many of the inherent problems associated with glass electrode pH measurement (e.g., liquid junction potential, drift) can be avoided using this method. Also, calibrating buffers are not required in the spectrophotometric method once the dissociation constants and molar absorptivities of the dye are determined in the salinity and temperature range of interest. Spectrophotometric pH measurements also have a higher precision than glass electrode measurements (e.g., variance in replicate measurements of ±0.0004 and ±0.0005 pH units respectively for seawater (Clayton and Byrne, 1993); ±0.001 to 0.01 respectively for estuarine water and freshwater (Yao and Byrne, 2001; Lai et al., 2016).

Indicator dyes have been used previously to determine the pH of soils using colorimetric methods (Snyder, 1935; Raupach and Tucker, 1959). In the Snyder (1935) approach, an individual indicator dye was added to a centrifuged soil extract and the color compared to prepared color standards representing different pH values. In the Raupach and Tucker (1959) approach, a mixed indicator dye solution was combined with the soil, the soil dusted with white barium sulfate powder (to highlight color), and the color compared visually to a standard color chart (Raupach and Tucker, 1959; Rayment and Lyons, 2011). The indicator pH measurements generally compared quite well to glass electrode measurements in 1:5 soil/water suspensions (Raupach and Tucker, 1959). However, the standard color charts used in these soil pH colorimetric methods have a much lower accuracy (±0.5 pH units) than glass electrode methods (±0.1 pH units with careful calibration) (Rayment and Lyons, 2011). Another potential issue with the Raupach and Tucker method is that the barium sulfate and concentrated dye solution addition to the soil may introduce a pH perturbation which was not assessed in its development.

The aim of this study was to examine whether the use of indicator dyes in combination with modern spectrophotometric methods can be used for determination of pH in soil extracts. Two sulfonephthalein indicators, bromocresol purple and phenol red, were used for spectrophotometric pH measurement in the approximate soil pH range of 5 to 8.5. The performance of spectrophotometric and electrode methods was compared for pH measurement in both water and $CaCl_2$ extracts at different soil/extractant ratios for a range of different soils.

MATERIALS AND METHODS

Soils and Preparation of Soil Extracts

Thirteen soils with a wide range of properties (Table 1) were utilized in the study. These soils were collected from various locations in South Australia, mostly collected from the surface (0–10 cm) layer, although four samples were included from a 0- to 55-cm depth profile at one site (Mobilong). The soils were oven-dried and sieved to obtain a <2 mm size fraction.

Four different soil extracts were prepared from each soil (1:1 w/v 25 g soil/25 mL water, 1:1 w/v 25 g soil/25 mL 0.01 mol L^{-1} $CaCl_2$, 1:5 w/v 5 g soil/25 mL water, 1:5 w/v 5 g soil/25 mL 0.01 mol L^{-1} $CaCl_2$). Three replicates of each soil and soil ratio/extract mixture were prepared. The soil solutions were shaken for 1 h on an orbital shaker, and then centrifuged (1915.2 relative centrifugal force) for 30 min as per standard methods (Rayment and Lyons, 2011). After centrifuging, approximately 10 mL of the soil extract supernatant was carefully pipetted into a clean polyethylene tube for immediate analysis.

Spectrophotometric Soil pH Measurement

The spectrophotometric pH method is based on measurement of the dissociation of a protonated (acid) indicator dye species (HI^-) to its unprotonated (base) form (I^{2-}) (Robert-Baldo et al., 1985; Clayton and Byrne, 1993):

$$HI^- \rightleftharpoons I^{2-} + H^+ \quad [1]$$

The equilibrium constant (K_2, second dissociation constant for the fully protonated dye species H_2I) for this equation can be defined as:

$$K_2 = [H^+][I^{2-}]/[HI^-] \quad [2]$$

Table 1. Soil physical and chemical properties.

Soil	Depth	Sand	Silt	Clay	Exchangeable cations					CEC	Total C
					Ca	Mg	Na	K	Total		
	cm	%			cmol(+) kg^{-1}						%
Monarto	0–10	84.6	7.1	8.3	4.9	1.01	<0.10	0.53	6.4	8.2	1.0
Arboretum	0–10	50	35	15	6.1	1.2	0.5	1.8	9.6	15	2.9
Lock siliceous	0–10	95	0	5	7.7	0.8	0.4	1.0	9.9	7.7	1.6
Karoonda	0–10	97.4	0.2	2.4	1.15	0.33	<0.17	<0.15	1.5	2.0	0.35
Ngarkat	0–10	95.8	1.0	3.2	2.19	0.35	<0.17	<0.15	2.5	3.1	0.67
Lock Horizon	0–10	97.5	2.5	0	3.2	1.0	0.4	0.1	4.7	2.5	3.7
Mt Compass	0–10	97.2	1.7	1.1	1.5	0.31	<0.1	0.08	1.8	3.6	0.5
Modra	0–10	65	5	30	18	3.2	0.6	3.5	25	28	2
Tumby Bay	0–10	51	21.5	27.5	4.7	1.5	0.2	0.9	7.4	10.0	2.9
Mobilong	0–10	53	9	38	7.2	14.0	19.4	1.2	41.8	43.6	11.1
	10–20	8.5	19	72.5	3.6	6.8	11.1	0.5	22.0	36.9	5.9
	20–35	15	12	73	6.7	11.1	15.2	1.2	34.1	43.7	7.0
	35–55	2	27	71	5.1	8.5	11.5	0.9	26.1	36.5	2.4

The pH on the free hydrogen ion concentration (mol H^+ kg^{-1}) scale is obtained from the following equation (Yao and Byrne, 2001):

$$pH = -\log[H^+] = pK_2 + \log\frac{(R - e_1)}{(e_2 - Re_3)} - 4A\left(\frac{\mu^{1/2}}{1+\mu^{1/2}} - 0.3\mu\right) \quad [3]$$

where $pK_2 = -\log K_2$; R is the ratio of light absorbance (Abs.) at the absorbance maxima of base (I^{2-}, λ_2) and acid (HI^-, λ_1) dye forms respectively ($R = \lambda_2$Abs.$/\lambda_1$Abs.); e_1 to e_3 denote indicator molar absorbance ratios which are constants based on an individual dye's absorbance characteristics; the last term is the Davies equation for correcting for ionic strength effects on ion activity where μ is ionic strength (mol L^{-1}), which is applicable to <0.5 mol L^{-1} solutions (Stumm and Morgan, 1996); and $A = 0.5092 + (T - 298.15) \times 8.5 \times 10^{-4}$ where T is the temperature in kelvin. The Supplemental Material contains a full derivation and explanation of the spectrophotometric method theory.

Bromocresol purple and phenol red dye stock solutions were prepared at a concentration of 3×10^{-3} mol L^{-1} and adjusted to a pH where approximately equal concentrations of acid and base forms were present (pH ≈ 7.5 and 5.9 for phenol red and bromocresol purple, respectively) using 0.1 mol L^{-1} HCl and NaOH. Indicators were not specifically tested for the potential impurities present in this study either but the magnitude of the pH errors these introduce (<0.01 pH units, Mosley et al., 2004) are not expected to be important for the large pH ranges found in soil.

UV-visible spectra were collected using matched glass cuvettes with a 1-cm path length on a double-beam spectrophotometer (GBC UV/VIS 916) equipped with Cintral software. The ratio of indicator absorbances (R) at their absorbance maxima were determined from these spectra. For phenol red, the acid and base indicator species were measured at wavelengths of 433 nm (λ_1) and 558 nm (λ_2), respectively. For bromocresol purple, the acid and base indicator species were measured at wavelengths of 432 nm (λ_1) and 589 nm (λ_2), respectively.

A spectrophotometric cell holder equipped with a water thermostat maintained the cuvette solution temperature at 25°C. Before measurement, sample tubes were placed in a separate water bath adjusted to 25°C to pre-equilibrate for approximately 30 min. After temperature equilibration, 4 mL of sample and 0.03 mL of dye stock was pipetted into the cuvette, which was capped, inverted to mix the dye, and placed in the spectrophotometer. Sample solution without dye was placed in the reference beam of the instrument. The full absorbance spectra with and without dye was recorded between 350 and 750 nm (example spectra in Fig. 1a).

To account for any minor pH perturbation following dye addition, the ratio R used for pH calculation (Eq. [3]) was that extrapolated to zero dye addition via linear regression of the R values calculated for three sequential dye additions versus the volume (0.03, 0.06, 0.09 mL) of dye addition (Clayton and Byrne, 1993) (example shown in Fig. 1b). Addition of these volumes of dye gave a final dye concentration in the range of approximately 2×10^{-5} to 6×10^{-5} mol L^{-1} (refer to Fig. 1a for the corresponding absorbance values). Three replicates were analyzed for each extract. The respective molar absorbance ratios of e_1 to e_3 and thermodynamic dissociation constants (pK_2) of the two (phenol red and bromocresol purple) indicator dyes (Eq. [4] and [5]) at 25°C used for the pH calculations were those previously reported by Yao and Byrne (2001).

$$pK_2 = 5.798 + 666.7/T \text{ (phenol red)} \quad [4]$$

$$pK_2 = 5.226 + 378.1/T \text{ (bromocresol purple)} \quad [5]$$

where T is the temperature in kelvin, and the pK_2 values are at infinite dilution for impure indicators.

Ionic strength (μ) was calculated from measured electrical conductivity (EC, mS cm^{-1}) in each soil solution using a calibrated conductivity electrode (TPS Glass K = 1.0 Cond Sensor) using the equation (Griffin and Jurinak, 1973; Gillman and Bell, 1978):

$$\mu = EC \times 0.0127 \quad [6]$$

To assess the accuracy of the spectrophotometric method in the absence of soil, a standard phosphate buffer solution was

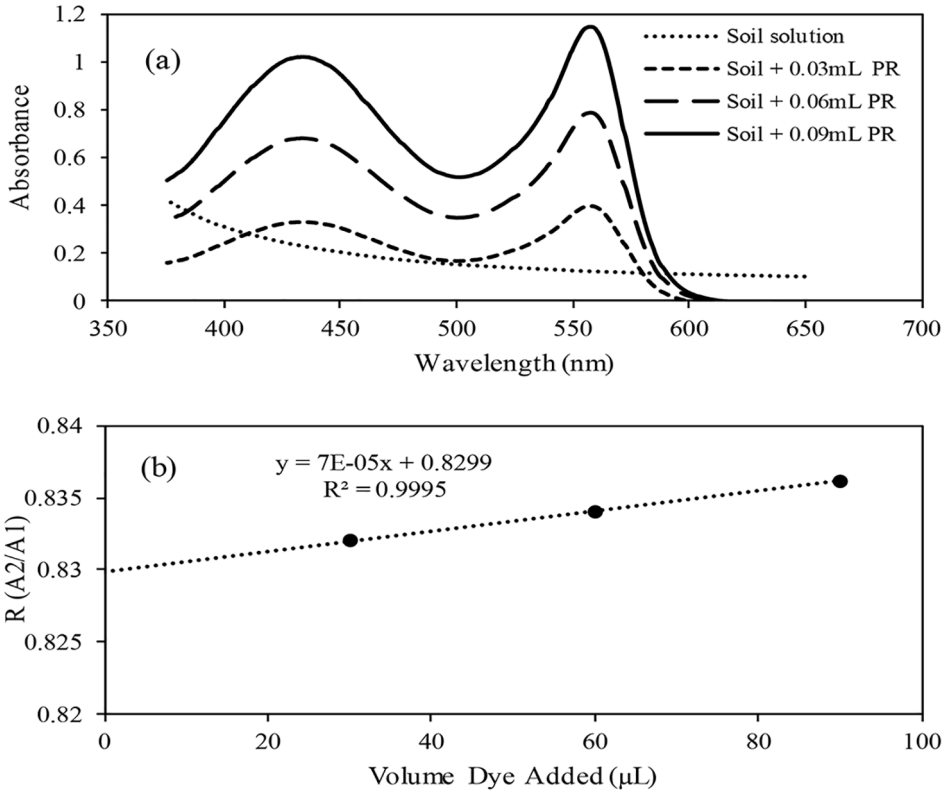

Fig. 1. (a) Absorbance vs. wavelength for base (I^{2-}) and acid (HI^{-}) forms of phenol red (PR) in a 1:1 soil extract before and after addition of 0.03, 0.06 and 0.09 mL of dye; (b) plot of the absorbance ratio (*R*) in the Modra 1:1 soil/water soil extract following sequential addition of 0.03, 0.06 and 0.09 mL dye solution. A linear equation is fitted with the *y*-intercept taken to represent the *R* value at zero dye addition.

prepared (NIST Standard Reference Material 186 g, refer to certification documentation on NIST website for details). The phosphate buffer had a certified pH = 6.77 on the free hydrogen ion concentration pH scale (pH 6.86 on NIST/NBS pH scale based on hydrogen ion activity as provided by the NIST certification and Bates and Acree, 1945; refer to Eq. [7] below for detail on this conversion). A spectrophotometric pH = 6.772 ± 0.002 was measured for this buffer which indicated the method was accurate in the absence of soil.

Glass Electrode Soil pH Measurement

The pH of each of the soil extracts was concurrently monitored with pH electrodes (Orion SureFlow) connected to a TPS model pH meter after calibration with two different ionic strength buffers: one low ionic strength buffer (μ = 0.005 mol L^{-1}) using potassium hydrogen phthalate and dihydrogen/hydrogen phosphate NIST buffers at approximately pH 4.0 and pH 6.86, respectively, and commercially manufactured (Australian Chemical Reagents) standard high ionic strength buffers ($\mu \approx 0.1$ mol L^{-1}) at pH 7 and 4 at 25°C. Three replicates of each sample were analyzed at 25°C as per the spectrophotometric measurements.

The pH measured using the glass electrode is defined on the NBS/NIST scale as $pH_{NBS/NIST} = -\log a_{H+}$, where a_{H+} is the hydrogen ion activity. To enable comparison between the pH values obtained by the spectrophotometric method, the NIST/NBS pH electrode measurements were corrected to the hydrogen ion concentration scale (pH_{free}) using the equation:

$$pH_{free} = -\log[H^+] = pH_{NBS/NIST} + \log\gamma_{H+} \quad [7]$$

where the activity coefficient for H^+ (γ_{H+}) was calculated via the Davies equation (refer to the Supplemental Material Eq. [12]) using the ionic strength of the soil extract measured as outlined above.

Reflectance Probe in situ Soil pH Measurement

The spectrophotometric pH measurement method was also tested in reflectance mode following dye application directly to 1:1 soil/water mixtures. A StellarNet Black Comet spectrometer with a R600-8-visible-near infrared fiber optic reflectance probe for VIS-NIR was utilized. During reflectance measurements the seven exterior fibers on the fiber optic probe are illuminated by a high output power light source and the single interior read fiber collects the reflected light and returns the signal to the spectrometer. To test the method, 1:1 soil/water mixtures of Mobilong and Tumby Bay soil samples were prepared but not centrifuged. A reference spectrum (350–750 nm) was collected of the soil mixture in the absence of dye. The phenol red and bromocresol purple dye stock solution (approximately 0.12 mL) was then mixed directly into the 1:1 soil mixture, the reflectance spectrum recorded and the reference spectrum subtracted. The pH_{spec} was then calculated as described above.

RESULTS

Comparison of Spectrophotometric and Glass Electrode pH Measurements

The relationship between pH values determined by spectrophotometric and glass electrode (calibrated with high ionic strength buffer at 25°C) methods across the 13 soils (pH range approximately 5–8.5) for the four different soil extract conditions is shown in Fig. 2. There was a strong linear correlation between pH_{elec} and pH_{spec} in 1:1 water ($y = 0.9626x + 0.3111$, $r^2 = 0.9916$), 1:5 water ($y = 0.9599x + 0.258$, $r^2 = 0.989$), 1:1 0.01 mol L^{-1} $CaCl_2$ ($y = 0.9966x + 0.1128$, $r^2 = 0.9887$), and 1:5 0.01 mol L^{-1} $CaCl_2$ ($y = 0.9717x + 0.2148$, $r^2 = 0.9802$) extracts. In general, samples plotted close to the linear (pH_{spec} vs. pH_{elec}) regression line although there is some deviation for some soils. Figure 3 shows the difference between spectrophotomet-

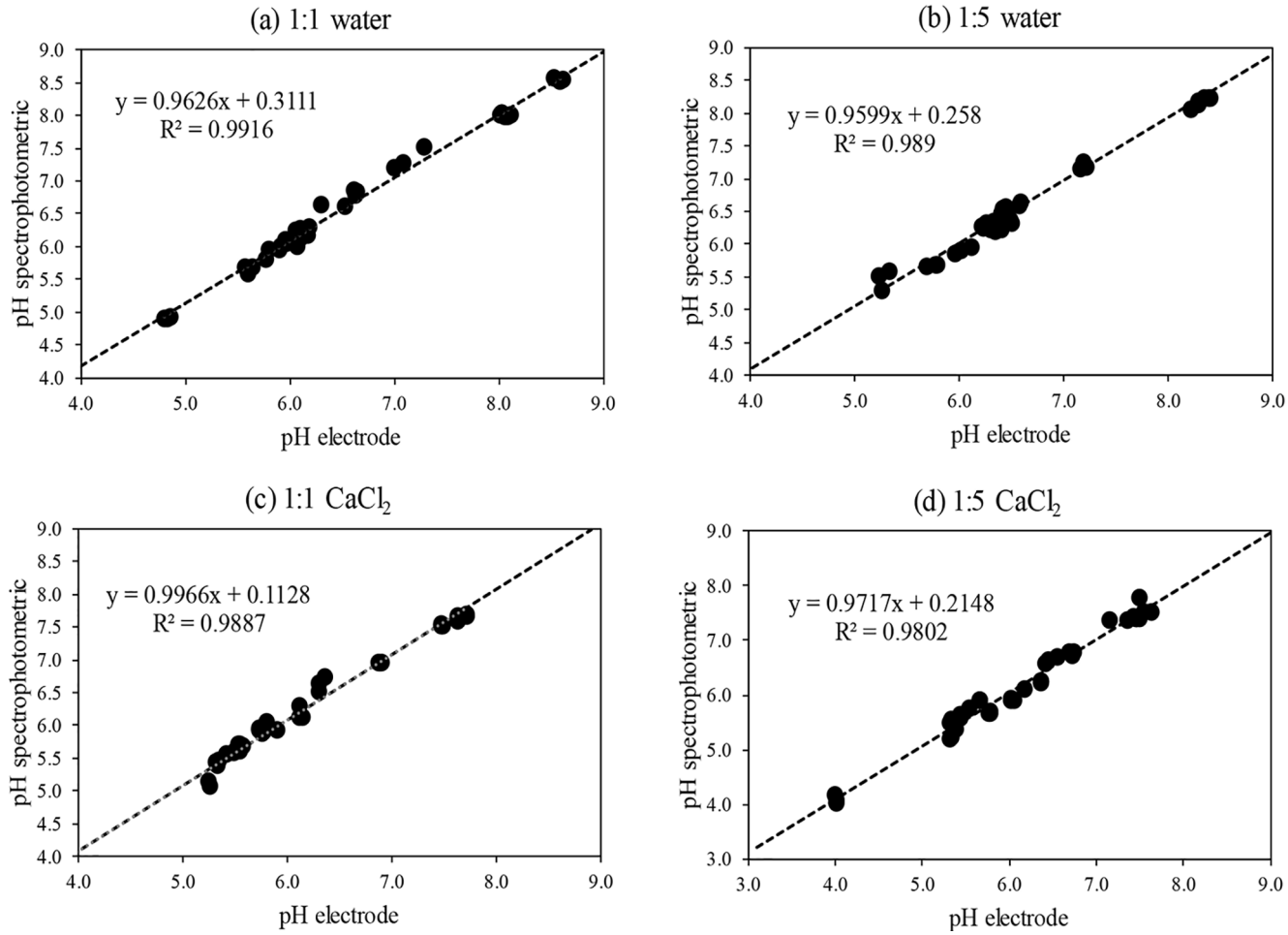

Fig. 2. Comparison of spectrophotometric and glass electrode pH measurements (calibrated with high ionic strength commercial buffer) for different soil extractant solutions: (a) 1:1 water, (b) 1:5 water, (c) 1:1 0.01 mol L^{-1} $CaCl_2$ and (d) 1:5 0.01 mol L^{-1} $CaCl_2$.

ric and electrode pH measurements calibrated with high ionic strength buffers is generally within ± 0.2 pH units.

Calibration of the pH electrode with different (low vs. high) ionic strength buffers gave different pH readings for the same soil extract (Fig. 3). The pH readings from the electrode calibrated with the low ionic strength buffer were generally lower (approximately 0.1–0.8 pH units) than the spectrophotometric pH readings respectively (Fig. 3). This was a much larger difference than the difference between pH values determined by spectrophotometric pH readings and pH readings with the electrode calibrated with high ionic strength buffers (Fig. 3). This is also reflected in a greater divergence (lower slope) from the linear regression line (Supplemental Fig. S1) compared with the high ionic strength buffer calibration results (Fig. 2).

Effect of Soil Extractant Solutions on pH in Individual Soils

Spectrophotometric and glass electrode mean pH values for all soils and every combination of soil/solution ratio and extractant are shown in Table 2. The standard deviation of triplicate pH measurements for individual soils and extractant ratios/solutions was generally small and similar for each measurement technique (approximately ±0.02 to 0.08 pH units, refer to Table 2). Similar patterns can be seen for most soil samples when comparing values determined for the four different extraction conditions. In general, pH was slightly lower for 1:1 water extracts than for 1:5 water extracts. Large differences (up to 1 pH unit) were observed between water and $CaCl_2$ extracts, with $CaCl_2$ generally decreasing the pH. The soil/solution ratio (1:1 vs. 1:5) had a much smaller effect on pH for $CaCl_2$ extracts than for water extracts.

For soils with a low EC (e.g., Mt Compass 0.16 mS cm^{-1}, Monarto 0.31 mS cm^{-1}; refer to Supplemental Table S1), the difference in pH between $CaCl_2$ and water extracts was relatively large, on the order of 0.2 to 1 pH units. On the other hand, for the Mobilong soils, which had high EC values of 8.2 to 68.3 (mS cm^{-1}) (Supplemental Table S1), the difference in pH between $CaCl_2$ and water extracts was smaller (0.0003 to 0.1 units) for both 1:1 and 1:5 extracts (Table 2).

Measuring in situ Soil pH with a Spectrophotometric Reflectance Probe

Absorbance spectra measured using a reflectance probe for two samples where dye solution was directly applied to the 1:1 soil/water mixture are shown in Fig. 4. The in situ soil pH determined using the reflectance probe was 7.71 and 5.85 for the Monarto and Tumby soils, respectively; there were differences

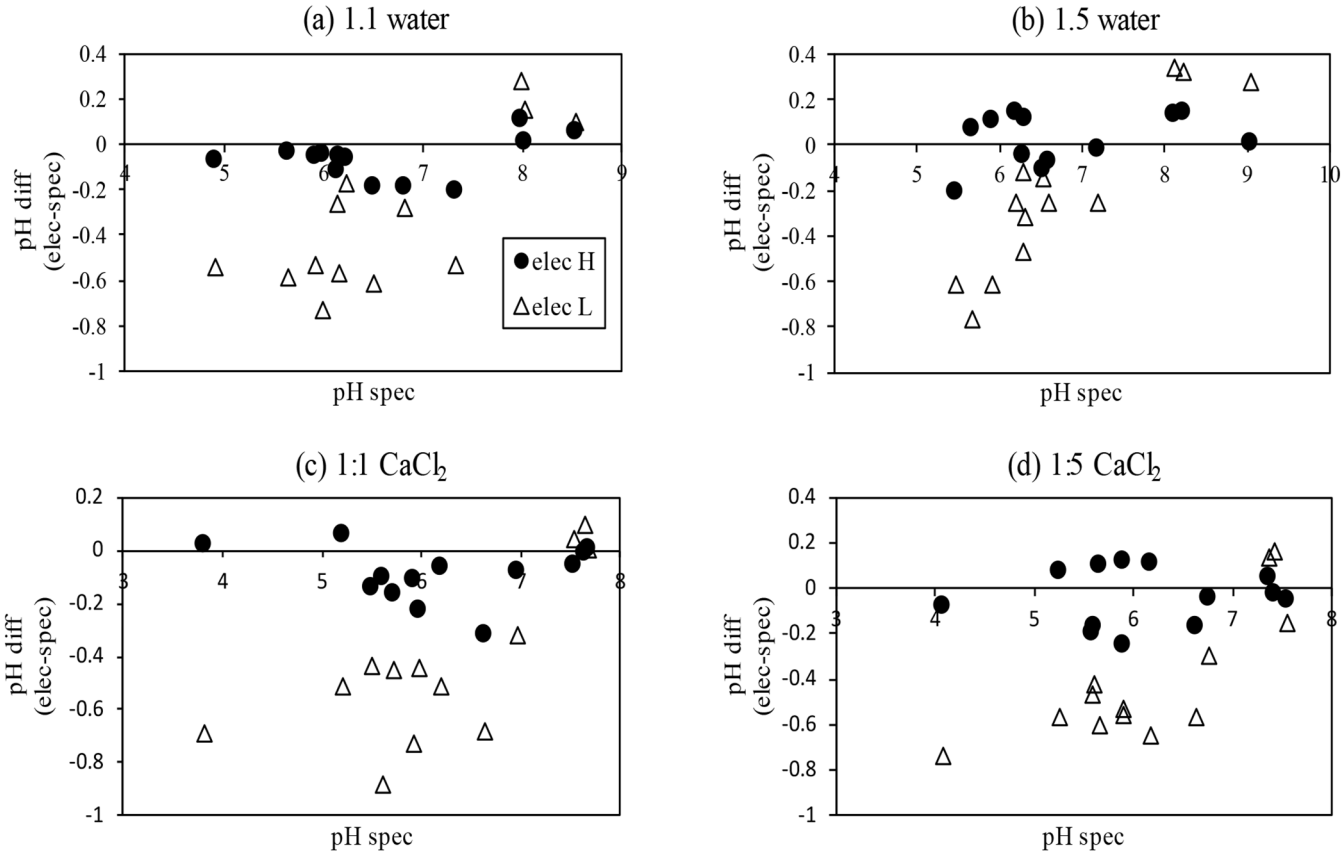

Fig. 3. pH difference between the spectrophotometric and glass electrode methods calibrated with buffer ≈ 0.1 mol L^{-1} (elec H) and with buffer ≈ 0.005 mol L^{-1} (elec L) versus spectrophotometric pH values for different soil/solutions: (a) 1:1 water, (b) 1:5 water, (c) 1:1 0.01 mol L^{-1} $CaCl_2$ and (d) 1:5 0.01 mol L^{-1} $CaCl_2$.

of 0.03 to 0.27 pH units compared to the pH measured on the centrifuged soil extract using the bench spectrophotometer (pH = 7.98 and 5.82 on the 1:1 soil/water extract, respectively). The reflectance spectra appear noisier at wavelengths <450 nm than the corresponding absorbance spectra of the centrifuged extracts (compare Fig. 4c-d with Fig. 4a-b, respectively). This noise is due to a higher and more variable background absorbance from the soil matrix, and, while this is corrected for by subtracting the reference spectrum (i.e., the reflectance spectrum of the corresponding 1:1 soil/water mixture without added dye) in the software, it introduced greater uncertainty in determining R values.

DISCUSSION

A novel spectrophotometric soil pH measurement method was developed in this study. The new method produced pH values that correlated strongly (r^2 > 0.95) with conventional soil pH measurements determined using a glass electrode in 1:1 and 1:5 soil/water and soil/$CaCl_2$ extracts. This indicates the spectrophotometric method is a viable alternative to the widely used electrode method, providing very similar results, and can be readily applied to a wide range of soils using conventional extraction procedures. The indicator dyes used (bromocresol purple and phenol red) provide the ability to measure soil pH in the range of 5 to 8.5, which is within the typical range of many soils. However, the method can be readily adapted for use with different indicator dyes to expand this pH range (e.g., bromocresol green for acidic soils, thymol blue for alkaline soils). Use of a mixture of dyes would also be worth testing. Indeed, the Raupach and Tucker (1959) color chart technique already uses a mixed indicator dye solution to provide a wider pH range and it would be useful to couple use of mixed dyes with the greatly improved precision that spectrophotometric measurement provides.

The average standard deviation of triplicate measurements using the spectrophotometric method was comparable to that for the electrode method (approximately ±0.08 pH units). This precision is less than has been achieved for spectrophotometric pH measurement in natural waters (<0.01 units; Clayton and Byrne, 1993; French et al., 2002; Mosley et al., 2004). We also undertook repeated measurements of a single soil extract split into five replicates which gave an improved precision of ±0.01 pH units. This indicates the lower precision of the spectrophotometric method in soils is due to additional processing steps required such as weighing out the soil, adding extractant solutions, shaking, centrifuging, storing of extracted samples and potential degassing of the CO_2 of the samples (Zabowski and Sletten, 1991).

The accuracy of the spectrophotometric method relative to the glass electrode method cannot be readily assessed as there is no independently measured and certified pH standard for soils. It would be useful to determine if the differences in pH between electrode and spectrophotometric methods are significant with respect to thermodynamic (equilibria) calculations (e.g., via simultaneous measurement of inorganic carbonate equilibria and

calculating pH). The relatively good comparison which was found in this study between electrode and spectrophotometric measurements may have been due in part to very careful measurement protocols (e.g., temperature control, electrodes with free flowing junctions designed for soil). Less care in making electrode measurements may produce higher discrepancies.

The spectrophotometric method has some potential advantages compared to soil electrode measurements. The spectrophotometric method does not require the addition of stabilizing electrolytes (although it has been demonstrated that it can also perform well in 0.01 mol L^{-1} $CaCl_2$ extracts). Hence spectrophotometric measurements may more closely estimate the true pH of the soil (rather than an arbitrary pH after addition of cations such as Ca^{2+}) across a wide range of soil salinities. The spectrophotometric pH measurements do not suffer from drift and/or errors associated with the "suspension effect" arising from glass electrodes being in contact with soil mixtures. Markedly different pH_{elec} readings (Fig. 3) were obtained in soils depending on the ionic strength of the buffer solution the electrode was calibrated in, and the low ionic strength buffer calibrated electrode measurements showed poorer agreement with the spectrophotometric pH. This variability suggests that liquid junction errors were likely occurring. This is consistent with the findings of other researchers (Bates and Popovych, 1981; Covington et al., 1983; Davison and Woof, 1985). Hence another key advantage of the spectrophotometric method is that it does not require calibration at different ionic strengths as the impact of the sample's ionic strength on the indicator dye dissociation constant can be corrected for by use of the Davies equation (Eq. [3], used at <0.5 mol L^{-1} ionic strength, EC of <40 mS cm^{-1}), while for the glass electrode method, calibration of the pH meter with the same ionic strength buffer as samples is necessary to achieve accurate measurements (Wiesner et al., 2006). Due to the difficulty and time consuming process of making different buffers to match soil solution composition, such calibrations are typically not performed in practice (Miller and Kissel, 2010). Hence the spectrophotometric method can be more readily applied to soils with a wide range of salinities.

The effect of different extraction conditions was also assessed for individual soils and the spectrophotometric pH results showed similar trends to the electrode method. The measured pH generally increased when the soil/water ratio was changed from 1:1 to 1:5. This appears to be due to dilution effects in agreement with the findings of Keaton (1938). In samples with low ionic strength, use of $CaCl_2$ as extractant caused a large decrease in soil pH which is also consistent with previous research that found a difference in pH values between water and $CaCl_2$ extracts of up to 1 pH unit (Miller and Kissel, 2010; Rayment and Lyons, 2011). However, for soils with high ionic strength (e.g., those from Mobilong), pH values determined on $CaCl_2$ extracts were quite close to those of water extracts. This is in agreement with the results of Kissel et al. (2009) who reported a difference of less than 0.2 pH units for soils with high ionic strength. The small differences observed for high ionic

Table 2. Mean and standard deviation (SD) of pH measured with glass electrode ($pH_{elec\ H, L}$, at high and low ionic strength buffer) and with spectrophotometry (pH_{spec}).

	1:1 water			1:5 water			1:1 $CaCl_2$			1:5 $CaCl_2$		
Soil	pH_{elec} H ± SD	pH_{elec} L	pH_{spec}	pH_{elec} H ± SD	pH_{elec} L	pH_{spec}	pH_{elec} H ± SD	pH_{elec} L	pH_{spec}	pH_{elec} H ± SD	pH_{elec} L	pH_{spec}
Arboretum	6.16 ± 0.05	6.05 ± 0.04	6.22 ± 0.07	6.42 ± 0.02	6.38 ± 0.03	6.53 ± 0.05	5.55 ± 0.02	5.26 ± 0.02	5.72 ± 0.01	5.44 ± 0.01	5.18 ± 0.00	5.60 ± 0.02
Monarto	8.03 ± 0.01	8.18 ± 0.01	8.02 ± 0.01	8.37 ± 0.03	8.55 ± 0.08	8.23 ± 0.00	7.48 ± 0.01	7.58 ± 0.01	7.54 ± 0.01	7.43 ± 0.06	7.52 ± 0.07	7.38 ± 0.03
Lock Siliceous	8.09 ± 0.03	8.26 ± 0.02	7.98 ± 0.01	8.26 ± 0.04	8.46 ± 0.13	8.13 ± 0.06	7.63 ± 0.01	7.74 ± 0.00	7.64 ± 0.03	7.40 ± 0.21	7.59 ± 0.03	7.43 ± 0.08
Karoonda	6.02 ± 0.05	5.88 ± 0.07	6.14 ± 0.08	6.25 ± 0.02	6.18 ± 0.03	6.30 ± 0.02	5.36 ± 0.05	5.06 ± 0.03	5.5 ± 0.07	5.40 ± 0.12	5.13 ± 0.14	5.59 ± 0.15
Ngarkat	6.64 ± 0.01	6.54 ± 0.01	6.82 ± 0.03	6.52 ± 0.09	6.35 ± 0.16	6.60 ± 0.05	5.75 ± 0.04	5.54 ± 0.06	5.98 ± 0.06	5.66 ± 0.01	5.38 ± 0.01	5.91 ± 0.00
Lock Horizon B	8.58 ± 0.04	8.63 ± 0.11	8.53 ± 0.02	9.06 ± 0.03	9.33 ± 0.04	9.06 ± 0.07	7.68 ± 0.05	7.67 ± 0.05	7.67 ± 0.03	7.52 ± 0.10	7.41 ± 0.16	7.57 ± 0.17
Mt Compass	4.83 ± 0.03	4.37 ± 0.04	4.91 ± 0.01	5.27 ± 0.05	4.86 ± 0.03	5.47 ± 0.15	3.84 ± 0.01	3.13 ± 0.02	3.82 ± 0.10	4.01 ± 0.02	3.35 ± 0.04	4.09 ± 0.07
Modra	7.13 ± 0.15	6.80 ± 0.17	7.33 ± 0.16	7.18 ± 0.03	6.94 ± 0.04	7.20 ± 0.05	6.89 ± 0.01	6.65 ± 0.02	6.97 ± 0.00	6.72 ± 0.03	6.47 ± 0.06	6.76 ± 0.03
Tumby	5.78 ± 0.08	5.39 ± 0.12	5.92 ± 0.11	6.26 ± 0.06	5.83 ± 0.04	6.30 ± 0.05	5.28 ± 0.05	4.70 ± 0.01	5.21 ± 0.17	5.34 ± 0.03	4.70 ± 0.01	5.27 ± 0.10
Mobilong (5–10 cm)	6.32 ± 0.21	5.89 ± 0.24	6.50 ± 0.21	6.43 ± 0.11	6.00 ± 0.15	6.32 ± 0.07	6.32 ± 0.03	5.96 ± 0.03	6.63 ± 0.10	6.47 ± 0.07	6.07 ± 0.11	6.64 ± 0.05
Mobilong (10–20 cm)	6.10 ± 0.01	5.58 ± 0.04	6.15 ± 0.04	6.36 ± 0.03	5.95 ± 0.02	6.21 ± 0.02	6.12 ± 0.02	5.67 ± 0.02	6.19 ± 0.10	6.29 ± 0.11	5.54 ± 0.14	6.19 ± 0.08
Mobilong (20–35 cm)	5.96 ± 0.13	5.27 ± 0.09	6.00 ± 0.06	6.02 ± 0.08	5.3 ± 0.14	5.91 ± 0.05	5.81 ± 0.08	5.19 ± 0.10	5.92 ± 0.02	6.03 ± 0.02	5.36 ± 0.03	5.91 ± 0.02
Mobilong (35–55 cm)	5.61 ± 0.03	5.06 ± 0.12	5.64 ± 0.05	5.75 ± 0.05	4.91 ± 0.10	5.68 ± 0.02	5.51 ± 0.03	4.73 ± 0.02	5.62 ± 0.01	5.77 ± 0.01	5.07 ± 0.06	5.67 ± 0.01
Average SD	0.06	0.08	0.06	0.05	0.08	0.05	0.03	0.03	0.06	0.06	0.07	0.06

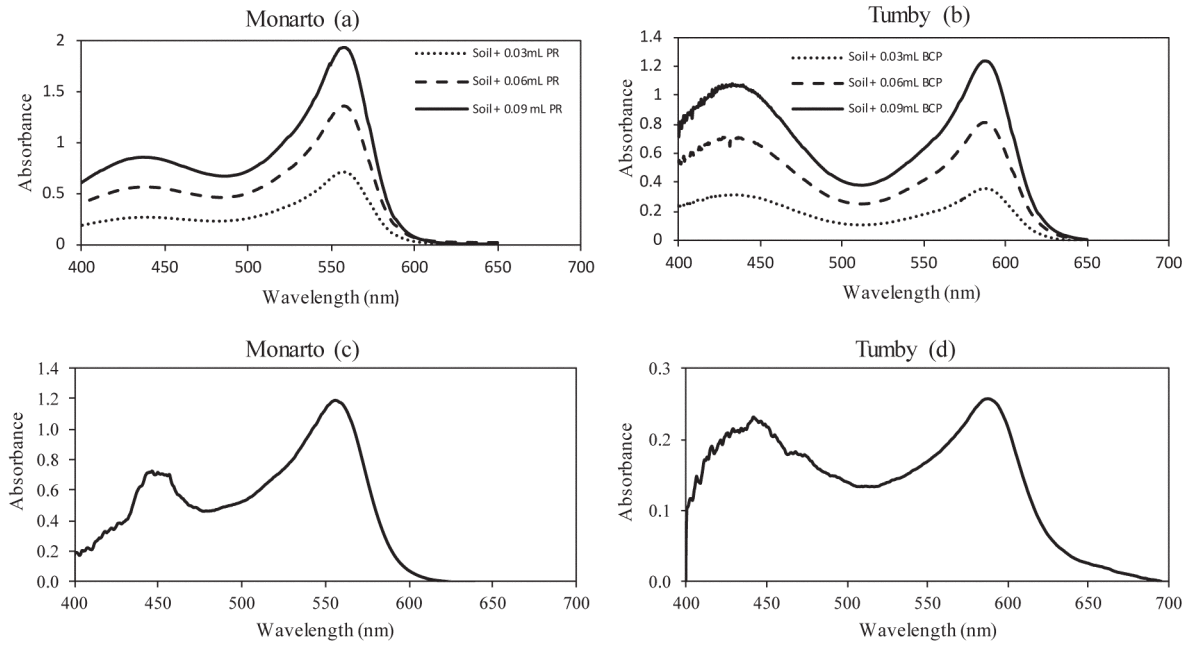

Fig. 4. Absorbance spectra of phenol red (PR) and bromocresol purple (BCP) indicator dyes for Monarto and Tumby Bay samples using the conventional spectrophotometer (a-b) on soil extracts (three dye additions shown) and reflectance probe (c-d) in situ on the soil paste.

strength soils reflects the fact that the addition of $CaCl_2$ electrolyte has much less of an effect on cation exchange and other reactions in saline soils.

The laboratory-based spectrophotometric soil pH method outlined is not readily applicable to in situ field application as shakers, centrifuges and bench spectrophotometers are required. However, the reflectance probe has shown that there is potential for the spectrophotometric method to be adapted for use in in situ applications. Further research is required to refine this reflectance approach and apply it to soils in the field.

CONCLUSIONS

A novel method for pH measurement in soils was developed using precise spectrophotometric measurement of the acid and base forms of indicator dyes added to soil extracts. The pH measured spectrophotometrically on a range of different soils and extraction conditions (1:1 and 1:5 soil/water and soil/0.01 mol L^{-1} $CaCl_2$) compared well to pH measurements using glass electrodes. The indicators dyes (phenol red and bromocresol purple) used in this study enable measurement in the pH range of most soils (pH 5–8.5) but other dyes are available to expand this range to more acidic or alkaline soils. The application of the spectrophotometric pH method to soils appears, however, to provide many potential benefits over electrode methods (e.g., readily applicable to wide range of soil salinities, no need to extract soils in stabilizing electrolytes which alter the pH, no drift or suspension effect). Therefore, this method could help improve prediction of other pH-dependent processes (e.g., metal binding, Sauvé et al., 2000). Further testing of the method and comparison to other soil chemical properties and processes is recommended.

SUPPLEMENTAL MATERIAL

The Supplemental Material contains a complete description of the spectrophotometric pH equations, along with one supplementary table and one supplementary figure as detailed below. Table S1: The mean values of electrical conductivity (EC) and absorbance ratio (*R*). Figure S1: Comparison of spectrophotometric and glass electrode pH measurements (low ionic strength buffer) for different soil extractant solutions.

ACKNOWLEDGMENTS

We would like to acknowledge Colin Rivers who provided some of the soils used in this study and Dr. Cameron Grant who assisted with soil texture measurements. We are also grateful for the very constructive comments of two anonymous reviewers which helped us to improve the draft manuscript.

REFERENCES

Bates, R.G., and S. Acree. 1945. pH of aqueous mixtures of potassium dihydrogen phosphate and disodium hydrogen phosphate at 0 to 60 C. J. Res. Natl. Bur. Stand. 34:373–394. doi:10.6028/jres.034.020

Bates, R.G., and O. Popovych. 1981. The modern meaning of pH. Crit. Rev. Anal. Chem. 10:247–278. doi:10.1080/10408348108085499

Bond-Lamberty, B., and A. Thomson. 2010. Temperature-associated increases in the global soil respiration record. doi:10.1038/nature08930

Clayton, T.D., and R.H. Byrne. 1993. Spectrophotometric seawater pH measurements: Total hydrogen ion concentration scale calibration of m-cresol purple and at-sea results. Deep Sea Res. Part I, Oceanogr. Res. Pap. 40:2115–2129. doi:10.1016/0967-0637(93)90048-8

Conyers, M., and B. Davey. 1988. Observations on some routine methods for soil pH determination. Soil Sci. 145:29–36. doi:10.1097/00010694-198801000-00004

Covington, A.K., P.D. Whalley, and W. Davison. 1983. Procedures for the measurement of pH in low ionic strength solutions including freshwater. Analyst (Lond.) 108:1528–1532. doi:10.1039/an9830801528

Davison, W., and C. Woof. 1985. Performance tests for the measurement of pH with glass electrodes in low ionic strength solutions including natural waters. Anal. Chem. 57:2567–2570. doi:10.1021/ac00290a031

Essington, M.E. 2015. Soil and water chemistry: An integrative approach. 2nd ed. CRC Press, New York.

French, C.R., J.J. Carr, E.M. Dougherty, L.A. Eidson, J.C. Reynolds, and M.D. DeGrandpre. 2002. Spectrophotometric pH measurements of freshwater.

Anal. Chim. Acta 453:13–20. doi:10.1016/S0003-2670(01)01509-4
Heintze, S.G. 1934. The use of the glass electrode in soil reaction and oxidation-reduction potential measurements. J. Agric. Sci. 24:28–41. doi:10.1017/S0021859600012429
Gillman, G.P., and L.C. Bell. 1978. Soil Solution Studies on Weathered Soils from tropical North Queensland. Aust. J. Soil Res. 16:67–77. doi:10.1071/SR9780067
Griffin, B., and J.J. Jurinak. 1973. Estimation of activity coefficients from the electrical conductivity of natural aquatic systems and soil extracts. Soil Sci. 116:26–30. doi:10.1097/00010694-197307000-00005
Keaton, C.M.A. 1938. Theory explaining the relation of soil-water ratios to pH values. Soil Sci. 46:259–266. doi:10.1097/00010694-193809000-00006
Kissel, D.E., L. Sonon, P.F. Vendrell, and R.A. Isaac. 2009. Salt concentration and measurement of soil pH. Commun. Soil Sci. Plant Anal. 40:179–187. doi:10.1080/00103620802625377
Lai, C.Z., M.D. DeGrandpre, B.D. Wasser, T.A. Brandon, D.S. Clucas, E.J. Jaqueth, Z.D. Benson, C.M. Beatty, and R.S. Spaulding. 2016. Spectrophotometric measurement of freshwater pH with purified meta-cresol purple and phenol red. Limnol. Oceanogr. Methods 14:864–873. doi:10.1002/lom3.10137
Manov, G.G., N.J. DeLollis, and S.F. Acree. 1944. Liquid junction potentials, and relative activity coefficients of chloride ions, in concentrated mixed chlorides and nitrates at 25°C. J. Res. Natl. Bur. Stand. 33:273–285. doi:10.6028/jres.033.012
Miller, R.O., and D.E. Kissel. 2010. Comparison of soil pH methods on soils of North America. Soil Sci. Soc. Am. J. 74:310–316. doi:10.2136/sssaj2008.0047
Millero, F.J. 1986. The pH of estuarine waters. Limnol. Oceanogr. 31:839–847. doi:10.4319/lo.1986.31.4.0839
Mosley, L.M., S.L. Husheer, and K.A. Hunter. 2004. Spectrophotometric pH measurement in estuaries using thymol blue and m-cresol purple. Mar. Chem. 91:175–186. doi:10.1016/j.marchem.2004.06.008
Raupach, M., and B. Tucker. 1959. The field determination of soil reaction. J. Aust. Inst. Agric. Sci. 25:129–133.
Rayment, G.E., and D.J. Lyons. 2011. Soil chemical methods. CSIRO publishing, Melbourne, Victoria, Australia.
Robert-Baldo, G.L., M.J. Morris, and R.H. Byrne. 1985. Spectrophotometric determination of seawater pH using phenol red. Anal. Chem. 57:2564–2567. doi:10.1021/ac00290a030
Sauvé, S., W. Hendershot, and H.E. Allen. 2000. Solid-solution partitioning of metals in contaminated soils. Environ. Sci. Technol. 34:1125–1131. doi:10.1021/es9907764
Skoog, D.A., F.J. Holler, and S.R. Crouch. 2007. Principles of instrumental analysis. Cengage Learning, Inc., Belmont, CA.
Snyder, E.F. 1935. Methods for determining the hydrogen ion concentration of soils. USDA Circular No. 56. US Department of Agriculture Washington, DC.
Stumm, W., and J. Morgan. 1996. Aquatic chemistry: Chemical equilibria and rates in natural waters. 3rd ed. Wiley Interscience, New York.
Suarez, D.L. 1977. Ion activity products of calcium carbonate in waters below the root zone. Soil Sci. Soc. Am. J. 41:310–315. doi:10.2136/sssaj1977.03615995004100020027x
Wiesner, A.D., L.E. Katz, and C.C. Chen. 2006. The impact of ionic strength and background electrolyte on pH measurements in metal ion adsorption experiments. J. Colloid Interface Sci. 301:329–332. doi:10.1016/j.jcis.2006.05.011
Yao, W., and R.H. Byrne. 2001. Spectrophotometric determination of freshwater pH using bromocresol purple and phenol red. Environ. Sci. Technol. 35:1197–1201. doi:10.1021/es001573e
Yuan, S., and M.D. DeGrandpre. 2008. Evaluation of indicator-based pH measurements for freshwater over a wide range of buffer intensities. Environ. Sci. Technol. 42:6092–6099. doi:10.1021/es800829x
Zabowski, D., and R.S. Sletten. 1991. Carbon dioxide degassing effects on the pH of spodosol soil solutions. Soil Sci. Soc. Am. J. 55:1456–1461. doi:10.2136/sssaj1991.03615995005500050043x

Supplemental Material for: Development of a spectrophotometric pH method for soils and comparison with glass electrode measurements

Sima Bargrizan[a]*, Ronald J. Smernik*[a]*, and Luke M. Mosley*[b]

[a] The School of Agriculture, Food and Wine, The University of Adelaide, South Australia

[b] Acid Sulfate Soils Centre, School of Biological Sciences, The University of Adelaide, South Australia

Summary of the supplemental material:

1 justification of the spectrophotometric pH equations

1 table

1 figure

Theory and derivation of equations that underpin the spectrophotometric pH measurement method

Sulfonephthalein indicator dyes can exist in three forms H_2I, HI^-, and I^{2-}, each of which has distinctive light absorption characteristics. The chemical equilibria among these three forms is dependent on pH and can be described by the first and second dissociation constants of the fully protonated (H_2I) dye species:

$$H_2I \rightleftharpoons HI^- + H^+ \qquad K_1 = [HI^-]\,[H^+] / [H_2I] \qquad [1a]$$

$$HI^- \rightleftharpoons I^{2-} + H^+ \qquad K_2 = [I^{2-}]\,[H^+] / [HI^-] \qquad [1b]$$

The total indicator concentration ($I_T = H_2I + HI^- + I^{2-}$) can be expressed in terms of [HI], K_1, K_2, and proton concentration by:

$$I_T = [HI^-]\,([H^+]/K_1 + 1 + K_2 / [H^+]) \qquad [2]$$

Using the Beer-Lambert law as the basis, the absorbance of an indicator dye in solution can be expressed by:

$$_\lambda A = l\,(_\lambda\varepsilon_{H2I}\,[H_2I] + {}_\lambda\varepsilon_{HI}\,[HI^-] + {}_\lambda\varepsilon_I\,[I^{2-}]) \qquad [3]$$

where $_\lambda A$ is the absorbance at wavelength λ, $_\lambda\varepsilon_x$ is the molar absorptivity of each individual dye species (x = I^{2-} or HI^- or H_2I), and l is the optical (spectrophotometer cell) path length. As per equation (2), equation (3) can be expressed in terms of the species HI by:

$$_\lambda A / l = [HI^-]\,(_\lambda\varepsilon H_2I\,[H^+]/K_1 + {}_\lambda\varepsilon HI + {}_\lambda\varepsilon I\,K_2\,/[H^+]) \qquad [4]$$

Dividing equation (4) by equation (2) yields:

$$\frac{_\lambda A}{I_T\,l} = \frac{_\lambda\varepsilon_{H2I}\,[H^+]/K_1 + {}_\lambda\varepsilon_{HI} + {}_\lambda\varepsilon_I\,K_2/[H^+]}{[H^+]/K_1 + 1 + K_2/[H^+]} \qquad [5]$$

Except at low pH the H_2I concentration is insignificant, hence ignoring the first dissociation reaction, equation (5) can be reduced to:

$$\frac{_\lambda A}{I_T\,l} = \frac{_\lambda\varepsilon_{HI} + {}_\lambda\varepsilon_I\,K_2/[H^+]}{1 + K_2/[H^+]} \qquad [6]$$

Using equation (6) and specifying R as the ratio of indicator absorbances at λ_2 and λ_1 (i.e. R = $_2A/_1A$) we can derive:

$$R = \frac{{}_2\varepsilon_{HI} + {}_2\varepsilon_I K_2/[H^+]}{{}_1\varepsilon_{HI} + {}_1\varepsilon_I K_2/[H^+]} \quad [7]$$

Dividing each term in the numerator and denominator by ${}_1\varepsilon_{HI}$,

$$R = \frac{{}_2\varepsilon_{HI}/{}_1\varepsilon_{HI} + {}_2\varepsilon_I K_2/{}_1\varepsilon_{HI}[H^+]}{{}_1\varepsilon_{HI}/{}_1\varepsilon_{HI} + {}_1\varepsilon_I K_2/{}_1\varepsilon_{HI}[H^+]} = \frac{e_1 + e_2 K_2/[H^+]}{1 + e_3 K_2/[H^+]} \quad [8a]$$

Where $e_1 = {}_2\varepsilon HI/{}_1\varepsilon HI$, $e_2 = {}_2\varepsilon I/{}_1\varepsilon HI$, $e_3 = {}_1\varepsilon I/{}_1\varepsilon HI$, and then multiplying each term in the numerator and denominator by H^+,

$$R = \frac{e_1[H^+] + e_2 K_2}{[H^+] + e_3 K_2} \quad [8b]$$

clearing the fraction,

$$R[H^+] + Re_3K_2 = e_1[H^+] + e_2K_2 \quad [8c]$$

rearranging the $e_1[H^+]$ and Re_3K_2 terms,

$$e_2K_2 - Re_3K_2 = R[H^+] - e_1[H^+] \quad [8d]$$

factoring both sides of the equation,

$$K_2(e_2 - Re_3) = [H^+](R - e_1) \quad [8e]$$

rearranging terms,

$$\frac{K_2}{[H^+]} = \frac{(R - e_1)}{(e_2 - Re_3)} \quad [8f]$$

and taking logs,

$$\log K_2 - \log [H^+] = \log \frac{(R - e_1)}{(e_2 - Re_3)} \quad [8g]$$

leads to the final equation for pH as a function of the 2nd dissociation constant ($pK_2 = -\log K_2$) of an indicator dye, the ratio of the absorbance of base and acid forms of the dye in solution (R, measured at the wavelength of maximum absorbance for each form), and the molar absorptivity ratios (e_1-e_3) for the dye as defined above:

$$pH = -\log [H^+] = pK_2 + \log \frac{(R - e_1)}{(e_2 - Re_3)} \quad [9]$$

Which is equivalent to the well known Henderson–Hasselbalch equation:

$$pH = -\log [H^+] = pK_2 + \log \frac{[I^{2-}]}{[HI^-]} \quad [10]$$

Equations (9) and (10) are only valid for ideal solutions when the dye and background electrolyte concentration approaches infinite dilution. For non-ideal solutions (i.e. as in natural water and soil solutions) such equations must be modified to account for the effect of ionic strength on ion activity. Ion activity (a_i) is related to concentration by:

$$a_i = c_i \gamma_i \quad [11]$$

Where c_i is the molar concentration of the solution species i and γ_i is the activity coefficient for this species. Individual ion activity coefficients (γ) can be estimated using the Davies equation:[1]

$$\log \gamma = -Az^2 \left(\frac{\mu^{1/2}}{1+\mu^{1/2}} - 0.3\mu\right) \quad [12]$$

Where A is the ion size parameter[2], z is the charge on the ion, and μ is ionic strength. The Davies equation is considered reliable at ionic strengths <0.5 M[1].

Therefore for the application of this equation to the 2nd dissociation constant of a sulfonephthalein indicator dye, the individual ion activity coefficient terms (γ_{I2-}, γ_{H+}, γ_{HI-}) are included for the dye dissociation:

$$pH = -\log [H^+] \gamma_{H+} = pK_{2+} \log [I^{2-}] \gamma_{I2-} / [HI^-] \gamma_{HI-} \quad [13a]$$

$$pH = pK_2 + \log [I^{2-}]/[HI^-] + \log (\gamma_{I2-} \gamma_{H+} / \gamma_{HI-}) \quad [13b]$$

While each individual ion activity coefficient could be calculated separately using the Davies equation (12), the charge (z^2) terms for calculation of the individual ion activity coefficients of the

[1] Stumm, W., and J. Morgan. 1996. Aquatic chemistry: chemical equilibria and rates in natural waters. 3rd ed. Wiley Interscience, New York, p. 1022.

[2] $A = 0.5092 + (T - 298.15) * 8.5 * 10^{-4}$ where T is temperature in Kelvin.

dye can be combined (as other parameters in the Davies equation are constant for a given solution) to calculate an overall mixed z^2 value ($z_{\pm}^2$) such that:

$$z_{\pm}^2 = \frac{z_{I2-}^2 z_{H+}^2}{z_{HI-}^2} = \frac{-2^2 \times 1^2}{-1^2} = 4 \quad [14]$$

By combining equation (9) with the Davies equation (12) to account for how the I^{2-}, HI^-, and H^+ activity coefficients change with ionic strength, and using z^2 =4 in the Davies equation, pH can now be calculated for a solution with indicator dye added via:

$$\mathrm{pH} = -\log[\mathrm{H}^+] = \mathrm{pK}_2 + \log\frac{(\mathrm{R}-e_1)}{(e_2 - Re_3)} - 4A\left(\frac{\mu^{1/2}}{1+\mu^{1/2}} - 0.3\mu\right) \quad [15]$$

Supplemental Table S1. The mean values of electrical conductivity (EC) and absorbance ratio at zero dye addition (R).

Soil (cm)	**1:1 water**		**1:5 water**		**1:1 CaCl2**		**1:5 CaCl2**	
	EC mS/cm Mean	**R**	**EC mS/cm Mean**	**R**	**EC mS/cm Mean**	**R**	**EC mS/cm Mean**	**R**
Arboretum	0.403	0.06	0.32	0.11	2.63	0.89	2.39	0.66
Lock Siliceous	0.36	2.88	0.21	3.63	2.65	2.08	2.41	1.26
Karoonda	0.37	0.05	0.17	0.06	2.5	0.55	2.32	0.66
Ngarkat	0.27	0.22	0.75	0.15	2.34	1.68	2.4	1.34
Lock Horizon B	0.83	8.67	0.39	15.32	2.49	2.12	3.26	1.5
Mt Compass	0.16	0.094	1.13	0.47	2.52	0.016	2.37	0.03
Monarto	0.31	3.07	0.14	4.32	2.57	1.6	2.43	1.13
Modra	1.86	0.94	1.56	0.66	3.69	0.5	3.09	0.3
Tumby	2.05	1.31	0.59	2.19	3.12	0.32	2.38	0.33
Mobilong (5-10)	52	5.66	12.92	5.63	68.27	10.61	14.66	11.65
Mobilong (10-20)	33.38	4.32	8.22	3.98	44.53	4.70	10.46	4.04
Mobilong (20-35)	16.28	2.93	11.02	2.19	45.23	2.5	12.39	2.24
Mobilong (35-55)	37.33	1.33	12.81	1.32	63.03	1.12	13.59	1.33

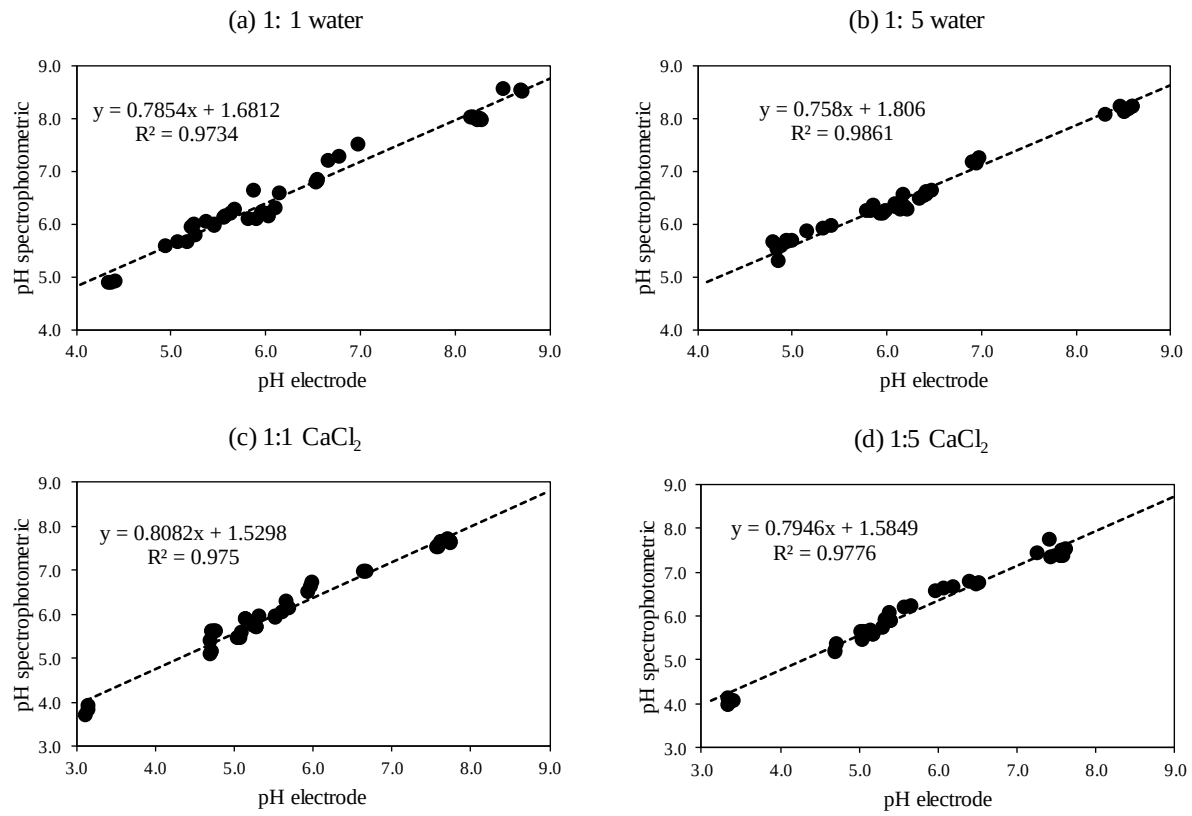

Supplemental Figure S1. Comparison of spectrophotometric and glass electrode pH measurements (low ionic strength phosphate buffer ≈ 0.005 M) for different soil extractant solutions: (a) 1:1 water, (b) 1:5 water, (c) 1:1 0.01 M $CaCl_2$ and (d) 1:5 0.01 M $CaCl_2$.

CHAPTER 3

The application of a spectrophotometric method to determine pH in acidic (pH < 5) soils

Sima Bargrizan[a], Ronald J. Smernik[a], Rob Fitzpatrick[b], and Luke M. Mosley[b]

[a] The School of Agriculture, Food and Wine, The University of Adelaide, South Australia

[b] Acid Sulfate Soils Centre, School of Biological Sciences, The University of Adelaide, South Australia

Bargrizan S, Smernik RJ, Fitzpatrick RW, Mosley LM (2018). The application of a spectrophotometric method to determine pH in acidic (pH < 5) soils. *Talanta* **186**, 421-426.

Statement of Authorship

Title of Paper	The application of a spectrophotometric method to determine pH in acidic (pH < 5) soils.
Publication Status	☑ Published ☐ Accepted for Publication ☐ Submitted for Publication ☐ Unpublished and Unsubmitted w ork w ritten in manuscript style
Publication Details	2018, Talanta, **186,** 421-426.

Principal Author

Name of Principal Author (Candidate)	Sima Bargrizan		
Contribution to the Paper	Accomplished experiment, data collection, data analysis and interpretation, wrote manuscript.		
Overall percentage (%)	70%		
Certification:	This paper reports on original research I conducted during the period of my Higher Degree by Research candidature and is not subject to any obligations or contractual agreements with a third party that would constrain its inclusion in this thesis. I am the primary author of this paper.		
Signature		Date	21.01.2019

Co-Author Contributions

By signing the Statement of Authorship, each author certifies that:

i. the candidate's stated contribution to the publication is accurate (as detailed above);

ii. permission is granted for the candidate in include the publication in the thesis; and

iii. the sum of all co-author contributions is equal to 100% less the candidate's stated contribution.

Name of Co-Author	Luke Mosley		
Contribution to the Paper	Supervised development of work, data interpretation and manuscript evaluation and correction, and acted as corresponding author.		
Signature		Date	21.01.2019

Name of Co-Author	Ron Smernik		
Contribution to the Paper	Supervised development of work, data interpretation, manuscript evaluation and correction.		
Signature		Date	21.01.2019

Please cut an

Name of Co-Author	Rob Fitzpatrick		
Contribution to the Paper	Supervised soil material collection, manuscript evaluation and correction.		
Signature		Date	21.01.2019

d paste additional co-author panels here as required.

Talanta 186 (2018) 421–426

Contents lists available at ScienceDirect

Talanta

journal homepage: www.elsevier.com/locate/talanta

The application of a spectrophotometric method to determine pH in acidic (pH < 5) soils

Sima Bargrizan[a], Ronald J. Smernik[a], Rob W. Fitzpatrick[b], Luke M. Mosley[b,*]

[a] The School of Agriculture, Food and Wine, The University of Adelaide, South Australia, Australia
[b] Acid Sulfate Soils Centre, School of Biological Sciences, The University of Adelaide, South Australia, Australia

ARTICLE INFO

Keywords:
Soil pH
Acid sulfate soils
Indicator dye
Bromocresol green

ABSTRACT

pH is a "master variable" controlling many biogeochemical processes in soils. Acid sulfate soils undergo rapid and large pH changes from circumneutral pH under anaerobic soil conditions to sulfuric soils with ultra (pH < 3.5) and extremely (pH 3.5–4.4) acidic properties following oxidation. Measuring soil pH using a glass electrode has several potential drawbacks including liquid junction errors, drift, suspension effects and clogging. Spectrophotometric pH measurement, involving addition of an indicator dye to the sample, is widely used in seawater and has recently been developed for soil extracts at circumneutral pH ranges. The aim of this study was to extend the spectrophotometric method for application in ultra and extremely acidic soils. The acid dissociation constant (pK_a = 5.02) and molar absorptivities of the indicator dye bromocresol green were determined and shown to enable spectrophotometric pH measurement between pH 3 − 5.3. To demonstrate the performance and application of the method, pH and metal availability (Fe, Al, Zn) were measured during the incubation of two acid sulfate soils, which both classified as hypersulfidic soils (pH > 4) and transformed to sulfuric soils (pH < 4) after incubation for 12 weeks. The method compared well (r^2 > 0.99) to glass electrode measurements under acidic conditions with high metal availability. The method has potential to improve understanding of biogeochemical processes in ultra and extremely acidic soils.

1. Introduction

Soil chemical reactions can result in the exchange or generation of protons. Therefore, soil pH is regarded as a key chemical variable [1]. For example, metal activity typically increases with decreasing pH in soils due to: (1) desorption of metals from surface binding sites due to increased protonation and (2) dissolution of mineral phases [2–5]. As pH is a log scale, even a +/−0.1 pH unit measurement error could have a substantive effect on the accuracy of prediction of metal speciation and partitioning in soils. For example, Sauvé et al. [6] reported that the partition coefficient, K_d (i.e. the ratio of sorbed metal concentration to the dissolved metal concentration) for Zn is best described by the relationship ($\log_{10} K_d^{Zn2+}$ = 0.62 pH − 0.97); the logarithmic nature of the relationship results in large changes in K_d around a pH of 6 (K_d = 562 at pH 6, 488 at pH 5.9 and 648 at pH 6.1). Soil pH has also been widely used as a key parameter in classifying soils (e.g. Isbell and National Committee on Soils and Terrain [7] and Soil Survey Staff [8]).

The most common method for measuring soil pH uses a glass electrode but such measurements have been recognized to have several potential problems such as inherent drift [9], liquid junction potential errors on the order of 0.1 pH units [10], clogging of the porous fibre of electrodes [11], and a suspension effect in which the function of the electrode is affected by soil cation exchange capacity [1]. Moreover, the need for calibration buffers makes accurate pH measurement quite difficult to perform for soils with varying salinity, as for accurate measurement the calibration buffer must have the same ionic strength and composition as the sample solution [12].

Spectrophotometric pH measurement methods using indicator dyes represent an alternative to the glass electrode method for pH measurement and eliminate the problems mentioned above [13]. The capability and accuracy (> 0.01 pH units) of this method emerges from swift indicator equilibrium as well as consistently measured absorbance of indicator species [13–15]. Prior to our recent study [16], which established the application of spectrophotometric pH measurement method for soils in the pH range 5 − 8.5, this method had been used most widely for estuarine and marine applications at pH 7 − 8 [13,17–19].

It would be useful to extend the application of spectrophotometric methods to pH < 5 for assessing acidification of soils that are ultra (< 3.5), extremely (3.5–4.4) and very strongly (4.5–5.0) acidic (Soil

* Correspondence to: Waite Campus, University of Adelaide, PMB 1 Glen Osmond, SA 5064, Australia.
E-mail address: luke.mosley@adelaide.edu.au (L.M. Mosley).

https://doi.org/10.1016/j.talanta.2018.04.074
Received 29 January 2018; Received in revised form 23 April 2018; Accepted 23 April 2018
Available online 24 April 2018
0039-9140/ © 2018 Elsevier B.V. All rights reserved.

Survey Staff, [8]). Bromocresol green (BCG) is a potentially suitable indicator dye for use with acid soil extracts, and has been used for determining seawater alkalinity titration endpoints within the range of pH 3.4–4.6 [20–22]. However, very limited information is available on the dissociation constant and molar absorptivities of BCG at lower ionic strength; these are critical parameters required for spectrophotometric pH measurement in soils. Further, the influence of high metal availability (e.g. Al^{3+}) under acidic conditions on dye properties needs assessment.

Acid sulfate soils provide an ideal case for testing and developing pH methods as they undergo large pH changes during oxidation. Acid sulfate soils (ASS) are those soils in which sulfuric acid (H_2SO_4) may be produced, is being produced, or has been produced in amounts that have a lasting effect on the main soil characteristics [23]. The production of acidity is caused by the oxidation of pyrite (FeS_2). The classification of acid sulfate soil materials (i.e. sulfuric, hypersulfidic, hyposulfidic or monosulfidic) is based mainly on the initial pH (pH at time zero) and after moist and aerobic incubation [24,25] for at least 16 weeks (Isbell and National Committee on Soils and Terrain [7]). Acid sulfate soils are identified as soils which classify as hypersulfidic soils (pH > 4) and transform to sulfuric soils (pH < 4) after incubation within 12 weeks (see Supplementary material Appendix 1 for more details). Sulfuric soils and rocks (at acid mine sites) may result in solubilisation of large amounts of metals (e.g. Al, Fe, Mn, Ni, Zn) and metalloids (As, Se) [26–31]. The transformation of hypersulfidic soils to sulfuric soils has been documented across the world, as a result of drought, anthropogenic and global climate change conditions [32,33].

The aim of this study was to develop and test spectrophotometric pH measurement methods for application in acidic (pH < 5) soil conditions. To do this, the properties of the indicator dye BCG were determined and used in spectrophotometric pH measurement during oxidation of two acid sulfate soils. The pH results under acidic conditions were compared to conventional electrode measurements and metal availability (Al, Fe, Zn) was also assessed. The method developed is applicable to a wide range of soils and waters under acidic conditions.

2. Materials and methods

2.1. Soil sample collection and incubation

Acid sulfate soil samples were collected from two localities: 1. Wally´s Landing (WL) and 2. Garden Island (GI). Sampling site “Wally´s Landing” (Finniss River; S 35°24′27.3″ and E 138°49′53.3″) in the Lower Lakes area of South Australia is a permanently flooded, anoxic wetland zone located in the Finniss River. The soil at this site is classified as a Hypersulfidic, Subaqueous Hydrosol (Isbell and National Committee on Soils and Terrain [7]), Typic Sulfiwassent (Soil Survey Staff [34]) and Hypersulfidic subaqueous soil [35]. A soil sample was taken at a depth of approximately 1 m below the water surface by a using a Russian D-auger (Dormer Australia) to a soil depth of 1.8 m and partitioned according to soil horizons (see Supplementary Table 1).

Sampling site “Garden Island” (GI; S 34°48′21.2″ and E 138°32′29.0″) is in a coastal mangrove near Port Adelaide in South Australia. The Garden Island area is intertidal and the soil at this site is classified as a Histic-Hypersulfidic, Intertidal Hydrosol, Hypersulfidic (Isbell and National Committee on Soils and Terrain [7]), Typic Sulfisaprist (Soil Survey Staff [34]) and Hypersulfidic organic soil [35]. The GI soil was collected using a 90 mm standard soil auger from the 90–110 cm soil layer (Supplementary Table 1).

In the field, soils were placed in plastic bags, sealed tightly to exclude oxygen and placed on ice for transportation to the laboratory. In the laboratory, GI soil samples were kept airtight in a fridge. The WL soil was kept uncovered at room temperature for almost 48 h to allow surplus water to evaporate prior to starting the incubation. In order to aerobically incubate, 50 g aliquots of homogenized field-moist soil, spread into a 10 mm thick layer, were transferred into plastic containers with lids equipped with holes so as to ensure soil exposure to oxygen. Throughout the incubation, soil water content was adjusted (to remain moist), if required, weekly for 12 weeks (method derived from Fitzpatrick et al. [24] and Creeper et al. [25]).

2.2. The principles of spectrophotometric pH measurement

The pH on the free hydrogen ion concentration scale can be calculated from spectrophotometric measurement of an indicator dye added to the sample solution using Eq. (1) [13,16]:

$$pH = -\log[H^+] = pK_a + \log\frac{(R-e_1)}{(e_2 - Re_3)} - 4A\left(\frac{\mu^{1/2}}{1+\mu^{1/2}} - 0.3\mu\right) \quad (1)$$

Where pK_a represents the negative logarithm of K_a (the second dissociation constant of BCG), R is the ratio of maximum absorbance of base to acid indicator forms at wavelengths λ_2 and λ_1 respectively, e_1-e_3 are indicator molar absorbance ratios, and the last term is the Davies equation where μ is ionic strength (M) and A = 0.5092 at 25 °C ([36]; equation is applicable when μ < 0.5 M). Further details, including justification of the use of Eq. (1) can be found in Supplementary Appendix 2 and Bargrizan et al. [16].

2.3. Determination of molar absorption ratios (e_1-e_3) and pK_a for bromocresol green

Molar absorption ratios (e_1-e_3) at wavelengths of peak maxima (λ_1 = 444 nm and λ_2 = 616 nm) for BCG were calculated as follows (Table 1):

$$e_1 = \frac{616\varepsilon_{HI}}{444\varepsilon_{HI}} \quad e_2 = \frac{616\varepsilon_I}{444\varepsilon_{HI}} \quad e_3 = \frac{444\varepsilon_I}{444\varepsilon_{HI}} \quad (2)$$

Where $_\lambda\varepsilon_{HI}$ and $_\lambda\varepsilon_I$ are the molar absorption coefficients (L mol^{-1} cm^{-1}) of acid and base forms of the indicator measured at wavelength λ and calculated using Beer's Law from measured absorbance, indicator concentrations, and path length (l) [13]. To achieve this, maximum absorbance of acid and base forms of BCG ($_{\lambda1,2}A_{HI}$ and $_{\lambda1,2}A_I$) at (λ_1 = 444 nm and λ_2 = 616 nm) were determined at extreme pH values where only the acid (approx. pH 1 − 2) or base (approx. pH 8 − 9) form of BCG, respectively, was present [17]. This was achieved by addition of diluted HCl and NaOH, respectively, into 1 mL of diluted stock BCG solution (2×10^{-3} mol L^{-1}) in a 100 mL volumetric flask. The maximum absorbance of base and acid forms of the indicator dye was measured via placing the solutions in a 1 cm cuvette in a double-beam spectrophotometer (GBC UV/VIS 916) thermostatted at 25 °C and supplied with Cintral™ software. Examples of the acid and base spectra under these extreme conditions are shown in Fig. 1.

In order to determine pK_a of BCG at μ = 0 and 25 °C, BCG stock solution (2×10^{-3} mol L^{-1}) was added in 30 μL increments to 4 mL certified (NIST Standard Reference Material 185i) phthalate buffer (0.05 mol kg^{-1}) with $pH_{NBS/NIST}$ = 4.00 (based on hydrogen ion activity; refer to certification documentation on NIST website for the

Table 1
BCG molar absorbance ratios (e_1-e_3) and pK_a values at zero ionic strength and 25 °C.

Replicate	e_1	e_2	e_3	pK_a
1	0.003	2.415	0.179	5.03
2	0.003	2.38	0.186	5.02
3	0.015	2.327	0.182	5.02
4	0.017	2.384	0.182	5.04
5	0.008	2.330	0.172	5.02
6	0.004	2.350	0.159	5.02
7	0.015	2.328	0.177	5.02
Average	0.009	2.359	0.177	5.02
SD	0.006	0.034	0.009	0.007

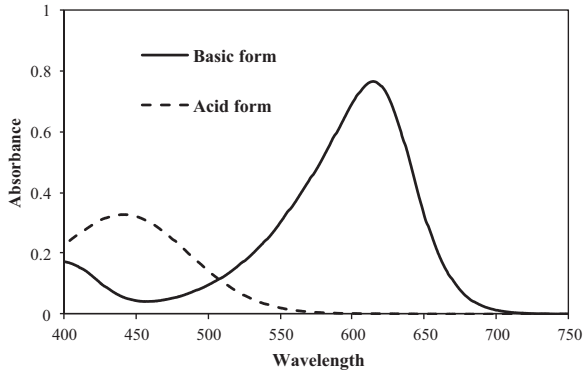

Fig. 1. Absorbance Vs wavelength for the base (I^{2-}) and acid (HI^{-}) forms of bromocresol Green (BCG).

protocol of preparation) in a 1 cm glass cuvette and R (ratio of maximum absorbance of base to acid forms of BCG) was measured. pK_a was then calculated using Eq. (1), where the buffer's ionic strength value was obtained using ($\mu=\frac{1}{2}\sum c_i Z_i^2$ where c_i is the concentration of ions (mol L^{-1}) and Z is the charge number of ions), the molar absorptivities of BCG (e_1-e_3) are as described and measured above, and the pH of the NIST buffer is on the free hydrogen scale. The pH of the NIST buffer on this scale (pH_{free} 3.91) was calculated based on converting the buffer $pH_{NBS/NIST}$ value based on hydrogen ion activity to hydrogen ion concentration using Eq. (3) [16]:

$$pH_{free} = -log[H^+] = pH_{NBS/NIST} + log\gamma_{H+} \quad (3)$$

Where γ_{H+} is the activity coefficient for the hydrogen ion calculated using the Davies equation.

2.4. Preparation of soil extracts and spectrophotometric pH measurement

Soil extracts (three replicates) were prepared by shaking 25 g soil (wet weight) with 25 mL water on an orbital shaker for 1 h [37] and then centrifuging at 1915.2 RCF (Relative Centrifugal Force) for 30 min. The supernatant was transferred to a clean polyethylene tube and brought to 25 °C using a water bath [16]. Aliquots (5–10 mL) of soil extracts were then set aside and acidified by adding concentrated HNO_3 to achieve a concentration of 2% v/v, and then analysed for metal content using ICP-OES. The pH was also measured using a calibrated glass electrode (Orion Sure Flow™) for soil extracts that were acidic (in the pH range of BCG dye, 3 − 5.3) to enable comparison with spectrophotometric pH values.

Other indicators, specifically phenol red (PR) and bromocresol purple (BCP), were used to obtain spectrophotometric pH values at the start and early stage of the soil incubation [16]. The pK_a and molar absorptivity values used for PR and BCG were those provided by Yao and Byrne [13] and are also provided in the Supplementary material Table 2.

Three indicator stock solutions (PR, BCP and BCG at the concentration of 2×10^{-3} mol L^{-1} were made and adjusted to pH ≈ 7.5 and 5.9 and 4.5, respectively) using 0.1 mol L^{-1} HCl or NaOH. Indicator concentration in analysed soil extracts ranged from 2×10^{-5} mol L^{-1} to 6×10^{-5} mol L^{-1} based upon sequential addition of three 0.03 mL aliquots of indicator stock solution (i.e. total addition of 0.03, 0.06, 0.09 mL) into 4 mL soil extract in a 1 cm glass cuvette (Bargrizan et al., 2017). The soil solutions before adding the dye had some colour and absorbance, especially towards the UV range. We measured the reference spectra of each soil extract and this was subtracted from the measurement spectra with the dye added.

During the pH measurement, the temperature of soil solutions was kept constant at 25 °C using a water thermostat installed on the spectrophotometer. The ratio of maximum absorbance of base to acid forms of the indicator (R) was measured as described above. The pH perturbation caused by indicator addition was corrected for each sample by plotting R vs dye volume, and obtaining R at zero dye volume by linear regression [16,17]. The ionic strength of the soil solution (μ) required to correct activity coefficients as per Eq. (1) was estimated by measuring electrical conductivity (EC) in a 1:1 soil:water extract (giving values of 17.5 and 6.5 mS cm^{-1} for GI and WL soils, respectively) and calculating using Eq. (4) [38,39]:

$$\mu = EC(mS\ cm^{-1}) \times 0.0127 \quad (4)$$

Ionic strength of the soil solution could also be calculated following measurement of the major ion composition of the soil solution and using $\mu = \frac{1}{2}\sum c_i Z_i^2$ where c is the concentration of ion *i* in mol L^{-1} and z is the charge of ion *i*. However, the pH_{spec} difference is no higher than 0.001 pH units when there is a 10% error between ionic strengths calculated using Eq. (4) and $\mu = \frac{1}{2}\sum c_i Z_i^2$.

3. Results and discussion

3.1. Dye properties

The BCG molar absorptivity ratios (e_1-e_3) and dissociation constant (pK_a) at 25 °C are presented in Table 1. The average results for e_1, e_2 and e_3 (± standard deviation, n = 7) were 0.009, 2.359 and 0.177, respectively. In comparison, results reported for BCG molar absorptivity ratios in seawater were e_1 = 0.0013, e_2 = 2.314 and e_3 = 0.129 [21]. An average pK_a of 5.02 ± 0.007 (standard deviation, n = 7) for BCG (μ = 0, 25 °C) was obtained based on measurement in the NIST phthalate buffer and correction to the free hydrogen ion concentration scale (Table 1). This was 0.12 higher than the pK_a for BCG reported by Bishop ([40], pK_a = 4.90). This difference could be due to dye impurities which can influence the measured e_i and consequently pK_a [19]. The BCG dye source and method of pK_a determination is not reported by Bishop [40].

The pK_a of BCG in seawater (μ ≈ 0.7) is approximately 4.42, as reported by Byrne et al. [20], King and Kester [22] and Breland and Byrne [21]. The difference of approximately 0.6 pK_a units between our pK_a for BCG at zero ionic strength and pK_a for BCG in seawater, is comparable to the difference reported for other indicator dyes, m-cresol purple and thymol blue [18,41]. The measurement of molar absorptivity ratios and pK_a for BCG in our study provides the ability to measure pH spectrophotometrically in acidic soils and solutions at lower ionic strengths (μ < 0.5) via Eq. (1).

3.2. Soil acidification and spectrophotomteric pH measurement method

To demonstrate the application of the spectrophotometric method using BCG under acidic conditions, the spectrophotometric pH values during a 12-week oxic incubation of two hypersulfidic soils (GI and WL) are shown in Fig. 2A and B, respectively. After 5 and 3 weeks of incubation, respectively, the pH for GI and WL reached ≤ 4 (i.e. soil qualified for classification as a sulfuric soil in accordance with the Australian Acid Sulfate Soil Identification key [35].

The pH of GI and WL hypersulfidic soils continued to decrease by ≤ 0.6 and ≤ 0.2 pH units, respectively, until a stable acidic pH was reached, suggesting oxidation of pyrite had ended.

There was a strong correlation ($r^2 > 0.99$) between the spectrophotometric and glass electrode methods for both soils (see Fig. 2C and D).

3.3. Relationship between spectrophotometric pH and metal availability in soil

Metal (Al, Fe and Zn) concentrations in the soil pore water over time for the two sites are shown in Fig. 3. The concentration of all metals (Fe, Al and Zn) in the GI soil began to increase substantially after about 5

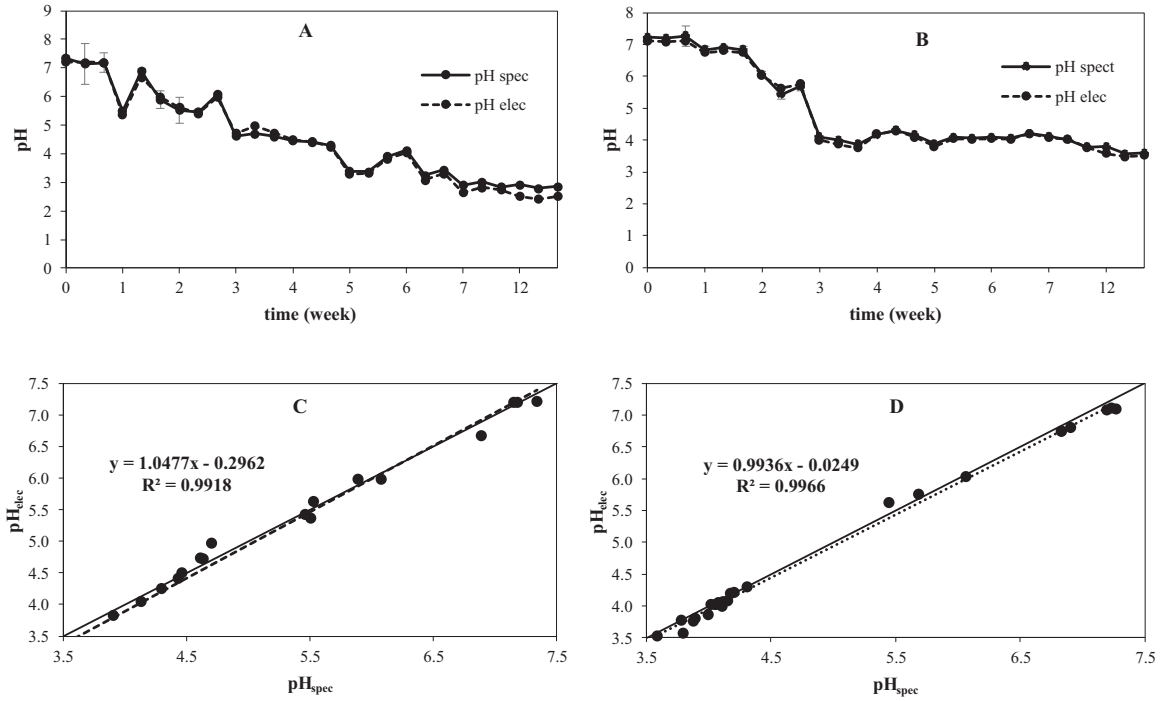

Fig. 2. Spectrophotometric (pH_{soec}) and glass electrode (pH_{elec}) pH values and correlation between pH_{spec} and pH_{elec} during incubation of two soil samples (A-C) GI, (B-D) WL for 12 weeks. Spectrophotometric pH in the incubation was measured between pH ≈ 3 − 5.3 with BCG, and with dyes PR and BCP for the pH ranges 6.8 − 8.3 and 5.3 − 6.8, respectively. Error bars representing the standard deviation for triplicate samples, where not visible, are smaller than the symbols. On (C) and (D) the solid line is the 1:1 line and the dashed line is the linear regression line.

weeks and remained elevated until the end of incubation. For the WL soil, the Fe concentration increased after 3 weeks and then stabilized at a high concentration until the end of the experiment, while for Al and Zn, two increases in concentration can be observed in weeks 5 and 12. Overall, the relative concentration of metals towards the end of the incubation was Fe > Al > Zn for both soils.

When metal concentrations are plotted versus pH (Fig. 4), the results highlight how soil acidification released metals once pH has decreased below approximately 5. The large pH decrease and Fe release is due to pyrite oxidation during the incubation of the hypersulfidic soils. The acidification results in the release of Al, Fe and Zn due to dissolution of Al and Fe oxides and clay minerals [30]. This is consistent with the findings of Mosley et al. [30] in sulfuric soils at pH < 4. In the WL soil, during acidification, a lower concentration of Al is observed at low pH compared with the GI soil, which could potentially be related to the difference in clay content and the amount of Al found between these two soils. According to the geochemical model of Shaw et al. [42], in the WL soil, most of the Al is likely to be isolated within the clay particles and released slowly through aluminosilicate dissolution as pH decreases.

A question with spectrophotometric pH measurements under acidic conditions is whether metal ions released from soil could react with the dye, potentially changing its acid-base properties. Fig. 5 shows the pH difference of electrode and spectrophotometric measurements under acidic conditions versus spectrophotometric pH measurements (approx. 0.01–0.2 pH units) with BCG (± 0.2 and 0.1, similar average standard deviation of triplicate measurements between two methods for GR and WL respectively). There was a greater difference between spectrophotometric pH and glass electrode measurements below pH 3 for GI soil (excluded from plot but see Fig. 2A), this may be due to exceedance of the working range of BCG. The spectrophotometric method produces values slightly lower than those measured with the glass electrode, a similar finding to Bargrizan et al. [16] at more neutral soil pH. However, in general there was a very good correlation ($r^2 > 0.99$) between the two measurement methods (Fig. 2), despite mg L^{-1} dissolved metal concentrations. This suggests that, at least for the dye and metal concentrations used in our study, interactions between the dye and metals do not appear to significantly affect pH determination using indicator dyes in acidic conditions.

4. Conclusion

The measurement of the properties of the bromocresol green indicator dye in this study enables spectrophotometric pH measurement

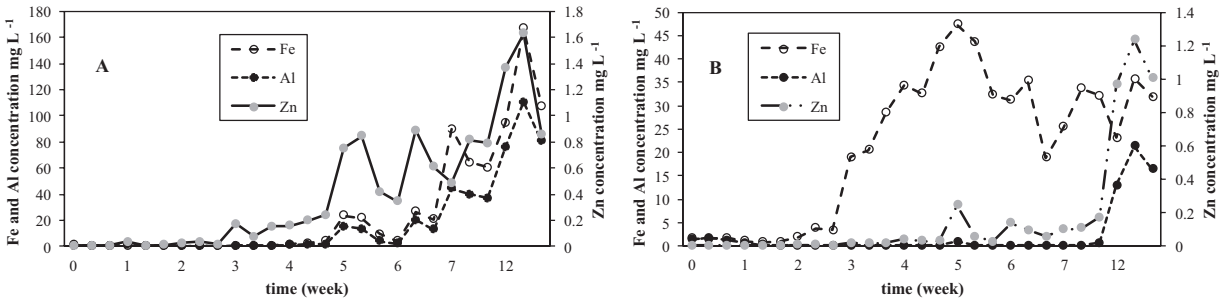

Fig. 3. Dissolved metal concentration (Fe, Al and Zn) over 12 weeks soil incubation for two soil samples (A) GI and (B) WL.

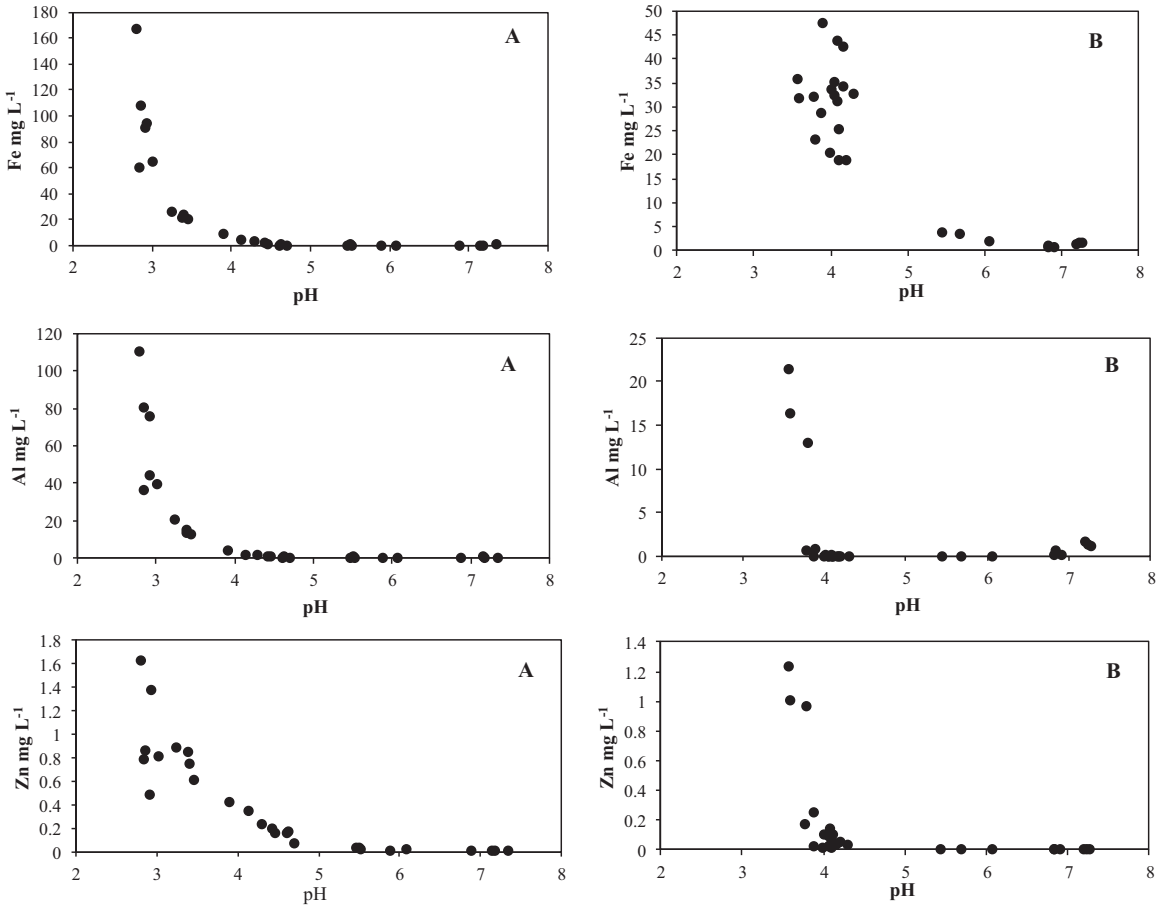

Fig. 4. Dissolved metal concentrations (Al, Fe, Zn), versus spectrophotometric pH (1.1 soil/water) for two samples: (A) GI, (B) WL.

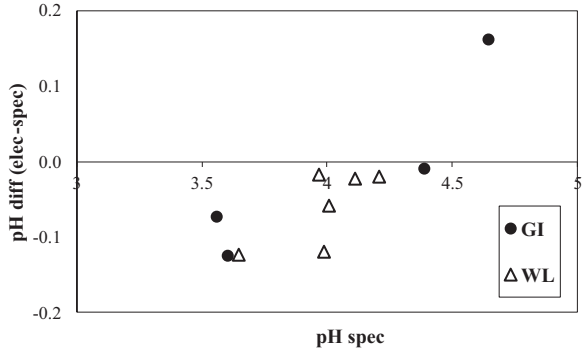

Fig. 5. pH difference between the glass electrode (elec) and spectrophotometric (spec) methods versus spectrophotometric pH values in the extremely acidic range (pH 3 − 4.5) for GI and WL soil samples during 12 weeks incubation. pH values < 3 were excluded due to their exceedance of the working range of BCG.

between pH 3 − 5.3 at ionic strengths < 0.5 (soil $EC_{1:1}$ < approx. 20 mS cm^{-1}). This extends the capability of the spectrophotometric soil pH method to measure lower pH conditions, such as that found in acidified agricultural land and acid sulfate soils. The application of the spectrophotometric method for measuring soil pH in the acidic range was demonstrated during a 12-week incubation of two hypersulfidic soils (pH > 4), which transformed to sulfuric soils (pH < 4). As the indicator dye spectra are, unlike glass electrodes, directly related to the acid-base equilibria in solution, spectrophotometric measurements could potentially reduce pH measurement errors in soils. This includes the elimination of liquid junction errors which, given they can be on the order of +/−0.1 pH units, could affect metal speciation calculations.

Further research using the spectrophotometric pH measurement method in a wider range of soils to assess whether it can be used to better understand geochemical processes (e.g. predict metal availability) in soils is recommended. The accuracy of the spectrophotometric method could be further assessed by concurrent measurement of two other carbonate system parameters (e.g. pCO_2 and dissolved inorganic carbon) and calculating pH for comparison to measured spectrophotometric and electrode pH. The advantage of the spectrophotometric method using indicator dyes is that it can potentially be used to study pH in two dimensions [43], which is critically important for better assessment of geochemical and plant-metal interactions in acidic soil.

Acknowledgments

We would like to thank Ms Bogumila Tomczak for assisting with the measurement of metals. This work was supported by the assistance of the Australian Commonwealth Government through an Australian Research Council Discovery Project Grant DP170104541 for RF and LM, and a University of Adelaide postgraduate scholarship for SB. We thank the Editor and two anonymous reviewers for their comments which enabled us to improve the manuscript.

Appendix A. Supporting information

Supplementary data associated with this article can be found in the online version at http://dx.doi.org/10.1016/j.talanta.2018.04.074.

References

[1] M.E. Essington, Soil and Water Chemistry: An Integrative Approach, second ed, CRC Press, New York, 2015.
[2] W.L. Lindsay, Chemical Equilibria in Soils, John Wiley & Sons Ltd, UK, 1979.
[3] L. Gandois, A. Probst, C. Dumat, Modelling trace metal extractability and solubility in French forest soils by using soil properties, Eur. J. Soil. Sci. 61 (2010) 271–286.
[4] S.L. Simpson, R.W. Fitzpatrick, P. Shand, B.M. Angel, D.A. Spadaro, L. Mosley, Climate-driven mobilisation of acid and metals from acid sulfate soils, Mar. Freshw. Res. 61 (2010) 129–138.
[5] S.L. Simpson, C.R. Vardanega, C. Jarolimek, D.F. Jolley, B.M. Angel, L.M. Mosley, Metal speciation and potential bioavailability changes during discharge and neutralisation of acidic drainage water, Chemosphere 103 (2014) 172–180.
[6] S. Sauvé, W. Hendershot, H.E. Allen, Solid-solution partitioning of metals in contaminated soils: dependence on pH, total metal burden, and organic matter, Environ. Sci. Technol. 34 (2000) 1125–1131.
[7] R.F. IsbellNational Committee on Soils and Terrain, The Australian Soil Classification, second ed, CSIRO Publishing, Clayton, Victoria, Australia, 2016.
[8] Soil Science Division Staff, Soil Survey Manual: Handbook of Department of Agriculture. No. 18. USDA-NRCS, U.S. Gov. Print. Office, Washington, D.C. USA, 2017.
[9] S. Yuan, M.D. DeGrandpre, Evaluation of indicator-based pH measurements for freshwater over a wide range of buffer intensities, Environ. Sci. Technol. 42 (2008) 6092–6099.
[10] F.J. Millero, The pH of estuarine waters, Limnol. Oceanogr. 31 (1986) 839–847.
[11] D.A. Skoog, F.J. Holler, S.R. Crouch, Principles of Instrumental Analysis, Cengage Learning, Inc, Belmont, (CA), 2007.
[12] A.D. Wiesner, L.E. Katz, C.C. Chen, The impact of ionic strength and background electrolyte on pH measurements in metal ion adsorption experiments, J. Colloid Interface Sci. 301 (2006) 329–332.
[13] W. Yao, R.H. Byrne, Spectrophotometric determination of freshwater pH using bromocresol purple and phenol red, Environ. Sci. Technol. 35 (2001) 1197–1201.
[14] R.G. Bates, A.K. Vijh, Determination of pH: theory and practice, J. Electrochem. Soc. 120 (1973) (263C-263C).
[15] R.H. Byrne, J.A. Breland, High precision multiwavelength pH determinations in seawater using cresol red, Deep-Sea Res. 36 (5) (1989) 803–810.
[16] S. Bargrizan, R.J. Smernik, L.M. Mosley, Development of a spectrophotometric method for determining pH of soil extracts and comparison with glass electrode measurements, Soil Sci. Soc. Am. J. 81 (2017) 1350–1358.
[17] T.D. Clayton, R.H. Byrne, Spectrophotometric seawater pH measurements: total hydrogen ion concentration scale calibration of m-cresol purple and at-sea results, Deep-Sea Res. Part I: Oceanogr. Res. Pap. 40 (1993) 2115–2129.
[18] L.M. Mosley, S.L. Husheer, K.A. Hunter, Spectrophotometric pH measurement in estuaries using thymol blue and m-cresol purple, Mar. Chem. 91 (2004) 175–186.
[19] C.Z. Lai, M.D. DeGrandpre, B.D. Wasser, T.A. Brandon, D.S. Clucas, E.J. Jaqueth, Z.D. Benson, C.M. Beatty, R.S. Spaulding, Spectrophotometric measurement of freshwater pH with purified meta-cresol purple and phenol red, Limnol. Oceanogr. Methods 14 (2016) 864–873.
[20] R. Byrne, G. Robert-Baldo, S. Thompson, C. Chen, Seawater pH measurements: an at-sea comparison of spectrophotometric and potentiometric methods, Deep-Sea Res. Part A: Oceanogr. Res. Pap. 35 (1988) (1405-141).
[21] J.A. Breland, R.H. Byrne, Spectrophotometric procedures for determination of sea water alkalinity using bromocresol green, Deep-Sea Res. Part I: Oceanogr. Res. Pap. 40 (1993) 629–641.
[22] D.W. King, D.R. Kester, Determination of seawater pH from 1.5 to 8.5 using colorimetric indicators, Mar. Chem. 26 (1989) 5–20.
[23] L.J. Pons, Outline of the genesis, characteristics, classification and improvement of acid sulphate soils, in: H. Dost (Eds.), Proceedings of the 1972, International Acid Sulphate Soils Symposium, Volume 1, 18. International Land Reclamation Institute Publication, Wageningen, Netherlands, 1973, pp. 3–27.
[24] R.W. Fitzpatrick, G. Grealish, P. Shand, R. Merry, N. Creeper, M. Thomas, A. Baker, B. Thomas, W. Hicks, and N. Jayalath, Chip-tray incubation, A new field and laboratory method to support Acid Sulfate Soil Hazard Assessment, Classification and Communication, In: R.J. Gilkes, and N. Prakongkep (Eds.), Proceedings of the 19th World Congress of Soil Science; Soil Solutions for a Changing World, ISBN 987-0-646-53783-2; published on DVD. 〈http://www.iuss.org; Symposium WG 3.1 Processes in acid sulfate soil materials〉 Brisbane, Australia, IUSS, (Accessed 1–6 August 2010), pp. 28-31.
[25] N. Creeper, R. Fitzpatrick, P. Shand, A simplified incubation method using chip--trays as incubation vessels to identify sulphidic materials in acid sulphate soils, Soil Use Manag. 28 (2012) 401–408.
[26] M. Astrom, N. Corin, Abundance, sources and speciation of trace elements in humus-rich streams affected by acid sulphate soils, Aquat. Geochem. 6 (2000) 367–383.
[27] R. Sundstrom, M. Astrom, P. Osterholm, Comparison of the metal content in acid sulfate soil runoff and industrial effluents in Finland, Environ. Sci. Technol. 36 (2002) 4269–4272.
[28] B.C.T. Macdonald, I. White, M.E. Astrom, A.F. Keene, M.D. Melville, J.K. Reynolds, Discharge of weathering products from acid sulfate soils after a rainfall event, Tweed River. Eastern Australia, Appl. Geochem. 22 (2007) 2695–2705.
[29] J. Toivonen, P. Osterholm, Characterization of acid sulfate soils and assessing their impact on a humic boreal lake, J. Geochem. Explor. 110 (2011) 107–117.
[30] L.M. Mosley, R.W. Fitzpatrick, D. Palmer, E. Leyden, P. Shand, Changes in acidity and metal geochemistry in soils, groundwater, drain and river water in the lower Murray River after a severe drought, Sci. Total Environ. 485 (2014) 281–291.
[31] J. Chamier, M. Wicht, L. Cyster, N.P. Ndindi, Aluminium (Al) fractionation and speciation; getting closer to describing the factors influencing $Al^{(3+)}$ in water impacted by acid mine drainage, Chemosphere 130 (2015) 17–23.
[32] D. Fanning, M. Rabenhorst, R. Fitzpatrick, Historical developments in the understanding of acid sulfate soils, Geoderma 308 (2017) 191–206.
[33] C. Yuan, P. Marschner, R.W. Fitzpatrick, L.M. Mosley, Global risks of severe acidification of acid sulfate soils due to increasing drought and the importance of organic matter for mitigation, in: Soil Science Society of China (Ed.), Soil Science and Ecological Civilization, 1 Northwest A&FUniversity Press, Xi'an, China, 2016, pp. 176–186.
[34] Soil Survey Staff, Keys to Soil Taxonomy, twelfth ed., Department of Agriculture Natural Resources Conservation Service, Washington, D.C. USA, 2014.
[35] R.W. Fitzpatrick, Demands on soil classification and soil survey strategies: special-purpose soil classification systems for local practical use, in: S.A. Shahid, F.K. Taha, M.A. Abdelfattah (Eds.), Developments in soil Classification, Land Use Planning and Policy Implications, Springer, Netherlands, 2013, pp. 51–83.
[36] W. Stumm, J. Morgan, Aquatic Chemistry: Chemical Equilibria and Rates in Natural Waters, 3rd ed, Wiley Interscience, New York, 1996, p. 1022.
[37] G.E. Rayment, D.J. Lyons, Soil Chemical Methods, CSIRO publishing, Melbourne, (VIC), 2011.
[38] B. Griffin, J.J. Jurinak, Estimation of activity coefficients from the electrical conductivity of natural aquatic systems and soil extracts, Soil Sci. 116 (1973) 26–30.
[39] G.P. Gillman, L.C. Bell, Soil Solution Studies on Weathered Soils from tropical North Queensland, Aust. J. Soil Res. 16 (1978) 67–77.
[40] E. Bishop, Indicators, Pergamon Press, Oxford, 1972.
[41] N. Douglas, R. Byrne, Spectrophotometric pH measurements from river to sea: calibration of mCP for $0 \leq S \leq 40$ and $278.15 \leq T \leq 308.15$ K, Mar. Chem. 197 (2017) 64–69.
[42] S.A. Shaw, M.J. Hendry, Geochemical and mineralogical impacts of H_2SO_4 on clays between pH 5.0 and −3.0, Appl. Geochem. 24 (2009) 333–345.
[43] S. Blossfeld, D. Gansert, A novel non-invasive optical method for quantitative visualization of pH dynamics in the rhizosphere of plants, Plant Cell Environ. 30 (2) (2007) 176–186.

SUPPLEMENTARY MATERIAL

The application of a spectrophotometric method to determine pH in acidic (pH < 5) soils

Sima Bargrizan[a], Ronald J. Smernik[a], Rob Fitzpatrick[b], and Luke M. Mosley[b]

[a] The School of Agriculture, Food and Wine, The University of Adelaide, South Australia

[b] Acid Sulfate Soils Centre, School of Biological Sciences, The University of Adelaide, South Australia

*Corresponding author

Waite Campus, University of Adelaide, PMB 1 Glen Osmond, SA 5064, Australia

E-mail: luke.mosley@adelaide.edu.au Tel.: +61 8 8313 5453

Appendix 1. Acid Sulfate Soil Classification Description

A soil that classifies as a 'hypersulfidic soil' requires hypersulfidic material (i.e. decrease in pH to pH 4 or less after incubation for at least 16 weeks) to be identified in a layer or horizon, which is at least 10 cm thick within 150 cm of the soil surface [1,2].

A soil profile that classifies as a 'hyposulfidic soil' requires hyposulfidic material (i.e. decrease in pH to > pH 4 after incubation for at least 16 weeks) to be identified in a layer or horizon, which is at least 10 cm thick within 150 cm of the soil surface. A soil that classifies as a 'sulfuric soil' requires sulfuric material (i.e. pH < 4 at time zero incubation) to be identified in a layer or horizon, which is at least 10 cm thick within 150 cm of the soil surface. For example, after drainage of water saturated (anaerobic) acid sulfate soils with hypersulfidic material for agricultural purposes or during drought periods, oxidation of pyrite causes strong acidification with the formation of sulfuric material (pH < 4). All soils were classified in accordance with the Australian Soil classification (Isbell and National Committee on Soils and Terrain [3]), Soil Taxonomy [4] and the Australian Acid Sulfate Soil Identification key [1].

The Australian Acid sulfate soil identification key is designed for people who are not experts in soil classification systems, assisting them to easily identify five acid sulfate soil types (subaqueous, organic, cracking clay, sulfuric and hypersulfidic soils) and 18 sub-types based on the occurrence of sulfuric, hypersulfidic, hyposulfidic, or monosulfidic material, and clayey or sandy layers [2].

Table 1. pH values of the acid sulfate soil sites on Garden Island and at Wally's Landing during time course of an oxic incubation, Acid sulfate soil material classification, Soil Taxonomy, ASS subtype classification. Samples were collected in November 2015, additional oxidised samples collected during the extreme drought period in 2011 are also shown for Wally's Landing.

Depth (cm)	[1]**Material**	**pH$_{H2O}$** (1:1 soil:solution, oxic conditions)				
		2011[5]	*2015*			
			day 0	8 weeks	16 weeks	24 weeks
Garden Island: [2]Histic-Hypersulfidic, Intertidal Hydrosol, [3]Typic Sulfisaprist, [4]Hypersulfidic organic soil						
0-5	Hyposulfidic		7.5	7.04	7.15	7.20
5-30	Hyposulfidic		7.0	7.13	7.12	7.11
30-60	Hyposulfidic		6.9	6.81	6.82	6.82
60-80	**Hypersulfidic**		6.8	3.58	1.76	1.56
80-100	**Hypersulfidic**		6.8	3.64	1.87	1.50
100-120	**Hypersulfidic**		6.8	3.48	2.30	1.96
120-135	**Hypersulfidic**		6.6	3.28	2.10	1.85
Wally's Landing: [2]Hypersulfidic, Subaqueous Hydrosol, [3]Typic Sulfiwassent; [4]Hypersulfidic subaqueous soil,						
0-10	Hyposulfidic	4.3[5]	7.1	5.2	4.2	3.9
10-25	Hyposulfidic	4.3[5]	6.8	5.0	4.6	4.1
25-55	Hyposulfidic	3.5[5]	6.8	6.0	4.6	4.4
55-80	Hyposulfidic	3.6[5]	6.9	5.5	4.4	4.3
80-130	**Hypersulfidic**	n.d.	7.7	3.6	2.4	2.0
130-180	**Hypersulfidic**	n.d.	8.4	2.6	1.9	1.7

[1]Where acid sulfate soil material is based on the definition in the 2nd edition of the Australian Soil Classification (Isbell and National Committee on Soils and Terrain [3])

[2]Australian Soil Classification (Isbell and National Committee on Soils and Terrain [3]).

[3]Soil Taxonomy (Soil Survey Staff [4]).

[4]Acid Sulfate Soil classification (Soil identification key) used in Australia [1,2].[*]Where the soil classification is a Hypersulfidic soil, hypersulfidic material (pH decreased to < 4 after incubation of at least 16 weeks) has been identified in a layer or horizon (at least 10cm thick) within 150 cm of the soil surface. Where the soil classification is a Sulfuric soil, Sulfuric material (pH < 4 at time zero incubation) has been identified in a layer or horizon (at least 15cm thick) within 150 cm of the soil surface.

[5]The soil material is derived from sediments of the Finniss River catchment and described as a "sulfuric subaqueous clay soil" [5-7].The Millennium drought conditions across SE Australia between 2007 and early 2010 [8] caused drying of the river and subsequent acidification (pH < 4) of hypersulfidic material in the river sediment. After river levels returned to normal in 2011 [5], the site is permanently flooded and the pH values have slowly recovered to neutral pH values after five years as shown when pH was measured in 2015. Soil samples were taken at a depth of approximately 1m below the water surface by a peat sampler (gouge auger) to a soil depth of 1.8 m and partitioned according to soil horizons.

References

[1] R.W. Fitzpatrick, Demands on soil classification and soil survey strategies: Special-purpose soil classification systems for local practical use, In: S. A. Shahid, F. K. Taha, M. A. Abdelfattah (Eds.), Developments in soil classification, land use planning and policy implications, Springer, Netherlands, 2013, pp. 51-83.

[2] R.W. Fitzpatrick, L.M. Mosley, F.J. Cook, Understanding and managing irrigated acid sulfate and salt-affected soils, A handbook for the Lower Murray Reclaimed Irrigation Area. DOI: <https://doi.org/10.20851/murray-soils> University of Adelaide Press, 2017, p.127. Available at : https://www.adelaide.edu.au/press/titles/murray-soils/

[3] R.F. Isbell, and National Committee on Soils and Terrain, The Australian soil classification, second ed., CSIRO Publishing, Clayton, Victoria, Australia, 2016.

[4] Soil Survey Staff, Keys to Soil Taxonomy, twelfth ed., Department of Agriculture Natural Resources Conservation Service, Washington, D.C. USA, 2014.

[5] A.K.M. Baker, P. Shand, R.W. Fitzpatrick, Recovery of re-flooded acid sulfate soil environments around Lakes Alexandrina and Albert, South Australia, In: CSIRO: Water for a Healthy Country National Research Flagship, 2013.

[6] R.W. Fitzpatrick, A.K.M. Baker, P. Shand, R.H. Merry, G. Grealish, L.M. Mosley, A modern soil-landscape characterization approach to reconstructing and predicting pedogenic pathways of inland acid sulfate soils, In: P. Osterholm, M. Yli- Halla, P. Eden (Eds.), Proceedings of 7th International Acid Sulfate Soil Conference, Vaasa, Finland. Geological Survey of Finland, Guide 56, 26–30 August 2012, pp. 47–50.

[7] R.W. Fitzpatrick,. P. Shand, R.H. Merry, Acid sulfate soils, In: J.T. Jennings (Eds.), Natural History of the Riverland and Murraylands, Royal Society of South Australia, Adelaide, South Australia, 2009, pp. 65–111.

[8] M. Heberger, Australia's millennium drought: impacts and responses, The world's water, Springer, 2012, pp. 97–125.

Appendix 2. Theory and derivation of equations that underpin the spectrophotometric pH measurement method

Sulfonephthalein indicator dyes can exist in three forms H_2I, HI^-, and I^{2-}, each of which has distinctive light absorption characteristics. The chemical equilibria among these three forms is dependent on pH and can be described by the first and second dissociation constants of the fully protonated (H_2I) dye species:

$$H_2I \rightleftharpoons HI^- + H^+ \qquad K_1 = [HI^-]\,[H^+] / [H_2I] \qquad [1a]$$

$$HI^- \rightleftharpoons I^{2-} + H^+ \qquad K_2 = [I^{-2}]\,[H^+] / [HI^-] \qquad [1b]$$

The total indicator concentration ($I_T = H_2I + HI^- + I^{2-}$) can be expressed in terms of [HI], K_1, K_2, and proton concentration by:

$$I_T = [HI^-]\,([H^+]/K_1 + 1 + K_2 / [H^+]) \qquad [2]$$

Using the Beer-Lambert law as the basis, the absorbance of an indicator dye in solution can be expressed by:

$$_\lambda A = (_\lambda\varepsilon_{H2I}\,[H_2I] + {}_\lambda\varepsilon_{HI}\,[HI^-] + {}_\lambda\varepsilon_I\,[I^{2-}]\,)\,l \qquad [3]$$

where $_\lambda A$ is the absorbance at wavelength λ, $_\lambda\varepsilon_x$ is the molar absorptivity of each individual dye species (x = I^{2-} or HI^- or H_2I), and l is the optical (spectrophotometer cell) path length. As per equation (2), equation (3) can be expressed in terms of the species HI by:

$$_\lambda A / l = [HI^-]\,(_\lambda\varepsilon H_2I\,[H^+]/K_1 + {}_\lambda\varepsilon HI + {}_\lambda\varepsilon I\,K_2\,/[H^+]) \qquad [4]$$

Dividing equation (4) by equation (2) yields:

$$\frac{_\lambda A}{I_T\,l} = \frac{_\lambda\varepsilon_{H2I}\,[H^+]/K_1 + {}_\lambda\varepsilon_{HI} + {}_\lambda\varepsilon_I\,K_2/[H^+]}{[H^+]/K_1 + 1 + K_2/[H^+]} \qquad [5]$$

Except at low pH the H_2I concentration is insignificant, hence ignoring the first dissociation reaction, equation (5) can be reduced to:

$$\frac{{}_{\lambda}\mathrm{A}}{I_T\, l} = \frac{{}_{\lambda}\varepsilon_{HI} + {}_{\lambda}\varepsilon_I \mathrm{K}_2/[\mathrm{H}^+]}{1 + K_2/[\mathrm{H}^+]}$$ [6]

Using equation (6) and specifying R as the ratio of indicator absorbances at λ_2 and λ_1 (i.e. R = ${}_2\mathrm{A}/{}_1\mathrm{A}$) we can derive:

$$\mathrm{R} = \frac{{}_2\varepsilon_{HI} + {}_2\varepsilon_I \mathrm{K}_2/[\mathrm{H}^+]}{{}_1\varepsilon_{HI} + {}_1\varepsilon_I \mathrm{K}_2/[\mathrm{H}^+]}$$ [7]

Dividing each term in the numerator and denominator by ${}_1\varepsilon_{HI}$,

$$\mathrm{R} = \frac{{}_2\varepsilon_{HI}/{}_1\varepsilon_{HI} + {}_2\varepsilon_I \mathrm{K}_2/{}_1\varepsilon_{HI}[\mathrm{H}^+]}{{}_1\varepsilon_{HI}/{}_1\varepsilon_{HI} + {}_1\varepsilon_I \mathrm{K}_2/{}_1\varepsilon_{HI}[\mathrm{H}^+]} = \frac{e_1 + e_2\mathrm{K}_2/[\mathrm{H}^+]}{1 + e_3\mathrm{K}_2/[\mathrm{H}^+]}$$ [8a]

Where $e_1 = {}_2\varepsilon\mathrm{HI}/{}_1\varepsilon\mathrm{HI}$, $e_2 = {}_2\varepsilon\mathrm{I}/{}_1\varepsilon\mathrm{HI}$, $e_3 = {}_1\varepsilon\mathrm{I}/{}_1\varepsilon\mathrm{HI}$, and then multiplying each term in the numerator and denominator by H^+,

$$\mathrm{R} = \frac{e_1[\mathrm{H}^+] + e_2\mathrm{K}_2}{[\mathrm{H}^+] + e_3\mathrm{K}_2}$$ [8b]

clearing the fraction,

$$\mathrm{R}[\mathrm{H}^+] + \mathrm{R}e_3\mathrm{K}_2 = e_1[\mathrm{H}^+] + e_2\mathrm{K}_2$$ [8c]

rearranging the $e_1[\mathrm{H}^+]$ and $\mathrm{R}e_3\mathrm{K}_2$ terms,

$$e_2\mathrm{K}_2 - \mathrm{R}e_3\mathrm{K}_2 = \mathrm{R}[\mathrm{H}^+] - e_1[\mathrm{H}^+]$$ [8d]

factoring both sides of the equation,

$$\mathrm{K}_2(e_2 - \mathrm{R}e_3) = [\mathrm{H}^+](\mathrm{R} - e_1)$$ [8e]

rearranging terms,

$$\frac{\mathrm{K}_2}{[\mathrm{H}^+]} = \frac{(\mathrm{R} - e_1)}{(e_2 - \mathrm{R}e_3)}$$ [8f]

and taking logs,

$$\log \mathrm{K}_2 - \log [\mathrm{H}^+] = \log \frac{(\mathrm{R} - e_1)}{(e_2 - Re_3)}$$ [8g]

leads to the final equation for pH as a function of the 2nd dissociation constant ($\mathrm{pK}_2 = -\log \mathrm{K}_2$) of an indicator dye, the ratio of the absorbance of base and acid forms of the dye in solution

(R, measured at the wavelength of maximum absorbance for each form), and the molar absorptivity ratios (e_1-e_3) for the dye as defined above:

$$\mathrm{pH} = -\log[\mathrm{H^+}] = \mathrm{pK_2} + \log\frac{(\mathrm{R}-e_1)}{(e_2-Re_3)} \quad [9]$$

Which is equivalent to the well known Henderson–Hasselbalch equation:

$$\mathrm{pH} = -\log[\mathrm{H^+}] = \mathrm{pK_2} + \log\frac{[\mathrm{I^{2-}}]}{[\mathrm{HI^-}]} \quad [10]$$

Equations (9) and (10) are only valid for ideal solutions when the dye and background electrolyte concentration approaches infinite dilution. For non-ideal solutions (i.e. as in natural water and soil solutions) such equations must be modified to account for the effect of ionic strength on ion activity. Ion activity (a_i) is related to concentration by:

$$a_i = c_i\,\gamma_i \quad [11]$$

Where c_i is the molar concentration of the solution species i and γ_i is the activity coefficient for this species. Individual ion activity coefficients (γ) can be estimated using the Davies equation:[1]

$$\log\gamma = -Az^2\left(\frac{\mu^{1/2}}{1+\mu^{1/2}} - 0.3\mu\right) \quad [12]$$

Where A is the ion size parameter[1], z is the charge on the ion, and μ is ionic strength. The Davies equation is considered reliable at ionic strengths <0.5 M [36].

Therefore for the application of this equation to the 2nd dissociation constant of a sulfonephthalein indicator dye, the individual ion activity coefficient terms (γ_{I2-}, γ_{H+}, γ_{HI-}) are included for the dye dissociation:

$$\mathrm{pH} = -\log[\mathrm{H^+}]\,\gamma_{H+} = \mathrm{pK_2} + \log[\mathrm{I^{2-}}]\,\gamma_{I2-} / [\mathrm{HI^-}]\,\gamma_{HI-} \quad [13a]$$

$$\mathrm{pH} = \mathrm{pK_2} + \log[\mathrm{I^{2-}}]/[\mathrm{HI^-}] + \log(\gamma_{I2-}\,\gamma_{H+}/\gamma_{HI-}) \quad [13b]$$

[1]$A = 0.5092 + (T - 298.15) * 8.5 * 10^{-4}$ where T is temperature in Kelvin.

While each individual ion activity coefficient could be calculated separately using the Davies equation (12), the charge (z^2) terms for calculation of the individual ion activity coefficients of the dye can be combined (as other parameters in the Davies equation are constant for a given solution) to calculate an overall mixed z^2 value ($z\pm^2$) such that:

$$z_{\pm}^2 = \frac{z_{I2-}^2 \, z_{H+}^2}{z_{HI-}^2} = \frac{2^2 \times 1^2}{1^2} = 4 \qquad [14]$$

By combining equation (9) with the Davies equation (12) to account for how the I^{2-}, HI^-, and H^+ activity coefficients change with ionic strength, and using $z^2 = 4$ in the Davies equation, pH can now be calculated for a solution with indicator dye added via:

$$\mathrm{pH} = -\log[\mathrm{H}^+] = \mathrm{pK}_2 + \log\frac{(\mathrm{R}-e_1)}{(e_2 - Re_3)} - 4A\left(\frac{\mu^{1/2}}{1+\mu^{1/2}} - 0.3\mu\right) \qquad [15]$$

Table 2. PR and BCP (e_1-e_3) and pK_a values at zero ionic strength and 25˚C.

Indicator	Wavelength range (λ_1- λ_2)	e_1	e_2	e_3	pK_a
PR	433-558	0.00244	2.734	0.1075	8.03
BCP	432-589	0.00387	2.858	0.0181	6.49

From Yao and Byrne (2001), Spectrophotometric determination of freshwater pH using bromocresol purple and phenol red, Environ. Sci. Technol. 35 (2001) 1197−1201.

CHAPTER 4

Spectrophotometric measurement of the pH of soil extracts using a multiple indicator dye mixture

Sima Bargrizan[a], Ronald J. Smernik[a], and Luke M. Mosley[b]

[a] The School of Agriculture, Food and Wine, The University of Adelaide, South Australia

[b] Acid Sulfate Soils Centre, School of Biological Sciences, The University of Adelaide, South Australia

Bargrizan S, Smernik RJ, Mosley LM (2018). Spectrophotometric measurement of the pH of soil extracts using a multiple indicator dye mixture. *European Journal of Soil Science*, https://doi.org/10.1111/ejss.12745

Statement of Authorship

Title of Paper	Spectrophotometric measurement of the pH of soil extracts using a multiple indicator dye mixture.
Publication Status	☑ Published ☐ Accepted for Publication ☐ Submitted for Publication ☐ Unpublished and Unsubmitted w ork w ritten in manuscript style
Publication Details	2018, European Journal of Soil Science, doi: 10.1111/ejss.12745.

Principal Author

Name of Principal Author (Candidate)	Sima Bargrizan		
Contribution to the Paper	Accomplished experiment, data collection, data analysis and interpretation, wrote manuscript.		
Overall percentage (%)	70%		
Certification:	This paper reports on original research I conducted during the period of my Higher Degree by Research candidature and is not subject to any obligations or contractual agreements with a third party that would constrain its inclusion in this thesis. I am the primary author of this paper.		
Signature		Date	21.01.2019

Co-Author Contributions

By signing the Statement of Authorship, each author certifies that:

i. the candidate's stated contribution to the publication is accurate (as detailed above);

ii. permission is granted for the candidate in include the publication in the thesis; and

iii. the sum of all co-author contributions is equal to 100% less the candidate's stated contribution.

Name of Co-Author	Luke Mosley		
Contribution to the Paper	Supervised development of work, data interpretation and manuscript evaluation and correction, and acted as corresponding author.		
Signature		Date	21.01.2019

Name of Co-Author	Ron Smernik		
Contribution to the Paper	Supervised development of work, data interpretation, manuscript evaluation and correction.		
Signature		Date	21.01.2019

European Journal of Soil Science

European Journal of Soil Science, 2018 doi: 10.1111/ejss.12745

Spectrophotometric measurement of the pH of soil extracts using a multiple indicator dye mixture

S. Bargrizan[a], R. J. Smernik[a] & L. M. Mosley[b]

[a]*The School of Agriculture, Food and Wine, The University of Adelaide, Adelaide, South Australia, PMB 1, Glen Osmond, SA 5064, and* [b]*Acid Sulfate Soils Centre, School of Biological Sciences, The University of Adelaide, Adelaide, South Australia, PMB 1, Glen Osmond, SA 5064*

Summary

This paper describes the development of a spectrophotometric method with an expanded pH range of 3–9 that uses a mixed indicator solution (equimolar bromophenol blue, bromocresol purple, *m*-cresol purple and thymol blue). The method uses measurements of absorbance of the dye mixture at two wavelengths (434 and 585 nm), chosen to represent the average acid and base peak maxima of the individual dyes within the mixture. The ratio of absorbance at these two wavelengths was used to calculate pH based on measured dye properties (p*K*a, molar absorptivity) and fundamental equations derived from Beer's law. The mixed dye spectrophotometric pH measurement was tested using certified pH buffers ($pH_{(NBS/NIST)}$ 4.00, 6.86, 9.18) and was found to be accurate to within ± 0–0.06 pH units. Measurements made with the mixed dye showed good correlation against conventional soil pH measurement using a glass electrode ($r = 0.99$), and also an alkalinity titration ($r = 0.99$) through the pH range 3–9. The average standard deviation was 0.07 for spectrophotometric soil pH measurement ($n = 30$) using the dye mixture. The mixed dye technique expands the working range of spectrophotometric pH measurement methods in soils and other applications.

Highlights

- We developed a novel spectrophotometric method for measuring soil pH using a mixed indicator dye.
- The method greatly extends the working soil pH range of previous single indicator dye approaches.
- The results were well correlated with glass electrode measurements between pH 3 and 9.
- The method provides new opportunities to study soil chemical processes affected by pH.

Introduction

Soil pH is a master variable for chemical and biological processes such as equilibria among inorganic carbon species (Suarez, 1977), metal solubility, nutrient availability and microorganism activity (Miller & Kissel, 2010; Essington, 2015). A relatively minor change in pH (± 0.1 units) can induce significant changes in the availability of chemical species (e.g. metals, nutrients and carbonates) in soil (Lindsay, 1979).

Conventional soil pH measurement with a glass electrode (Heintze, 1934; Rayment & Lyons, 2011) suffers from several inherent deficiencies. Unpredictability in liquid junction potential (Millero, 1986) has been shown to cause an error of 0.03 pH units across a 10-unit alteration in salinity (Easley & Byrne, 2012). Other problems include considerable drift, especially in low ionic strength solutions (Yuan & DeGrandpre, 2008), and the requirement that electrode calibration procedures match the ionic strength of samples (Wiesner *et al.,* 2006; Miller & Kissel, 2010).

Spectrophotometric pH measurement involving addition of a single indicator dye is used widely in marine chemistry because of its reliability and high precision (Clayton & Byrne, 1993; Yao & Byrne, 2001; Mosley *et al.*, 2004; Lai *et al.*, 2016). Spectrophotometric methods avoid the problems associated with potentiometric pH measurement using a glass electrode (Yao & Byrne, 2001).

Spectrophotometric measurement has recently been adapted to determine soil pH, where it achieved a similar precision (0.02–0.08 pH unit) to conventional potentiometric techniques (Bargrizan *et al.*, 2017). However, the phenol red (p*K*a = 8.03) and bromocresol purple (p*K*a = 6.49) dyes used in that study, like other sulfonephthalein dyes, are useful only in a narrow pH range of approximately ± 1 pH unit from the pK_a of the individual dye (King & Kester, 1990; Yao & Byrne, 2001). A narrow working range has not been a major issue for spectrophotometric pH measurement in seawater (which has a relatively small pH range), but it causes problems for

Correspondence: L. Mosley. E-mail: luke.mosley@adelaide.edu.au
Received 29 October 2017; revised version accepted 12 September 2018

© 2018 British Society of Soil Science

spectrophotometric pH measurement in soils, which have a much wider variation in pH (Miller & Kissel, 2010), even within a single soil profile (pH range of 3–7) (Mosley *et al.*, 2017). Thus, conventional spectrophotometric measurement of soil pH with a single indicator dye would require prior knowledge of the likely pH or pretesting with different dyes.

There has been some previous research using multiple dye mixtures for pH measurement. King & Kester (1989) carried out spectrophotometric measurement of seawater pH and alkalinity titration using a mixture of two indicators, namely phenol red and bromocresol green (pKa = 7.492 and 4.410, respectively, in seawater). Their approach was limited by the fact that only low and high pH (end points) could be measured precisely within the range of 3–8.2 because the pKa values of these two dyes are separated by more than 2 pH units. Lin & Liu (2000) and Raghuraman *et al.* (2006) tested multiple (three to four) dye mixtures where the individual pK_a values of the dyes were approximately 2 pH units apart (i.e. chosen so that when the working range of one dye ends, the working range of another begins).

Raghuraman *et al.* (2006) formulated a theoretical basis for pH determination based on the ratio of absorbances of the mixed dye's acid and base peaks, measured at common wavelengths. However, the individual dyes chosen in their study had acid and base peak absorbance maxima at quite different wavelengths, which makes it difficult to find a suitable common wavelength. Moreover, their method did not appear to be validated against certified pH buffer solutions, tested against glass electrode pH measurement methods or optimized for soil solutions.

A multiple dye technique had also been developed for colorimetric pH measurement in soils (Raupach & Tucker, 1959). Although this method is still used for non-research applications (e.g. garden soil test kits), its accuracy is quite poor (±0.5 pH units) because pH has to be estimated visually by comparing the colour of soil treated with dye against a standard colour chart that has a resolution of only 0.5 pH units (Rayment & Lyons, 2011). In general, it is difficult to formulate a combination of sulfonephthalein dyes for colorimetric measurement because colour intensity changes with pH can be quite difficult to detect (Netto *et al.*, 1995). The advantage of the spectrophotometric method is that subtle changes in light absorbance spectra can be readily resolved and accurately related to the solution pH. A potential advantage of the spectrophotometric pH method using indicator dyes in soil is that it could be used to study pH in several dimensions, which is critically important for better assessment of geochemical reactions and plant–solute (e.g. nutrients, metals) interactions in soil. For example, Blossfield & Gansert (2007) demonstrated the use of high-resolution optical scanning methods to quantify *in situ* pH around the rhizosphere, which showed considerable complexity and provided more information than typical bulk soil measurements. Hyperspectral cameras and scanners potentially allow the full spectra to be measured, and therefore spectrophotometric pH in many spatial dimensions.

The aim of this study was to develop a spectrophotometric method, involving the addition of a multiple indicator dye solution, to enable measurement across the typical range of soil pH values (between 3 and 9). The accuracy of the method was tested against standard buffer solutions and the results were compared with conventional glass electrode measurements of soil extracts and an alkalinity titration.

Materials and methods

Theory

The pH can be calculated by spectrophotometric measurement using a single sulfonephthalein indicator dye as follows (Yao & Byrne, 2001; Bargrizan *et al.*, 2017):

$$\mathrm{pH} = -\log\left[H^+\right] = \mathrm{p}K_a + \log\frac{\left(R - e_1\right)}{\left(e_2 - Re_3\right)} - 4A\left(\frac{\mu^{\frac{1}{2}}}{1+\mu^{\frac{1}{2}}} - 0.3\mu\right), \quad (1)$$

where pKa is the second acid dissociation constant of the dye (at zero ionic strength), the second term in the equation is obtained by substitution for the ratio of the unprotonated base form (I^{2-}) to the protonated acid (HI^-) forms of the indicator in the Henderson–Hasselbalch (H–H) equation:

$$\left(\mathrm{pH} = \mathrm{p}K_a \quad + \log\left(\frac{I^{2-}}{HI^-}\right)\right),$$

and R is defined as the ratio of the absorbance of the base to acid forms of indicator measured at the wavelengths of maximum absorption (λ_2 and λ_1, respectively), e_1–e_3 are molar absorbance ratios (obtained by measuring molar absorption coefficients (ε) when only base and acid forms of dye are present at pH values much greater and less than the dye pKa, respectively), and the last term in Equation (1) is the Davies equation expression to calculate the mean activity coefficient for the dye where A is the ion size parameter (0.5092 at 25°C) and μ is ionic strength (note this equation is only appropriate for $\mu < 0.5$ M activity corrections (Stumm & Morgan, 1996)).

Similarly, for a mixture of two or more sulfonephthalein dyes, pH can be calculated using knowledge of the properties of the individual dyes in the mixture and measurement of their absorption spectra (Raghuraman *et al.*, 2006). Starting with a mixture of two dyes, each containing separate acid (A_1 and A_2) and base (B_1 and B_2) species, respectively, an expression for cumulative absorbance of the dye mixture at common wavelengths (λ_1 and λ_2, respectively) can be formulated:

$$\mathrm{abs}_{\lambda 1} = \varepsilon_{A1}^{\lambda 1} l\left[A_1\right] + \varepsilon_{B1}^{\lambda 1} l\left[B_1\right] + \varepsilon_{A2}^{\lambda 1} l\left[A_2\right] + \varepsilon_{B2}^{\lambda 1} l\left[B_2\right], \quad (2)$$

and

$$\mathrm{abs}_{\lambda 2} = \varepsilon_{A1}^{\lambda 2} l\left[A_1\right] + \varepsilon_{B1}^{\lambda 2} l\left[B_1\right] + \varepsilon_{A2}^{\lambda 2} l\left[A_2\right] + \varepsilon_{B2}^{\lambda 2} l\left[B_2\right], \quad (3)$$

where based on Beer's law, absorbance is proportional to the concentration (denoted by [ ]) of the absorbing dye species (A_i or B_i), the molar absorptivity coefficients ($\varepsilon_{\lambda i}$) at wavelengths λ_i for A_i and B_i, and the spectrophotometric cell pathlength (l). A ratio (R_{multi}) of the cumulative absorbance of the base and acid species in the two dyes at λ_2 to λ_1 can be calculated:

$$R_{\text{multi}} = \frac{\text{abs}^{\lambda 2}}{\text{abs}^{\lambda 1}} = \frac{\varepsilon_{A1}^{\lambda 2} l \left[A_1\right] + \varepsilon_{B1}^{\lambda 2} l \left[B_1\right] + \varepsilon_{A2}^{\lambda 2} l \left[A_2\right] + \varepsilon_{B2}^{\lambda 2} l \left[B_2\right]}{\varepsilon_{A1}^{\lambda 1} l \left[A_1\right] + \varepsilon_{B1}^{\lambda 1} l \left[B_1\right] + \varepsilon_{A2}^{\lambda 1} l \left[A_2\right] + \varepsilon_{B2}^{\lambda 1} l \left[B_2\right]}. \quad (4)$$

Equation (4) can be rewritten following substitution of $10^{-\left(\text{pH}-\text{p}K'_{ai}\right)}$ for $\frac{[A_i]}{[B_i]}$ (see H–H equation above) and extended to a mixture of n dyes:

$$R_{\text{multi}} = \frac{\sum_i \varepsilon_{Bi}^{\lambda 2} \frac{[B_i]}{[B_1]} \left(1 + \frac{\varepsilon_{Ai}^{\lambda 2}}{\varepsilon_{Bi}^{\lambda 2}} 10^{-\left(\text{pH}-\text{p}K'_{ai}\right)}\right)}{\sum_i \varepsilon_{Ai}^{\lambda 1} \frac{[B_i]}{[B_1]} \left(10^{-\left(\text{pH}-\text{p}K'_{ai}\right)} + \frac{\varepsilon_{Bi}^{\lambda 1}}{\varepsilon_{Ai}^{\lambda 1}}\right)}, \quad \text{for } i = 1, n \quad (5)$$

where

$$\frac{[B_i]}{[B_1]} = \frac{1 + 10^{-\left(\text{pH}-\text{p}K'_{a1}\right)}}{1 + 10^{-\left(\text{pH}-\text{p}K'_{ai}\right)}} \frac{f_i}{f_1}, \quad (6)$$

and f_i is the mole fraction of dye i determined by dividing each dye concentration (in mol l^{-1}) by the total concentration of mixed dye and pK'_a is the dissociation constant of the dye at the specific ionic strength of the sample solution, which is calculated by the Davies equation (as outlined above):

$$\text{p}K'_a = \text{p}K_a - 4A\left(\frac{\mu^{\frac{1}{2}}}{1 + \mu^{\frac{1}{2}}} - 0.3\mu\right). \quad (7)$$

For a full derivation of these equations, see the Supporting Information.

Experimental

Selection of dye mixture

The above theory relies on selecting a dye mixture that covers the pH range of interest and measurement at two wavelengths (λ_1 and λ_2) chosen to represent the absorbance of the acid and base species of all the indicator dyes in the mixture. Full spectral modelling of the multiple dye mixture could potentially enable a wider range of dyes to be assessed (Ohline *et al.*, 2007) because it would not rely on just the assessment at two wavelengths. However, this is likely to be more complex in terms of spectral analysis and might not be possible as many of the dyes have very similar absorption spectra (which makes separation of individual contributions difficult).

It is required that (i) the pK_a of the individual dyes in the mixture are collectively able to cover the entire desired range of pH by being within approximately 2 units of each other (the individual dyes have a limited working pH range as discussed above) and (ii) the individual dyes have similar wavelengths of maximum acid and base peak absorbance to maximize sensitivity at the wavelengths chosen for measurement (λ_1 and λ_2).

Different sulfonephthalein dyes have different absorbance spectra; Figure 1 shows spectra of six common indicator dyes: phenol red (PR), bromocresol purple (BCP), bromophenol blue (BPB), *m*-Cresol purple (*m*CP), bromocresol green (BCG) and thymol blue (TB). The acid peak wavelength is similar for all the dyes, but the base peak wavelengths for phenol red and bromocresol green are to the right and left, respectively, of the base peak wavelengths of the other four dyes. Therefore, in this study an indicator dye mixture comprising BPB, BCP, *m*CP and TB was chosen for testing because it fulfilled both requirements (i) and (ii) above. The vertical dashed lines in Figure 1(a,b) show the common wavelengths ($\lambda_1 = 434$ nm, $\lambda_2 = 585$ nm) that were chosen to represent the respective average acid and base peak maxima of the four-dye mixture. There are other dyes within the pH range of interest, such as cresol red (7–8.8), bromophenol red (5.2–6.8) and chlorophenol red (4.8–6.4), that could potentially be used in a mixture, taking into consideration the selection criteria above. Fewer dyes in the mixture could also be considered if the soils of interest covered a narrow soil pH range.

Molar absorption and pK_a determination

It is important to note that because the chosen wavelengths ($\lambda_1 = 434$ nm, $\lambda_2 = 585$ nm) did not correspond precisely with the peak maxima for each individual dye (Figure 1), the molar absorptivity (ε) had to be determined at these wavelengths. Previous literature values of ε for these dyes have typically been measured at the maximum peak absorbance, which is appropriate for individual dye measurement. Therefore, the molar absorptivities ($\varepsilon_{\lambda i}$) of the above dyes were measured at extreme pH values where either acid or base from of each dye was present (Clayton & Byrne, 1993) by adjusting a diluted stock solution of the dye using 1 mol l^{-1} HCl and 0.1 mol l^{-1} NaOH, respectively. The measured absorbance, known concentration of the diluted stock solution and cell pathlength (1 cm) were used to calculate $\varepsilon_{\lambda i}$ with Beer's law.

The pK_a value of BCP has been measured accurately for spectrophotometric pH measurement by Yao & Byrne (2001). The pK_a values of BPB, *m*CP and TB have received less attention and so they were determined at 25°C by the addition of a single indicator dye to certified pH buffer solutions (i.e. $\text{pH}_{\text{NBS/NIST}}$ 4.00 phthalate buffer (0.05 mol kg^{-1}), $\text{pH}_{\text{NBS/NIST}}$ 6.86 phosphate buffer (0.025 mol kg^{-1}) and $\text{pH}_{\text{NBS/NIST}}$ 9.18 disodium tetraborate buffer (0.01 mol l^{-1})). The standard reference materials used to prepare the phthalate and phosphate buffers were NIST 185i and 186g, respectively (they refer to certification documentation on the NIST website for buffer preparation), and Certipur® (traceable to NIST) was used for the disodium tetraborate buffer. To enable comparison with the pH defined in the spectrophotometric method based on hydrogen ion concentration (free hydrogen ion scale, pH_{free}, Equation (1)), correction of pH (based on the hydrogen ion activity scale, $\text{pH}_{\text{NBS/NIST}}$)

© 2018 British Society of Soil Science, *European Journal of Soil Science*

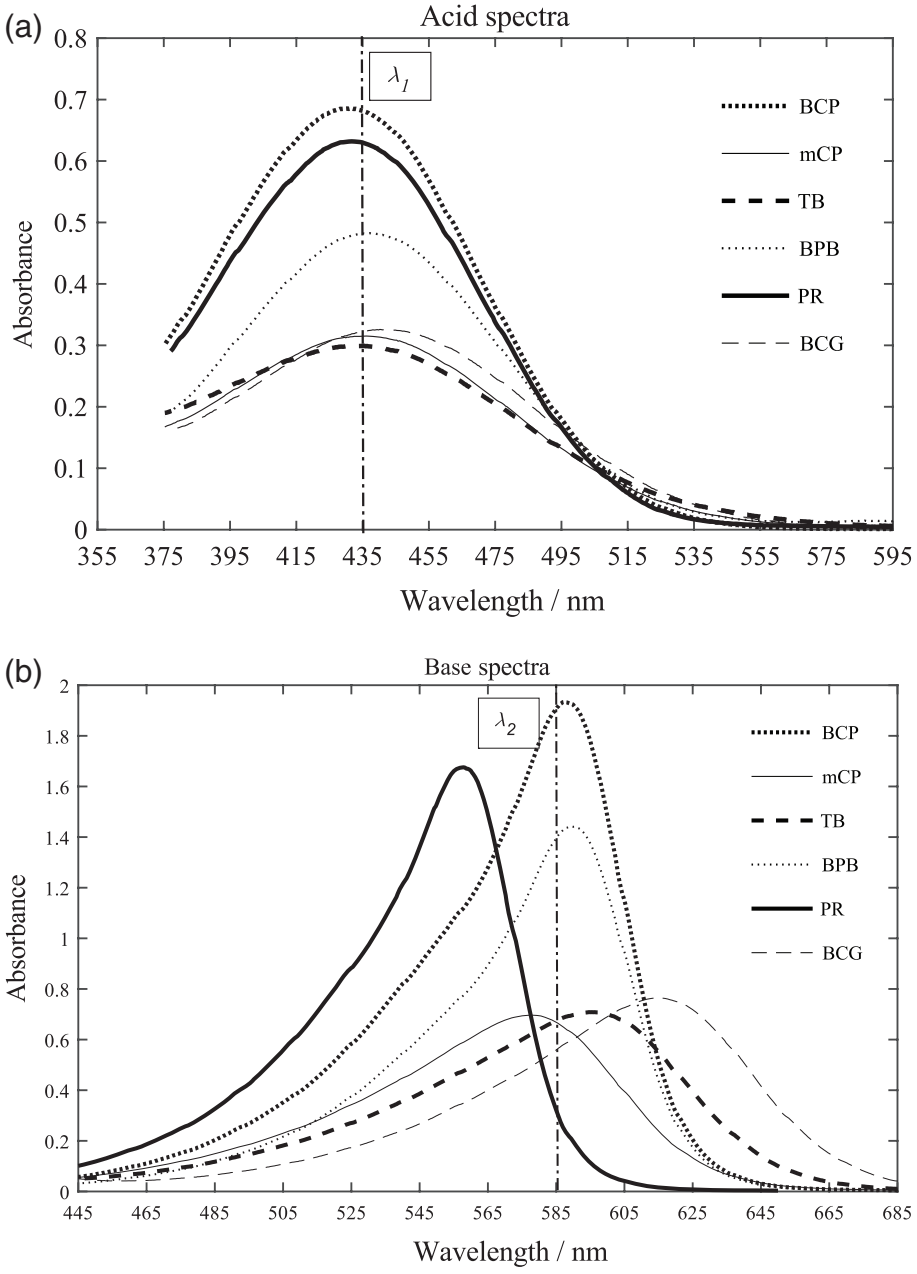

Figure 1 Comparison of (a) acid and (b) base spectra of different dyes (BPB, bromophenol blue; BCG, bromocresol green; BCP, bromocresol purple; PR, phenol red; *m*CP, *m*-cresol purple; TB, thymol blue). The vertical dashed lines are the chosen wavelengths where the multiple dye mixture acid (λ_1) and base peak (λ_2) absorbances were measured.

of these buffers was carried out using Equation (8) (Bargrizan *et al.*, 2017):

$$\mathrm{pH_{free}} = -\log\left[H^+\right] = \mathrm{pH_{NBS/NIST}} + \log\gamma_{H+}, \qquad (8)$$

where γ is the activity coefficient calculated with the Davies equation. This gave pH values of 3.91, 6.77 and 9.11 for the three buffers. With R at the peak maxima for three dye additions (0.01, 0.02, 0.03 ml) and corrected by linear interpolation to zero ionic strength to remove the small perturbations in dye pH (see Bargrizan *et al.*, 2017), Equation (1) and the Davies equation ionic strength correction for the dye (Yao & Byrne, 2001), the pK_a of each indicator was then calculated. All glass electrode pH measurements ($\mathrm{pH_{elec}}$) expressed later were also corrected to the free hydrogen ion scale. The certified pH buffers with known pH (4.00, 6.86, 9.18) were also used to test the accuracy of the mixed dye solution.

Spectrophotometric and glass electrode pH measurements

For multiple dye mixture measurements using the spectrophotometric method, a stock solution containing bromocresol purple (BCP), bromophenol blue (BPB), *m*-cresol purple (*m*CP) and thymol blue (TB) was prepared at a total dye concentration of 8×10^{-3} mol l^{-1} using equal mole fractions ($f = 0.25$) and adjusted to pH ≈ 7 using 0.1 mol l^{-1} NaOH. During sample measurement, the mixed dye stock solution concentration was 2×10^{-5} mol l^{-1}

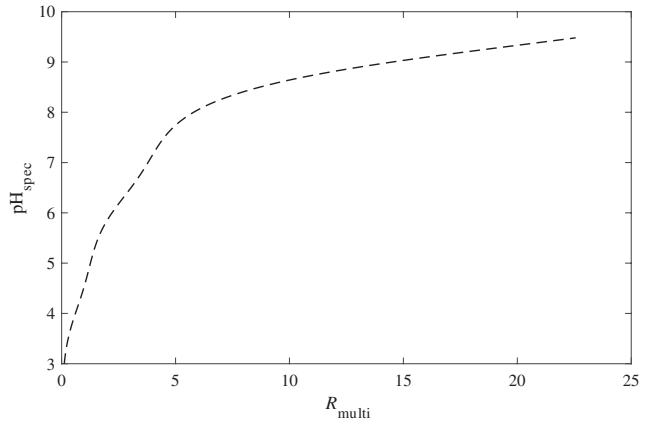

Figure 2 Theoretical curve to estimate pH_{spec} from the measured ratio (R_{multi}) of the mixed indicator dye base and acid species absorbances at the chosen wavelengths ($\lambda_1 = 434$ nm, $\lambda_2 = 585$ nm) at $\mu = 0.1$ M for standard phosphate buffer.

to 6×10^{-5} mol l^{-1} depending on the volume (0.01, 0.02, 0.03 ml sequential additions) of dye added into 4 ml of sample in a 1-cm glass cuvette. The reason for sequential addition of the dye is to account for the effect of any indicator-induced pH perturbation (Clayton & Byrne, 1993). Full details of the spectrophotometric procedure for soil pH measurement can be found in Bargrizan *et al.* (2017).

The maximum acid and base absorbances were at 434 and 585 nm on a dual-beam spectrophotometer (GBC UV/VIS 916, Melbourne, Australia) connected to Cintral™ software. With Equation (5), a theoretical relation for the dye mixture R_{multi} (measured at 434 and 585 nm) against pH was calculated from pH 3 to 9 (at 0.01 pH intervals) and this relation is plotted in Figure 2. Because of the complexity and difficulty of solving Equation (5) analytically, a look-up table was created in Microsoft Excel™ to convert a measured R_{multi} value to its corresponding pH value to the nearest 0.01 pH unit (Table S3, Supporting Information). The R_{multi} value is unique both to the dye mixture and the individual dye mole fractions comprising the mixture. Further, the ionic strength of the sample solution affects the relation between R_{multi} and pH. This effect is corrected implicitly by the Davies equation, which corrects pK_a (at $\mu = 0$) to pK_a' at variable ionic strength. The potential effect of any weighing errors on mole fractions of individual dyes used to calculate R_{multi} was assessed by changing mole fractions by a factor of 0.0025 (error of 1% on mole fraction of 0.25) and recalculating (Figure S3, Supporting Information). There was a difference in the R_{multi} calculated for the equal mole fraction of the order ± 0.001 to 0.1 units (Figure S4, Supporting Information). This difference increased as R and pH increased, and also varied depending on which dye pair the mole fraction was varied. This suggests care should be taken in preparing mole fractions of dyes to minimize any weighing and other errors in the preparation of the mixed dye solution.

The pH was measured simultaneously with a glass electrode (Orion SureFlow model™, Waltham, MA, U.S.A.) connected to a TPS™ model pH meter after calibrating with commercially available buffers ($\mu \approx 0.1$ mol l^{-1}) at 25°C. The pH electrode ($pH_{NBS/NIST}$) measurements were corrected to the pH_{free} scale using Equation (8) above.

Alkalinity titration

To compare pH determined by the mixed dye method, pH_{spec}, to pH_{elec} throughout the pH range of interest, an alkalinity titration was performed. Mixed dye solution (250 µl) was added to 100 ml of a Na_2CO_3 solution (400 mg l^{-1} as $CaCO_3$) and titrated using 1.600 N sulphuric acid. The volume of acid added by the digital titrator (HACH™) was recorded throughout the titration. The pH was measured using a glass electrode after every 20-µl incremental addition of sulphuric acid. Simultaneously, 4 ml of this solution was pipetted to the cuvette for spectrophotometric pH measurement and then tipped back into the titration flask. The titration was continued until pH < 3 was achieved.

Soil-solution preparation

To test the mixed dye method for use in soils, soil samples ($n = 10$) within the range of pH 3–9 were analysed (Table S4, Supporting Information). Three replicates of each soil extract (1:1 25 g soil to 25 ml water) were used for spectrophotometric and glass electrode measurements of pH at 25°C. Refer to Bargrizan *et al.* (2017) for more details on soil extract preparation and measurement.

Results and discussion

Indicator properties and comparison of results with previous studies

Table 1 and Table S1 (Supporting Information) summarize the characteristics of the individual indicators that made up the mixed dye. The pK_a value obtained for *m*CP (8.64) was very similar to the value of 8.63 reported by Mosley *et al.* (2004) and 8.66 by Lai *et al.* (2016). The measured pK_a values for TB and BPB determined in our study were 9.22 and 4.34, respectively. Our value for TB was slightly larger than those determined by Mosley *et al.* (2004, $pK_a = 9.12$) and Bishop (1972, $pK_a = 9.20$). The pK_a of BPB reported by Shokrollahi & Zare (2016) was exactly the same as the value we

Table 1 Individual indicator properties at 25°C

Dye	Peak absorbance of acid / nm	Peak absorbance of base / nm	$pK_a(\mu = 0)$	pH range
BPB	436	592	4.34	3.0–4.6
BCP	432	589	6.49[a]	5.3–6.8
*m*CP	434	578	8.64	7.4–9.0
TB	435	596	9.22	8.0–9.6

[a]From Yao & Byrne (2001).
BPB, bromophenol blue; BCP, bromocresol purple; *m*CP, *m*-cresol purple; TB, thymol blue.

© 2018 British Society of Soil Science, *European Journal of Soil Science*

Table 2 Molar absorption coefficients (ε) at the chosen mixed indicator dye wavelengths ($\lambda_1 = 434$ nm, $\lambda_2 = 585$ nm) at 25°C

	Indicator dye							
	BCP		mCP		BPB		TB	
Dye species	Acid	Base	Acid	Base	Acid	Base	Acid	Base
Extreme pH measured at	pH = 3	pH = 10	pH = 4.5	pH = 11.5	pH = 2	pH = 8.5	pH = 3.5	pH = 12
ε at λ_2 (585 nm)	135	64 893	215	33 721	741	68 277	233	33 875
ε at λ_1 (434 nm)	23 014	1289	15 761	2103	23 496	885	14 957	1370

BCP, bromocresol purple; *m*CP, *m*-cresol purple; BPB, bromophenol blue; TB, thymol blue.

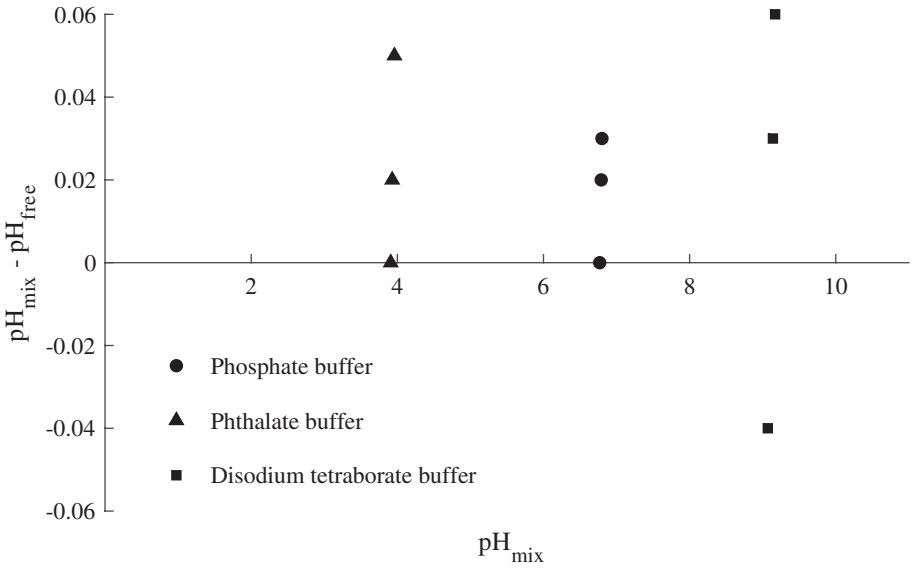

Figure 3 Difference between spectrophotometric pH measurement using mixed dye (pH_{spec}) and certified pH values (pH_{free}) of certified standard buffer solutions.

obtained. The pK_a value obtained for BPB was about 0.24 pH units higher than that provided by Bishop (1972). The reason for the larger discrepancies observed between our pK_a values and those of Shokrollahi & Zare (2016) and Bishop (1972) for BPB is unclear; however, it might relate in part to dye impurities (Liu *et al.*, 2011).

Table 2 shows the molar absorptivity results for individual indicators. These ε values, and the pK_a values shown in Table 1, were used in Equations (5) and (6) to calculate the value of R_{multi} as a function of pH.

Measurement on standard pH buffers

The accuracy of the pH values determined using the mixed indicator dye approach was tested against certified reference phosphate ($pH_{free} = 6.77$), phthalate ($pH_{free} = 3.91$) and disodium tetraborate ($pH_{free} = 9.11$) buffer solutions. Figure 3 shows the deviation (residual) of pH measured spectrophotometrically using the mixed dye (pH_{spec}) from the certified pH values. The accuracy was ±0–0.06 pH units using the mixed dye and there appears to be a slight (~0.02 pH unit) positive bias to the residuals. Accuracy was less for the pH 9.11 buffer than for the other buffers. The curve of R_{multi} against pH (Figure 2) suggests that the method is likely to be more sensitive and accurate at pH > 5 (lower slope, so any error in determination of R_{multi} would lead to less error in pH). The pH range through which the protonation of TB varies possibly also has less sensitivity because the base peak is slightly more offset from the common measurement wavelength than for the other dyes (Figure 1). Examination of the mixed dye spectra in the three buffers (Figure 4) indicates low absorbance for the acid peak of the mixed dye in the disodium tetraborate buffer. This is consistent with the range of the chosen dye mixture being limited to pH < 9, as is explored further below in the acid–base titration.

Acid–base titration with mixed indicator

Figure 5(a) shows the pH values for an alkalinity titration determined by spectrophotometric and glass electrode methods. A strong correlation ($r > 0.99$, root mean square error (RMSE) = 0.13) between pH_{elec} and pH_{spec} was observed throughout the pH range 3–9 (Figure 5b). The pH_{spec} readings are on average lower by 0.08 pH units than pH_{elec} throughout this range. For all pH values between 3 and 9, peaks from both acid and base species of at least one component of the mixed dye were present (Figure 6). There is weaker correlation outside this pH range (≤ 3 and ≥ 9) because all the individual dyes in the mixture were predominantly either in their acid (pH < 3) or base form (pH > 9). This is consistent with the findings of Raghuraman *et al.* (2006), who found that

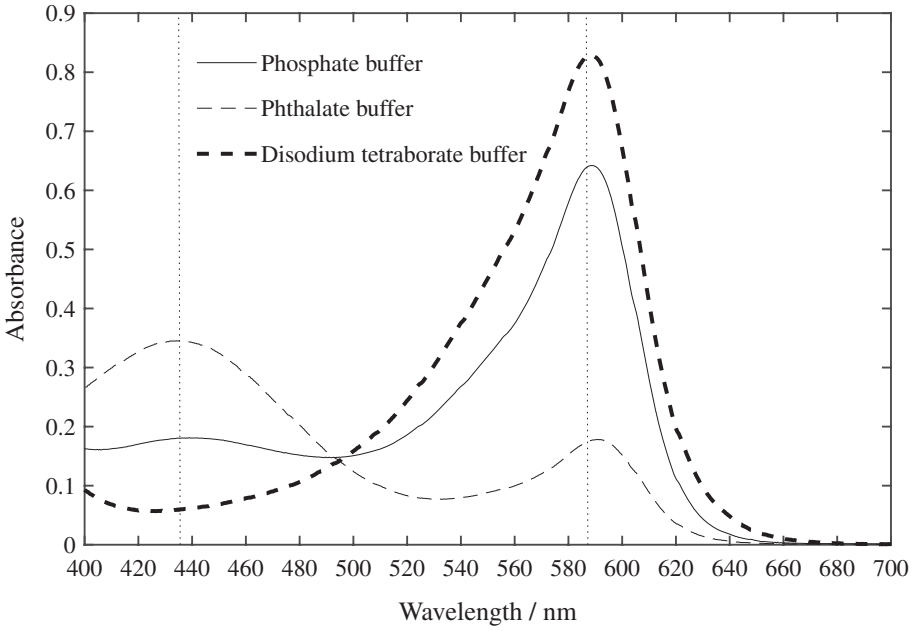

Figure 4 Absorbance plotted against wavelength for the basic (I^{2-}) and acidic (HI^{-}) forms of mixed dye in the certified reference buffer solutions. The vertical dashed red line indicates the selected wavelengths for measurement of 434 and 585 nm, respectively.

accuracy was less at extreme pH values. The colour of the dye at various points during the titration is shown in Table S2, Supporting Information.

The accuracy of spectrophotometric soil pH measurements could be assessed by comparing measured pH with pH calculated by measuring or constraining two other carbonate system parameters (e.g. alkalinity, pCO_2, by equilibrating samples with fixed pCO_2) (Patsavas *et al.*, 2015). This may give a clearer indication of measurement accuracy and comparison of accuracy between pH_{spec} and pH_{elec}.

Comparison of pH for soil extracts determined using spectrophotometric and glass electrode methods

The pH of ten soils across a pH range of 3–9 was analysed spectrophotometrically with the multiple indicator dye mixture and compared with glass electrode measurements (Figure 7). In general, the results obtained from both methods were strongly comparable ($r > 0.99$, RMSE = 0.17) across this wide range of soil pH. However, there was a difference between the two methods; pH_{spec} was + 0.12 units higher than pH_{elec} on average (Figure S1, Supporting Information).

These differences in average pH might relate to liquid junction errors and calibration difficulties with electrodes across variable ionic strengths (Miller & Kissel, 2010). The apparent differences also increase near the pK_a limits of the dye mixture (Figure S1, Supporting Information), which might result from larger errors in spectrophotometric measurements near the limits of the method. This difference does not appear to relate to ionic strength because a plot of residuals against μ showed no systematic pattern (Figure S2, Supporting Information). Errors from the use of non-purified dyes have been estimated to be typically of the order of 0.01–0.02 pH units, which could account for some of the differences (Yao *et al.*, 2007; Liu *et al.*, 2011). Large concentrations of dissolved organic matter in the soil solution might also introduce errors of the order of around 0.01–0.1 pH units (Muller *et al.*, 2018).

The average standard deviations (precision) for the measurement of pH of three replicates of each soil sample were 0.07 and 0.06 pH units for the mixed dye spectrophotometric method and electrode method, respectively. The precision was less than that of single dye measurements in water, which might relate to (i) the greater complexity and influence of the multiple dye mixture preparation and (ii) the fact that the determination of soil pH requires more preparation steps than determination of the pH of water (Bargrizan *et al.*, 2017). Soil samples are also more heterogeneous than water samples and also potentially more influenced by CO_2 produced by microbial respiration of the samples (Zabowski & Sletten, 1991).

Overall, precision of the spectrophotometric method using the mixed dye method is better than the precision of 0.1 pH units suggested as satisfactory for soil pH measurement by Miller & Kissel (2010) and Kalra (1995). The less stringent acceptable limits for precision in the measurement of pH for soil than for water reflects the fact that soil is more heterogeneous, can have a wide pH range and can undergo large fluctuations in pH from processes such as oxidation–reduction and respiration.

The multiple dye method has been designed to cover a wide range of pH that can occur in soil; if narrow pH ranges are the target of investigation use of a single dye approach is recommended (Bargrizan *et al.*, 2017).

A potential major advantage of spectrophotometric methods is that the dye could be readily applied to study spatial and temporal dynamics of pH at high resolution in soil. For example, plant-induced alteration of pH in the root–rhizosphere–soil interface occurs at < mm scales and is of great importance for understanding the (i) physicochemical conditions of plant nutrient acquisition and uptake, (ii) rhizosphere microbial network and

© 2018 British Society of Soil Science, *European Journal of Soil Science*

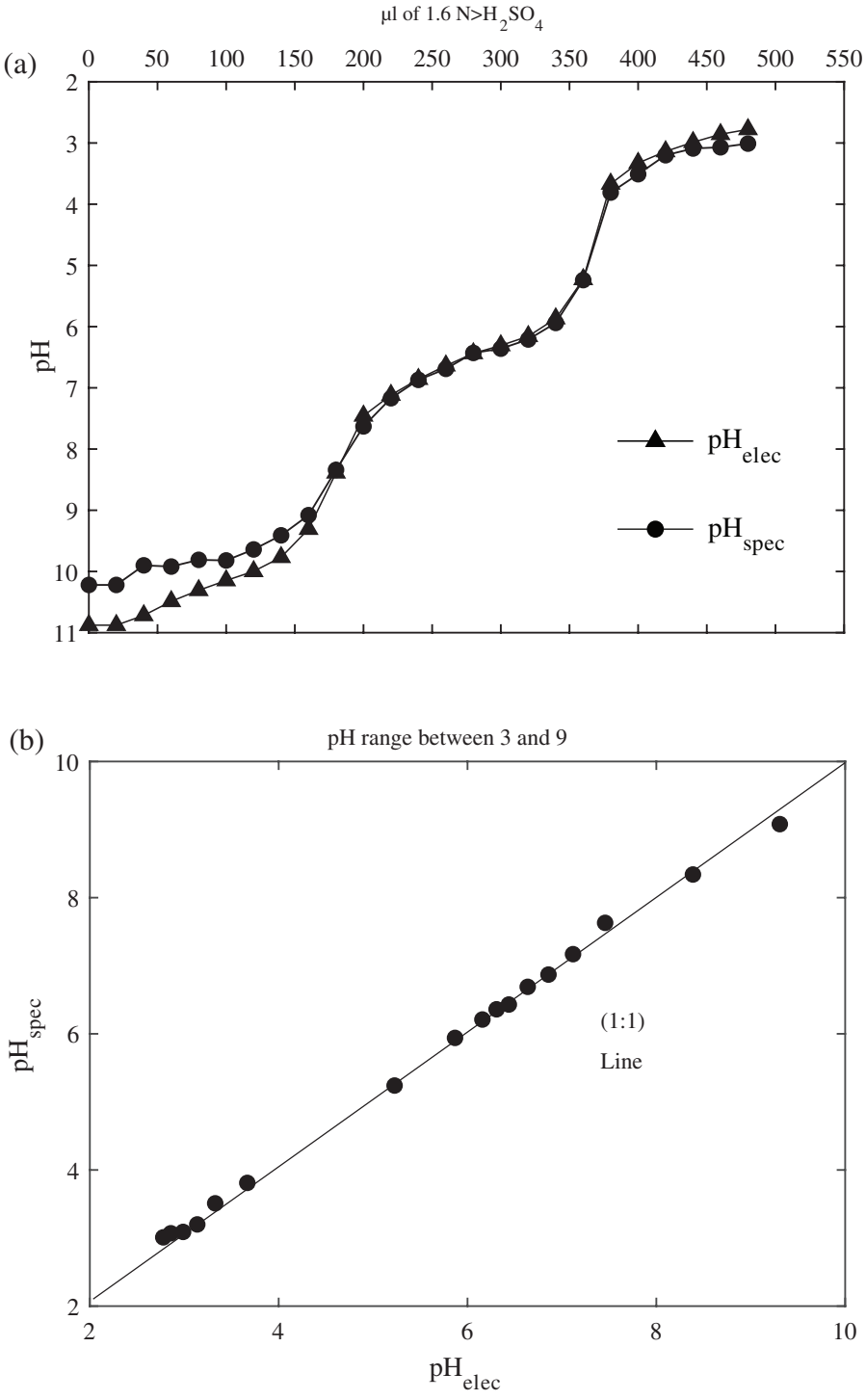

Figure 5 (a) Alkalinity titration of a sodium bicarbonate solution (400 mg l^{-1} as $CaCO_3$) with 1.6 N sulphuric acid. The pH was measured by a spectrophotometric method using the multiple dye mixture and a conventional potentiometric method with a glass electrode. (b) Comparison of spectrophotometric and glass electrode pH measurements over pH range 3–9 in the alkalinity titration ($r = 0.99$).

(iii) biogeochemical production of methane and dinitrous oxide in wetland soils (Blossfeld & Gansert, 2007).

Conclusion

A multiple indicator dye mixture, comprising equimolar concentrations of bromophenol blue, bromocresol purple, *m*-cresol purple and thymol blue, was used to extend the useful pH range of spectrophotometric methods using a single dye compound. The requirement of the individual dyes comprising the mixture to cover the desired pH range was satisfied using this dye mixture. In practical terms, this required that there was a difference of no more than 2 pH units between consecutive dye pK_a values, and that all dyes had approximately similar acid and base peak

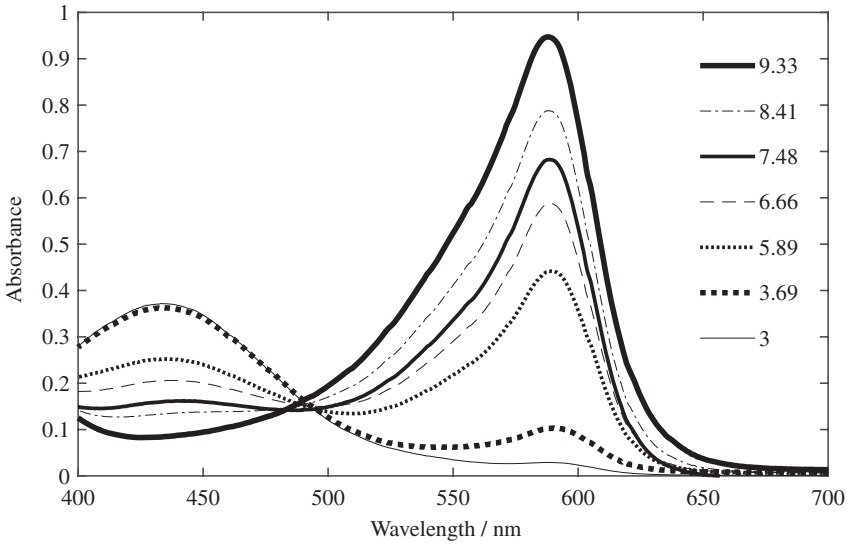

Figure 6 Spectra of the multiple dye mixture at different pH (9.33, 8.41, 7.48, 6.66, 5.89, 3.69, 3) during the alkalinity titration.

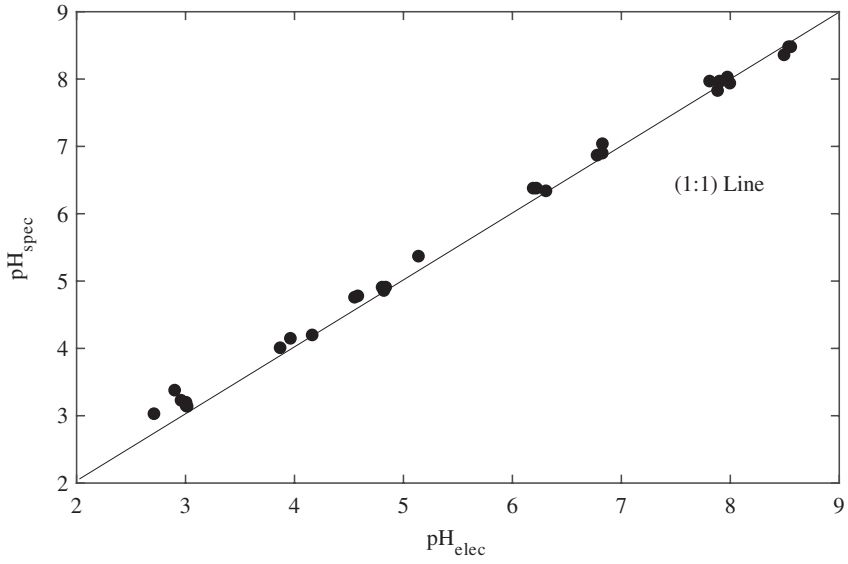

Figure 7 Correlation between spectrophotometric (pH_{spec}) and electrode methods (pH_{elec}) in different soil water extracts ($n = 30$, 10 soil samples × 3 replicates, $r = 0.99$).

wavelength maxima. Spectrophotometric pH measurements using the mixed dye showed an accuracy of approximately ±0–0.06 pH units based on measurement of certified pH standard buffer solutions. The multi-dye performance was further demonstrated in an alkalinity titration, which gave comparable results to the glass electrode method throughout a pH range of 3–9. The results indicate that the proposed mixed dye in this study may be applied to spectrophotometric soil pH measurement with high precision (±0.07), but it would be beneficial to test a wider range of soils with this method. In addition to the potential advantages noted above with spectrophotometric pH methods compared to electrode methods (i.e. lack of drift, liquid junctions or suspension effects), dyes could also be applied to study pH accurately in multiple dimensions (e.g. down a soil profile, around minerals or organic matter, or around the root zone). This opens up new opportunities for research to understand the role of pH better in influencing biogeochemical processes in soils and other systems.

Supporting Information

The following supporting information is available in the online version of this article:

Appendix S1. Derivation of spectrophotometric pH equations using a dye mixture.

Table S1. The mean molar absorption ratios and standard deviations (in brackets) at 25°C for mCP, BCP, BPB and TB (used for single indicator dye measurements at wavelengths of maximum absorption of acid and base forms of the dye).

Table S2. The mixed indicator colour change at selected points (pH values) in the alkalinity titration.

Table S3. The look-up table for Rmulti as a function of pH.

Table S4. Soil physical and chemical properties.

Figure S1. The difference in pH between the spectrophotometric and glass electrode methods plotted against electrode pH values.

© 2018 British Society of Soil Science, *European Journal of Soil Science*

Figure S2. The difference in pH between the spectrophotometric and glass electrode methods plotted against ionic strength (μ).
Figure S3. Effect of changing mole fractions of a four-dye mixture (mCP- BCP-BPB-TB) on R_{multi} as a function of pH.
Figure S4. The residual plot for R_{multi} calculated for the equal and different mole fractions against $R_{equl\text{-}mole.}$

Acknowledgements

We acknowledge the assistance of Zhoubin Maneshi (Heidelberg University) for assistance with justification of the theoretical equations for a mixed dye solution. Sima Bargrizan acknowledges the assistance of a University of Adelaide postgraduate scholarship, and LM acknowledges the assistance of the Australian Commonwealth Government through an Australian Research Council Discovery Project Grant DP170104541. We thank an Associate Editor and anonymous reviewers whose comments enabled us to improve the manuscript.

References

Bargrizan, S., Smernik, R.J. & Mosley, L.M. 2017. Development of a spectrophotometric method for determining pH of soil extracts and comparison with glass electrode measurements. *Soil Science Society of America Journal*, **81**, 1350–1358.

Bishop, E. 1972. *Indicators*. Pergamon Press, Oxford.

Blossfeld, S. & Gansert, D. 2007. A novel non-invasive optical method for quantitative visualization of pH dynamics in the rhizosphere of plants. *Plant, Cell & Environment*, **30**, 176–186.

Clayton, T.D. & Byrne, R.H. 1993. Spectrophotometric seawater pH measurements: total hydrogen ion concentration scale calibration of *m*-cresol purple and at-sea results. *Deep Sea Research Part I: Oceanographic Research Papers*, **40**, 2115–2129.

Easley, R.A. & Byrne, R.H. 2012. Spectrophotometric calibration of pH electrodes in seawater using purified *m*-cresol purple. *Environmental Science & Technology*, **46**, 5018–5024.

Essington, M.E. 2015. *Soil and Water Chemistry: an Integrative Approach*, 2nd edn. CRC Press, New York.

Heintze, S.G. 1934. The use of the glass electrode in soil reaction and oxidation-reduction potential measurements. *Journal of Agricultural Science.*, **24**, 28–41.

Kalra, Y.P. 1995. Determination of pH of soils by different methods: collaborative study. *Journal of AOAC International*, **78**, 310–324.

King, D.W. & Kester, D.R. 1989. Determination of seawater pH from 1.5 to 8.5 using colorimetric indicators. *Marine Chemistry*, **26**, 5–20.

King, D.W. & Kester, D.R. 1990. Spectral modeling of sulfonephthalein indicators: application to pH measurements using multiple indicators. *Applied Spectroscopy*, **44**, 722–727.

Lai, C.Z., DeGrandpre, M.D., Wasser, B.D., Brandon, T.A., Clucas, D.S., Jaqueth, E.J. *et al.* 2016. Spectrophotometric measurement of freshwater pH with purified meta-cresol purple and phenol red. *Limnology and Oceanography Methods*, **14**, 864–873.

Lin, J. & Liu, D. 2000. An optical pH sensor with a linear response over a broad range. *Analytica Chimica Acta*, **408**, 49–55.

Lindsay, W.L. 1979. *Chemical Equilibria in Soils*. John Wiley & Sons Ltd, Chichester.

Liu, X., Patsavas, M.C. & Byrne, R.H. 2011. Purification and characterization of meta-cresol purple for spectrophotometric seawater pH measurements. *Environmental Science & Technology*, **45**, 4862–4868.

Miller, R.O. & Kissel, D.E. 2010. Comparison of soil pH methods on soils of North America. *Soil Science Society of America Journal*, **74**, 310–316.

Millero, F.J. 1986. The pH of estuarine waters. *Limnology and Oceanography*, **31**, 839–847.

Mosley, L.M., Husheer, S.L. & Hunter, K.A. 2004. Spectrophotometric pH measurement in estuaries using thymol blue and *m*-cresol purple. *Marine Chemistry*, **91**, 175–186.

Mosley, L.M., Biswas, T.K., Cook, F.J., Marschner, P., Palmer, D., Shand, P. *et al.* 2017. Prolonged recovery of acid sulfate soils with sulfuric materials following severe drought: causes and implications. *Geoderma*, **308**, 312–320.

Muller, J.D., Schneider, B., Abmann, S. & Rehder, G. 2018. Spectrophotometric pH measurements in the presence of dissolved organic matter and hydrogen sulfide. *Limonology and Oceanography: Methods*, **16**, 68–82.

Netto, E.J., Peterson, J.I., Mcshane, M. & Hampshire, V. 1995. A fiber-optic broad-range pH sensor system for gastric measurements. *Sensors and Actuators B: Chemical*, **29**, 157–163.

Ohline, S.M., Reid, M.R., Husheer, S.L., Currie, K.I. & Hunter, K.A. 2007. Spectrophotometric determination of pH in seawater off Taiaroa Head, Otago, New Zealand: full-spectrum modelling and prediction of pCO_2 levels. *Marine Chemistry*, **107**, 143–155.

Patsavas, M.C., Byrne, R.H., Wanninkhof, R., Feely, R.A. & Cai, W.-J. 2015. Internal consistency of marine carbonate system measurements and assessments of aragonite saturation state: insights from two U.S. coastal cruises. *Marine Chemistry*, **176**, 9–20.

Raghuraman, B., Gustavson, G., Van Hal, R.E.G., Dressaire, E. & Zhdaneev, O. 2006. Extended-range spectroscopic pH measurement using optimized mixtures of dyes. *Applied Spectroscopy*, **60**, 1461–1468.

Raupach, M. & Tucker, B. 1959. The field determination of soil reaction. *Journal of the Australian Institute of Agricultural Science*, **25**, 129–133.

Rayment, G.E. & Lyons, D.J. 2011. *Soil Chemical Methods*. CSIRO Publishing, Melbourne.

Shokrollahi, A. & Zare, E. 2016. Determination of acidity constants of bromophenol blue and phenol red indicators by solution scanometric method and comparison with spectrophotometric results. *Journal of Molecular Liquids*, **219**, 1165–1171.

Stumm, W. & Morgan, J. 1996. *Aquatic Chemistry: Chemical Equilibria and Rates in Natural Waters*, 3rd edn. Wiley Interscience, New York.

Suarez, D.L. 1977. Ion activity products of calcium carbonate in waters below the root zone. *Soil Science Society of America Journal*, **41**, 310–315.

Wiesner, A.D., Katz, L.E. & Chen, C.C. 2006. The impact of ionic strength and background electrolyte on pH measurements in metal ion adsorption experiments. *Journal of Colloid and Interface Science*, **301**, 329–332.

Yao, W. & Byrne, R.H. 2001. Spectrophotometric determination of freshwater pH using bromocresol purple and phenol red. *Environmental Science & Technology*, **35**, 1197–1201.

Yao, W., Liu, X. & Byrne, R.H. 2007. Impurities in indicators used for spectrophotometric seawater pH measurements: assessment and remedies. *Marine Chemistry*, **107**, 167–172.

Yuan, S. & DeGrandpre, M.D. 2008. Evaluation of indicator-based pH measurements for freshwater over a wide range of buffer intensities. *Environmental Science & Technology*, **42**, 6092–6099.

Zabowski, D. & Sletten, R.S. 1991. Carbon dioxide degassing effects on the pH of spodosol soil solutions. *Soil Science Society of America Journal*, **55**, 1456–1461.

Supporting Information

Spectrophotometric measurement of soil pH using a multiple indicator dye mixture

S . Bargrizan[a], R. J. Smernik[a], & L. M. Mosley[b]

[a]*The School of Agriculture, Food and Wine, The University of Adelaide, South Australia,*

[b]*Acid Sulfate Soils Centre, School of Biological Sciences, The University of Adelaide, South Australia*

Summary of the Supporting Information:

1 Justification of the theory of spectrophotometric pH measurement method using a dye mixture

4 tables

4 Figures

Appendix S1. Derivation of spectrophotometric pH equations using a dye mixture:

The pH of a conjugate acid–base system can be calculated using the Henderson–Hasselbalch equation taking advantage of the dissociation constant (pK_a) of the weak acid for two dyes with base (B_i) and acid (A_i) species as follows:

$$\mathrm{pH} = \mathrm{p}K_{a1} + \log\frac{\gamma_{B1}}{\gamma_{A1}} + \log\frac{[B_1]}{[A_1]}, \quad \text{(A1a)}$$

$$\mathrm{pH} = \mathrm{p}K_{a2} + \log\frac{\gamma_{B2}}{\gamma_{A2}} + \log\frac{[B_2]}{[A_2]}. \quad \text{(A2a)}$$

where [ ] denotes the concentration and γ the activity coefficients of base (B_1 and B_2) and acid (A_1 and A_2) forms of the two indicator dyes.

The spectrophotometric pH using a two-indicator dye mixture can be determined as outlined below:

Let us define $\mathrm{p}K'_{a1} = \mathrm{p}K_{a1} + \log\frac{\gamma_{B1}}{\gamma_{A1}}$ and $\mathrm{p}K'_{a2} = \mathrm{p}K_{a2} + \log\frac{\gamma_{B2}}{\gamma_{A2}}$. Therefore, the relations in Equations (A1a) and (A2a) reduce to the following:

$$\mathrm{pH} = \mathrm{p}K'_{a1} + + \log\frac{[B_1]}{[A_1]}. \quad \text{(A1b)}$$

$$\mathrm{pH} = \mathrm{p}K'_{a2} + + \log\frac{[B_2]}{[A_2]}\,. \quad \text{(A2b)}$$

From the relations in Equations (A1b) and (A2b) we obtain:

$$\frac{[A_i]}{[B_i]} = 10^{-\left(\mathrm{pH} - \mathrm{p}K'_{ai}\right)} \quad \text{(A3)}$$

According to the Beer–Lambert Law, the absorbance (Abs) of acid and base forms of indicator at λ_1 and λ_2 is defined as:

$$\mathrm{Abs}_{\lambda 1} = \varepsilon_{A1}^{\lambda 1} l[A_1] + \varepsilon_{B1}^{\lambda 1} l[B_1] + \varepsilon_{A2}^{\lambda 1} l[A_2] + \varepsilon_{B2}^{\lambda 1} l[B_2]\,, \quad \text{(A4)}$$

$$Abs_{\lambda 2} = \varepsilon_{A1}^{\lambda 2} l[A_1] + \varepsilon_{B1}^{\lambda 2} l[B_1] + \varepsilon_{A2}^{\lambda 2} l[A_2] + \varepsilon_{B2}^{\lambda 2} l[B_2]\,, \quad \text{(A5)}$$

where ($\varepsilon_{\lambda 1}$ and $\varepsilon_{\lambda 2}$) are the molar absorptivity coefficients at wavelengths λ_1 and λ_2 for (A_1 and A_2), and (B_1 and B_2) and l is the spectrophotometric cell path length.

To obtain the ratio of maximum absorption of acid and base forms of two-dye mixture (R_{multi}), equation (A5) needs to be divided by equation (A4) as follows:

$$R_{multi} = \frac{Abs^{\lambda 2}}{Abs^{\lambda 1}} = \frac{\varepsilon_{A1}^{\lambda 2} l[A_1] + \varepsilon_{B1}^{\lambda 2} l[B_1] + \varepsilon_{A2}^{\lambda 2} l[A_2] + \varepsilon_{B2}^{\lambda 2} l[B_2]}{\varepsilon_{A1}^{\lambda 1} l[A_1] + \varepsilon_{B1}^{\lambda 1} l[B_1] + \varepsilon_{A2}^{\lambda 1} l[A_2] + \varepsilon_{B2}^{\lambda 1} l[B_2]} \quad \text{(A6a)}$$

Numerator and denominator can be written:

$$\text{Numerator:} \quad \varepsilon_{B1}^{\lambda 2}[B_1]\left(1 + \frac{\varepsilon_{A1}^{\lambda 2}}{\varepsilon_{B1}^{\lambda 2}}\frac{[A_1]}{[B_1]}\right) + \varepsilon_{B2}^{\lambda 2}[B_2]\left(1 + \frac{\varepsilon_{A2}^{\lambda 2}}{\varepsilon_{B2}^{\lambda 2}}\frac{[A_2]}{[B_2]}\right). \quad \text{(A6b)}$$

$$\text{Denominator:} \quad \varepsilon_{A1}^{\lambda 1}[B_1]\left(\frac{[A_1]}{[B_1]} + \frac{\varepsilon_{B1}^{\lambda 1}}{\varepsilon_{A1}^{\lambda 1}}\right) + \varepsilon_{A2}^{\lambda 1}[B_2]\left(\frac{[A_2]}{[B_2]} + \frac{\varepsilon_{B2}^{\lambda 1}}{\varepsilon_{A2}^{\lambda 1}}\right). \quad \text{(A6c)}$$

Equations (A6b) and (A6c) can be put in the following compact form:

$$\text{Numerator:} \quad \sum_{i=1,2} \varepsilon_{Bi}^{\lambda 2}\,[B_i]\left(1 + \frac{\varepsilon_{Ai}^{\lambda 2}}{\varepsilon_{Bi}^{\lambda 2}}\frac{[A_i]}{[B_i]}\right). \quad \text{(A6d)}$$

$$\text{Denominator:} \sum_{i=1,2} \varepsilon_{Ai}^{\lambda 1}\,[B_i]\left(\frac{[A_i]}{[B_i]} + \frac{\varepsilon_{Bi}^{\lambda 1}}{\varepsilon_{Ai}^{\lambda 1}}\right). \quad \text{(A6e)}$$

Substitution of Equation (A3) for equations (A6d) and (A6e), gives us the numerator and denominator as:

Numerator: $\sum_{i=1,2}^{2} \varepsilon_{Bi}^{\lambda 2}\ [B_i] \left(1 + \frac{\varepsilon_{Ai}^{\lambda 2}}{\varepsilon_{Bi}^{\lambda 2}}\ 10^{-(\mathrm{pH}-\mathrm{p}K'_{ai})}\right)$. (A6f)

Denominator: $\sum_{i=1,2}^{2} \varepsilon_{Ai}^{\lambda 1}\ [B_i] \left(\ 10^{-(\mathrm{pH}-\mathrm{p}K'_{ai})} + \frac{\varepsilon_{Bi}^{\lambda 1}}{\varepsilon_{Ai}^{\lambda 1}}\right)$. (A6g)

If both numerator and denominator Equations (A6e) and (A6f) are divided by the fixed factor $[B_1]$, Therefore, R_{multi} can be obtained as:

$$R_{\mathrm{multi}} = \frac{\sum_{i=1,2}^{2} \varepsilon_{Bi}^{\lambda 2} \frac{[B_i]}{[B_1]} \left(1 + \frac{\varepsilon_{Ai}^{\lambda 2}}{\varepsilon_{Bi}^{\lambda 2}} 10^{-(\mathrm{pH}-\mathrm{p}K'_{ai})}\right)}{\sum_{i=1,2}^{2} \varepsilon_{Ai}^{\lambda 1} \frac{[B_i]}{[B_1]} \left(10^{-(\mathrm{pH}-\mathrm{p}K'_{ai})} + \frac{\varepsilon_{Bi}^{\lambda 1}}{\varepsilon_{Ai}^{\lambda 1}}\right)}, \quad \text{(A7)}$$

$$\frac{[B_2]}{[B_1]} = \frac{1 + 10^{-(\mathrm{pH}-\mathrm{p}K'_{a1})}}{1 + 10^{-(\mathrm{pH}-\mathrm{p}K'_{a2})}} \frac{(1-f_1)}{f_1}, \quad \text{(A8a)}$$

where pK'_{a} is the dissociation constant of the dye at the specific ionic strength of the sample solution, and mole fraction of dye in the mixture defines as f_1:

$$f_1 = \frac{[A_1] + [B_1]}{[A_1] + [B_1] + [A_2] + [B_2]} = \frac{[B_1]\left(1 + \frac{[A_1]}{[B_1]}\right)}{[B_1]\left(1 + \frac{[A_1]}{[B_1]}\right) + [B_2]\left(1 + \frac{[A_2]}{[B_2]}\right)}, \quad \text{(A8b)}$$

where $[A_1]$, $[A_2]$ and $[B_1]$, $[B_2]$ are the concentrations of acid and base species of dyes 1 and 2.

Equation (A8a) can be justified as expressed below

The numerator and denominator of Equation (A8b) are divided by $[B_1]$ as follows:

$$f_1 = \frac{\left(1 + \frac{[A_1]}{[B_1]}\right)}{\left(1 + \frac{[A_1]}{[B_1]} + \frac{[B_2]}{[B_1]}\left(1 + \frac{[A_2]}{[B_2]}\right)\right)}, \quad \text{(A8c)}$$

and then we obtain the following:

$$f_1 \left[\left(1 + \frac{[A_1]}{[B_1]}\right) + \frac{[B_2]}{[B_1]}\left(1 + \frac{[A_2]}{[B_2]}\right)\right] = 1 + \frac{A_1}{B_1}, \quad \text{(A8d)}$$

$$(1 - f_1)\left(1 + \frac{[A_1]}{[B_1]}\right) = f_1 \frac{[B_2]}{[B_1]} \left(1 + \frac{[A_2]}{[B_2]}\right), \quad \text{(A8e)}$$

$$\frac{[B_2]}{[B_1]} = \frac{1 + \frac{[A_1]}{[B_1]}}{1 + \frac{[A_2]}{[B_2]}} \frac{(1-\mathrm{f})}{\mathrm{f}_1}. \quad \text{[A8f]}$$

From the relation (A3), the corresponding values are substituted for $\frac{[A_1]}{[B_1]}$ and $\frac{[A_2]}{[B_2]}$ to obtain the equation (A8a).

Table S1 The mean molar absorption ratios and standard deviations (in brackets) at 25°C for *m*CP, BCP, BPB and TB (used for single indicator dye measurements at wavelengths of maximum absorption of acid and base forms of the dye)

Indicator	e_1	e_2	e_3
*m*CP	0.015	2.24	0.13
	(0.00)	(0.02)	(0.01)
BCP	0.006	2.83	0.05
	(0.00)	(0.03)	(0.00)
BPB	0.032	2.96	0.04
	(0.01)	(0.02)	(0.01)
TB	0.0093	2.38	0.09
	(0.01)	(0.03)	(0.01)

Table S2 The mixed indicator colour change at selected points (pH values) in the alkalinity titration

pH 3.1	pH 3.67	pH 5.23	pH 5.87	pH 6.31
				
pH 6.64	pH 7.12	pH 8.39	pH 9.31	pH 10.49
				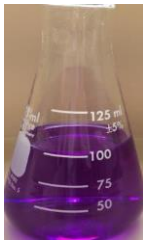

Table S3 The look -up table for R_{multi} as a function of pH

	*m*CP	BCP	BPB	TB
	Dye 1	Dye 2	Dye 3	Dye 4
$[B_i]/[B_1]$	1	2	3	4
pK_a (μ=0)	8.64	6.49	4.34	9.20
γ	–0.43	–0.43	–0.43	–0.43
pK_a'	8.21	6.06	3.91	8.77
$\varepsilon\lambda_2$ Base	33 721	64 893	68 277	33 875
$\varepsilon\lambda_2$ Acid	215	135	741	233
$\varepsilon\lambda_1$ Base	2103	1289	885	1370
$\varepsilon\lambda_1$ Acid	15 761	23 014	23 496	14 957
f_1	0.25			
f_2	0.25			
f_3	0.25			
f_4	0.25			

pH	**R (ODR)**	$[B_2]/[B_1]$	$[B_3]/[B_1]$	$[B_4]/[B_1]$
3.0	0.12	141.10	17 774.80	0.28
3.01	0.12	141.13	17 729.72	0.28
3.02	0.12	141.13	17 683.83	0.28
3.03	0.12	141.12	17 637.11	0.28
3.04	0.13	141.12	17 589.57	0.28
3.05	0.13	141.12	17 541.18	0.28
3.06	0.13	141.11	17 491.94	0.28
3.07	0.13	141.11	17 441.83	0.28
3.08	0.14	141.11	17390.86	0.28
3.09	0.14	141.10	17 339.0	0.28
3.10	0.14	141.10	17 286.26	0.28
3.11	0.14	141.10	17 232.62	0.28
3.12	0.15	141.09	17 178.07	0.28
3.13	0.15	141.09	17 122.61	0.28
3.14	0.15	141.09	17 066.23	0.28
3.15	0.15	141.08	17 008.92	0.28
3.16	0.16	141.08	16 950.67	0.28
3.17	0.16	141.07	16 891.47	0.28
3.18	0.16	141.07	16 831.32	0.28
3.19	0.17	141.07	16 770.21	0.28
3.20	0.17	141.06	16 708.14	0.28
3.21	0.17	141.06	16 645.09	0.28
3.22	0.17	141.05	16 581.07	0.28
3.23	0.18	141.05	16 516.06	0.28
3.24	0.18	141.04	16 450.07	0.28
3.25	0.18	141.04	16 383.08	0.28
3.26	0.19	141.03	16 315.09	0.28
3.27	0.19	141.03	16 246.11	0.28
3.28	0.19	141.02	16 176.11	0.28
3.29	0.20	141.02	16 105.11	0.28
3.30	0.20	141.01	16 033.1	0.28

3.31	0.21	141.01	15 960.07	0.28
3.32	0.21	141.00	15 886.02	0.28
3.33	0.21	140.99	15 810.96	0.28
3.34	0.22	140.99	15 734.89	0.28
3.35	0.22	140.98	15 657.79	0.28
3.36	0.23	140.98	15 579.68	0.28
3.37	0.23	140.97	15 500.55	0.28
3.38	0.23	140.96	15 420.40	0.28
3.39	0.24	140.96	15 339.24	0.28
3.40	0.24	140.95	15 257.08	0.28
3.41	0.25	140.94	15 173.90	0.28
3.42	0.25	140.93	15 089.72	0.28
3.43	0.25	140.93	15 004.54	0.28
3.44	0.26	140.92	14 918.36	0.28
3.45	0.26	140.91	14 831.20	0.28
3.46	0.27	140.90	14 743.06	0.28
3.47	0.27	140.90	14 653.94	0.28
3.48	0.28	140.89	14 563.85	0.28
3.49	0.28	140.88	14 472.80	0.28
3.50	0.29	140.87	14 380.81	0.28
3.51	0.29	140.86	14 287.87	0.28
3.52	0.30	140.85	14 194.01	0.28
3.53	0.30	140.84	14 099.23	0.28
3.54	0.31	140.83	14 003.54	0.28
3.55	0.31	140.82	13 906.96	0.28
3.56	0.32	140.81	13 809.49	0.28
3.57	0.32	140.80	13 711.16	0.28
3.58	0.33	140.79	13 611.98	0.28
3.59	0.33	140.78	13 511.97	0.28
3.60	0.34	140.77	13 411.13	0.28
3.61	0.35	140.76	13 309.50	0.28
3.62	0.35	140.75	13 207.08	0.28
3.63	0.36	140.74	13 103.89	0.28
3.64	0.36	140.72	12 999.95	0.28
3.65	0.37	140.71	12 895.29	0.28
3.66	0.37	140.70	12 789.92	0.28
3.67	0.38	140.69	12 683.86	0.28
3.68	0.39	140.67	12 577.14	0.28
3.69	0.39	140.66	12 469.77	0.28
3.70	0.40	140.65	12 361.79	0.28
3.71	0.40	140.63	12 253.21	0.28
3.72	0.41	140.62	12 144.05	0.28
3.73	0.42	140.60	12 034.36	0.28
3.74	0.42	140.59	11 924.13	0.28
3.75	0.43	140.57	11 813.41	0.28
3.76	0.44	140.56	11 702.23	0.28
3.77	0.44	140.54	11 590.59	0.28
3.78	0.45	140.52	11 478.55	0.28
3.79	0.46	140.51	11 366.11	0.28

3.80	0.46	140.49	11 253.31	0.28
3.81	0.47	140.47	11 140.18	0.28
3.82	0.48	140.45	11 026.74	0.28
3.83	0.48	140.44	10 913.03	0.28
3.84	0.49	140.42	10 799.07	0.28
3.85	0.50	140.40	10 684.90	0.28
3.86	0.50	140.38	10 570.54	0.28
3.87	0.51	140.36	10 456.02	0.28
3.88	0.52	140.34	10 341.38	0.28
3.89	0.53	140.32	10 226.63	0.28
3.90	0.53	140.29	10 111.83	0.28
3.91	0.54	140.27	9996.99	0.28
3.92	0.55	140.25	9882.14	0.28
3.93	0.55	140.23	9767.31	0.28
3.94	0.56	140.20	9652.55	0.28
3.95	0.57	140.18	9537.87	0.28
3.96	0.58	140.15	9423.30	0.28
3.97	0.58	140.13	9308.88	0.28
3.98	0.59	140.10	9194.64	0.28
3.99	0.60	140.07	9080.60	0.28
4.00	0.60	140.05	8966.80	0.28
4.01	0.61	140.02	8853.26	0.28
4.02	0.62	139.99	8740.02	0.28
4.03	0.63	139.96	8627.19	0.28
4.04	0.63	139.93	8514.54	0.28
4.05	0.64	139.90	8402.35	0.28
4.06	0.65	139.87	8290.57	0.28
4.07	0.66	139.84	8179.22	0.28
4.08	0.66	139.81	8068.33	0.28
4.09	0.67	139.77	7957.93	0.28
4.10	0.68	139.74	7848.05	0.28
4.11	0.69	139.70	7738.70	0.28
4.12	0.69	139.67	7629.91	0.28
4.13	0.70	139.63	7521.72	0.28
4.14	0.71	139.59	7414.13	0.28
4.15	0.72	139.56	7307.18	0.28
4.16	0.72	139.52	7200.89	0.28
4.17	0.73	139.48	7095.27	0.28
4.18	0.74	139.44	6990.36	0.28
4.19	0.75	139.39	6886.17	0.28
4.20	0.75	139.35	6782.71	0.28
4.21	0.76	139.31	6680.02	0.28
4.22	0.77	139.26	6578.10	0.28
4.23	0.78	139.22	6476.99	0.28
4.24	0.78	139.17	6376.68	0.28
4.25	0.79	139.12	6277.21	0.28
4.26	0.80	139.07	6178.58	0.28
4.27	0.81	139.02	6080.81	0.28
4.28	0.81	138.97	5983.91	0.28

4.29	0.82	138.92	5887.91	0.28
4.30	0.83	138.87	5792.81	0.28
4.31	0.84	138.81	5698.62	0.28
4.32	0.84	138.76	5605.36	0.28
4.33	0.85	138.70	5513.03	0.28
4.34	0.86	138.64	5421.65	0.28
4.35	0.86	138.58	5331.22	0.28
4.36	0.87	138.52	5241.76	0.28
4.37	0.88	138.46	5153.28	0.28
4.38	0.89	138.39	5065.77	0.28
4.39	0.89	138.33	4979.25	0.28
4.40	0.90	138.26	4893.72	0.28
4.41	0.91	138.19	4809.18	0.28
4.42	0.91	138.13	4725.65	0.28
4.43	0.92	138.05	4643.13	0.28
4.44	0.93	137.98	4561.62	0.28
4.45	0.93	137.91	4481.12	0.28
4.46	0.94	137.83	4401.63	0.28
4.47	0.95	137.75	4323.16	0.28
4.48	0.95	137.67	4245.71	0.28
4.49	0.96	137.59	4169.27	0.28
4.50	0.97	137.51	4093.85	0.28
4.51	0.97	137.42	4019.45	0.28
4.52	0.98	137.34	3946.07	0.28
4.53	0.99	137.25	3873.70	0.28
4.54	0.99	137.16	3802.34	0.28
4.55	1.00	137.07	3731.99	0.28
4.56	1.01	136.97	3662.65	0.28
4.57	1.01	136.87	3594.31	0.28
4.58	1.02	136.78	3526.97	0.28
4.59	1.03	136.68	3460.63	0.28
4.60	1.03	136.57	3395.28	0.28
4.61	1.04	136.47	3330.91	0.28
4.62	1.04	136.36	3267.52	0.28
4.63	1.05	136.25	3205.11	0.28
4.64	1.06	136.14	3143.66	0.28
4.65	1.06	136.02	3083.18	0.28
4.66	1.07	135.90	3023.65	0.28
4.67	1.07	135.79	2965.06	0.28
4.68	1.08	135.66	2907.42	0.28
4.69	1.09	135.54	2850.71	0.28
4.70	1.09	135.41	2794.93	0.28
4.71	1.10	135.28	2740.06	0.28
4.72	1.10	135.15	2686.11	0.28
4.73	1.11	135.01	2633.05	0.28
4.74	1.12	134.87	2580.88	0.28
4.75	1.12	134.73	2529.60	0.28
4.76	1.13	134.59	2479.19	0.28
4.77	1.13	134.44	2429.65	0.28

4.78	1.14	134.29	2380.96	0.28
4.79	1.14	134.13	2333.12	0.28
4.80	1.15	133.98	2286.11	0.28
4.81	1.16	133.82	2239.93	0.28
4.82	1.16	133.65	2194.57	0.28
4.83	1.17	133.48	2150.02	0.28
4.84	1.17	133.31	2106.26	0.28
4.85	1.18	133.14	2063.29	0.28
4.86	1.18	132.96	2021.10	0.28
4.87	1.19	132.78	1979.68	0.28
4.88	1.20	132.59	1939.02	0.28
4.89	1.20	132.41	1899.10	0.28
4.90	1.21	132.21	1859.92	0.28
4.91	1.21	132.02	1821.46	0.28
4.92	1.22	131.82	1783.73	0.28
4.93	1.22	131.61	1746.70	0.28
4.94	1.23	131.40	1710.37	0.28
4.95	1.24	131.19	1674.72	0.28
4.96	1.24	130.97	1639.75	0.28
4.97	1.25	130.75	1605.45	0.28
4.98	1.25	130.52	1571.80	0.28
4.99	1.26	130.29	1538.80	0.28
5.00	1.26	130.06	1506.44	0.28
5.01	1.27	129.82	1474.70	0.28
5.02	1.27	129.57	1443.58	0.28
5.03	1.28	129.33	1413.07	0.28
5.04	1.29	129.07	1383.15	0.28
5.05	1.29	128.81	1353.82	0.28
5.06	1.30	128.55	1325.07	0.28
5.07	1.30	128.28	1296.89	0.28
5.08	1.31	128.01	1269.27	0.28
5.09	1.32	127.73	1242.20	0.28
5.10	1.32	127.45	1215.66	0.28
5.11	1.33	127.16	1189.66	0.28
5.12	1.33	126.86	1164.18	0.28
5.13	1.34	126.56	1139.21	0.28
5.14	1.35	126.26	1114.75	0.28
5.15	1.35	125.94	1090.78	0.28
5.16	1.36	125.63	1067.30	0.28
5.17	1.36	125.30	1044.30	0.28
5.18	1.37	124.98	1021.77	0.28
5.19	1.38	124.64	999.69	0.28
5.20	1.38	124.30	978.08	0.28
5.21	1.39	123.96	956.90	0.28
5.22	1.40	123.60	936.16	0.28
5.23	1.40	123.25	915.85	0.28
5.24	1.41	122.88	895.96	0.28
5.25	1.42	122.51	876.48	0.28
5.26	1.42	122.13	857.41	0.28

5.27	1.43	121.75	838.73	0.28
5.28	1.44	121.36	820.45	0.28
5.29	1.44	120.96	802.54	0.28
5.30	1.45	120.56	785.02	0.28
5.31	1.46	120.15	767.85	0.28
5.32	1.46	119.73	751.06	0.28
5.33	1.47	119.31	734.61	0.28
5.34	1.48	118.88	718.51	0.28
5.35	1.49	118.45	702.75	0.28
5.36	1.49	118.00	687.33	0.28
5.37	1.50	117.55	672.23	0.28
5.38	1.51	117.10	657.46	0.28
5.39	1.52	116.63	642.99	0.28
5.40	1.52	116.16	628.84	0.28
5.41	1.53	115.68	614.99	0.28
5.42	1.54	115.20	601.43	0.28
5.43	1.55	114.71	588.17	0.28
5.44	1.56	114.21	575.19	0.28
5.45	1.57	113.70	562.48	0.28
5.46	1.57	113.19	550.05	0.28
5.47	1.58	112.67	537.89	0.28
5.48	1.59	112.14	525.99	0.28
5.49	1.60	111.60	514.35	0.28
5.00	1.61	111.06	502.96	0.28
5.51	1.62	110.51	491.81	0.28
5.52	1.63	109.96	480.91	0.28
5.53	1.64	109.39	470.24	0.28
5.54	1.64	108.82	459.81	0.28
5.55	1.65	108.25	449.60	0.28
5.56	1.66	107.66	439.61	0.28
5.57	1.67	107.07	429.84	0.28
5.58	1.68	106.47	420.29	0.28
5.59	1.69	105.86	410.94	0.28
5.60	1.70	105.25	401.79	0.28
5.61	1.71	104.63	392.85	0.28
5.62	1.72	104.01	384.10	0.28
5.63	1.73	103.37	375.55	0.28
5.64	1.74	102.73	367.18	0.28
5.65	1.76	102.09	358.99	0.28
5.66	1.77	101.43	350.98	0.28
5.67	1.78	100.77	343.15	0.28
5.68	1.79	100.11	335.50	0.28
5.69	1.80	99.43	328.01	0.28
5.70	1.81	98.75	320.68	0.28
5.71	1.82	98.07	313.52	0.28
5.72	1.83	97.38	306.52	0.28
5.73	1.85	96.68	299.67	0.28
5.74	1.86	95.98	292.97	0.28
5.75	1.87	95.27	286.42	0.28

5.76	1.88	94.55	280.01	0.28
5.77	1.89	93.83	273.75	0.28
5.78	1.91	93.11	267.62	0.28
5.79	1.92	92.38	261.63	0.28
5.80	1.93	91.64	255.77	0.28
5.81	1.94	90.90	250.05	0.28
5.82	1.96	90.16	244.45	0.28
5.83	1.97	89.41	238.97	0.28
5.84	1.98	88.65	233.62	0.28
5.85	2.00	87.89	228.38	0.28
5.86	2.01	87.13	223.26	0.28
5.87	2.02	86.36	218.26	0.28
5.88	2.04	85.59	213.37	0.28
5.89	2.05	84.82	208.58	0.28
5.90	2.07	84.04	203.91	0.28
5.91	2.08	83.26	199.33	0.28
5.92	2.09	82.47	194.86	0.28
5.93	2.11	81.68	190.49	0.28
5.94	2.12	80.89	186.22	0.28
5.95	2.14	80.10	182.04	0.28
5.96	2.15	79.03	177.96	0.28
5.97	2.17	78.51	173.96	0.28
5.98	2.18	77.71	170.06	0.28
5.99	2.20	76.91	166.24	0.28
6.00	2.21	76.10	162.51	0.28
6.01	2.23	75.30	158.86	0.28
6.02	2.24	74.50	155.30	0.28
6.03	2.26	73.69	151.81	0.28
6.04	2.27	72.88	148.41	0.28
6.05	2.29	72.08	145.07	0.28
6.06	2.31	71.27	141.82	0.28
6.07	2.32	70.46	138.63	0.28
6.08	2.34	69.65	135.52	0.28
6.09	2.35	68.85	132.48	0.28
6.10	2.37	68.04	129.51	0.28
6.11	2.39	67.24	126.60	0.28
6.12	2.40	66.43	123.76	0.28
6.13	2.42	65.63	120.98	0.28
6.14	2.43	64.83	118.27	0.28
6.15	2.45	64.03	115.61	0.28
6.16	2.47	63.23	113.02	0.28
6.17	2.48	62.43	110.48	0.28
6.18	2.50	61.64	108.00	0.28
6.19	2.52	60.85	105.58	0.28
6.20	2.53	60.06	103.21	0.28
6.21	2.55	59.27	100.90	0.28
6.22	2.57	58.49	98.63	0.28
6.23	2.59	57.71	96.42	0.28
6.24	2.60	56.93	94.26	0.28

6.25	2.62	56.16	92.15	0.28
6.26	2.64	55.39	90.08	0.28
6.27	2.65	54.63	88.06	0.28
6.28	2.67	53.87	86.09	0.28
6.29	2.69	53.11	84.16	0.28
6.30	2.70	52.36	82.28	0.28
6.31	2.72	51.61	80.43	0.28
6.32	2.74	50.87	78.63	0.28
6.33	2.76	50.13	76.87	0.28
6.34	2.77	49.40	75.15	0.28
6.35	2.79	48.67	73.47	0.28
6.36	2.81	47.95	71.83	0.28
6.37	2.82	47.24	70.22	0.28
6.38	2.84	46.52	68.65	0.28
6.39	2.86	45.82	67.11	0.28
6.40	2.88	45.12	65.61	0.28
6.41	2.89	44.43	64.15	0.28
6.42	2.91	43.74	62.71	0.28
6.43	2.93	43.06	61.31	0.28
6.44	2.94	42.38	59.95	0.28
6.45	2.96	41.71	58.61	0.28
6.46	2.98	41.05	57.30	0.28
6.47	2.99	40.40	56.02	0.28
6.48	3.01	39.75	54.77	0.28
6.49	3.03	39.11	53.55	0.28
6.50	3.04	38.47	52.36	0.28
6.51	3.06	37.84	51.19	0.28
6.52	3.08	37.22	50.05	0.28
6.53	3.09	36.60	48.94	0.28
6.54	3.11	36.00	47.85	0.28
6.55	3.13	35.39	46.79	0.28
6.56	3.14	34.80	45.75	0.28
6.57	3.16	34.21	44.73	0.28
6.58	3.18	33.63	43.74	0.28
6.59	3.19	33.06	42.77	0.28
6.60	3.21	32.49	41.82	0.28
6.61	3.22	31.94	40.89	0.28
6.62	3.24	31.38	39.98	0.28
6.63	3.26	30.84	39.10	0.28
6.64	3.27	30.30	38.23	0.28
6.65	3.29	29.77	37.39	0.28
6.66	3.30	29.25	36.56	0.28
6.67	3.32	28.73	35.75	0.28
6.68	3.33	28.22	34.96	0.28
6.69	3.35	27.72	34.19	0.28
6.70	3.36	27.23	33.44	0.28
6.71	3.38	26.74	32.70	0.28
6.72	3.39	26.26	31.98	0.28
6.73	3.41	25.79	31.27	0.28

6.74	3.42	25.32	30.59	0.28
6.75	3.44	24.86	29.91	0.28
6.76	3.45	24.41	29.26	0.28
6.77	3.47	23.96	28.61	0.28
6.78	3.48	23.52	27.99	0.28
6.79	3.50	23.09	27.37	0.28
6.80	3.51	22.67	26.77	0.28
6.81	3.53	22.25	26.19	0.28
6.82	3.54	21.84	25.61	0.28
6.83	3.56	21.43	25.06	0.28
6.84	3.57	21.03	24.51	0.28
6.85	3.58	20.64	23.97	0.28
6.86	3.60	20.25	23.45	0.28
6.87	3.61	19.88	22.94	0.28
6.88	3.63	19.50	22.44	0.28
6.89	3.64	19.14	21.95	0.28
6.90	3.65	18.78	21.48	0.29
6.91	3.67	18.42	21.01	0.29
6.92	3.68	18.07	20.56	0.29
6.93	3.70	17.73	20.11	0.29
6.94	3.71	17.39	19.68	0.29
6.95	3.72	17.06	19.25	0.29
6.96	3.74	16.74	18.84	0.29
6.97	3.75	16.42	18.43	0.29
6.98	3.76	16.11	18.04	0.29
6.99	3.78	15.80	17.65	0.29
7.00	3.79	15.50	17.27	0.29
7.01	3.80	15.20	16.90	0.29
7.02	3.82	14.91	16.54	0.29
7.03	3.83	14.62	16.18	0.29
7.04	3.84	14.34	15.84	0.29
7.05	3.86	14.07	15.50	0.29
7.06	3.87	13.80	15.17	0.29
7.07	3.88	13.53	14.85	0.29
7.08	3.90	13.27	14.53	0.29
7.09	3.91	13.02	14.23	0.29
7.10	3.92	12.77	13.93	0.29
7.11	3.94	12.52	13.63	0.29
7.12	3.95	12.28	13.34	0.29
7.13	3.96	12.04	13.06	0.29
7.14	3.97	11.81	12.79	0.29
7.15	3.99	11.58	12.52	0.29
7.16	4.00	11.36	12.26	0.29
7.17	4.01	11.14	12.00	0.29
7.18	4.03	10.93	11.75	0.29
7.19	4.04	10.72	11.51	0.29
7.20	4.06	10.51	11.27	0.29
7.21	4.07	10.31	11.03	0.29
7.22	4.08	10.11	10.81	0.30

7.23	4.10	9.92	10.58	0.30
7.24	4.11	9.73	10.37	0.30
7.25	4.12	9.54	10.15	0.30
7.26	4.14	9.36	9.94	0.30
7.27	4.15	9.18	9.74	0.30
7.28	4.16	9.00	9.54	0.30
7.29	4.18	8.83	9.35	0.30
7.30	4.19	8.66	9.16	0.30
7.31	4.21	8.50	8.97	0.30
7.32	4.22	8.33	8.79	0.30
7.33	4.24	8.18	8.61	0.30
7.34	4.25	8.02	8.44	0.30
7.35	4.27	7.87	8.27	0.30
7.36	4.28	7.72	8.11	0.30
7.37	4.29	7.57	7.94	0.30
7.38	4.31	7.43	7.79	0.30
7.39	4.33	7.29	7.63	0.30
7.40	4.34	7.15	7.48	0.30
7.41	4.36	7.02	7.33	0.31
7.42	4.37	6.89	7.19	0.31
7.43	4.39	6.76	7.05	0.31
7.44	4.40	6.63	6.91	0.31
7.45	4.42	6.51	6.78	0.31
7.46	4.44	6.39	6.64	0.31
7.47	4.45	6.27	6.52	0.31
7.48	4.47	6.16	6.39	0.31
7.49	4.49	6.04	6.27	0.31
7.50	4.50	5.93	6.15	0.31
7.51	4.52	5.82	6.03	0.31
7.52	4.54	5.72	5.92	0.31
7.53	4.56	5.61	5.80	0.31
7.54	4.57	5.51	5.69	0.32
7.55	4.59	5.41	5.59	0.32
7.56	4.61	5.32	5.48	0.32
7.57	4.63	5.22	5.38	0.32
7.58	4.65	5.13	5.28	0.32
7.59	4.67	5.04	5.18	0.32
7.60	4.69	4.95	5.09	0.32
7.61	4.71	4.86	5.00	0.32
7.62	4.73	4.77	4.91	0.32
7.63	4.75	4.69	4.82	0.32
7.64	4.77	4.61	4.73	0.33
7.65	4.79	4.53	4.64	0.33
7.66	4.81	4.45	4.56	0.33
7.67	4.83	4.37	4.48	0.33
7.68	4.86	4.30	4.40	0.33
7.69	4.88	4.23	4.32	0.33
7.70	4.90	4.15	4.25	0.33
7.71	4.92	4.08	4.17	0.33

7.72	4.95	4.01	4.10	0.33
7.73	4.97	3.95	4.03	0.34
7.74	5.00	3.88	3.96	0.34
7.75	5.02	3.82	3.90	0.34
7.76	5.05	3.75	3.83	0.34
7.77	5.07	3.69	3.76	0.34
7.78	5.10	3.63	3.70	0.34
7.79	5.12	3.57	3.64	0.34
7.80	5.15	3.52	3.58	0.35
7.81	5.18	3.46	3.52	0.35
7.82	5.21	3.41	3.46	0.35
7.83	5.23	3.35	3.41	0.35
7.84	5.26	3.30	3.35	0.35
7.85	5.29	3.25	3.03	0.35
7.86	5.32	3.20	3.25	0.35
7.87	5.35	3.15	3.20	0.36
7.88	5.38	3.10	3.15	0.36
7.89	5.41	3.05	3.10	0.36
7.90	5.45	3.01	3.05	0.36
7.91	5.48	2.96	3.00	0.36
7.92	5.51	2.92	2.96	0.36
7.93	5.54	2.87	2.91	0.37
7.94	5.58	2.83	2.87	0.37
7.95	5.61	2.79	2.83	0.37
7.96	5.65	2.75	2.79	0.37
7.97	5.68	2.71	2.74	0.37
7.98	5.72	2.67	2.70	0.38
7.99	5.76	2.64	2.67	0.38
8.00	5.79	2.60	2.63	0.38
8.01	5.83	2.56	2.59	0.38
8.02	5.87	2.53	2.55	0.38
8.03	5.91	2.49	2.52	0.39
8.04	5.95	2.46	2.48	0.39
8.05	5.99	2.43	2.45	0.39
8.06	6.03	2.39	2.42	0.39
8.07	6.07	2.36	2.39	0.40
8.08	6.12	2.33	2.35	0.40
8.09	6.16	2.30	2.32	0.40
8.10	6.20	2.27	2.29	0.40
8.11	6.25	2.24	2.26	0.41
8.12	6.29	2.22	2.24	0.41
8.13	6.34	2.19	2.21	0.41
8.14	6.39	2.16	2.18	0.41
8.15	6.44	2.14	2.15	0.42
8.16	6.49	2.11	2.13	0.42
8.17	6.53	2.08	2.10	0.42
8.18	6.59	2.06	2.08	0.42
8.19	6.64	2.04	2.05	0.43
8.20	6.69	2.01	2.03	0.43

8.21	6.74	1.99	2.00	0.43
8.22	6.80	1.97	1.98	0.43
8.23	6.85	1.95	1.96	0.44
8.24	6.91	1.92	1.94	0.44
8.25	6.96	1.90	1.92	0.44
8.26	7.02	1.88	1.89	0.45
8.27	7.08	1.86	1.87	0.45
8.28	7.14	1.84	1.85	0.45
8.29	7.20	1.82	1.84	0.46
8.30	7.26	1.81	1.82	0.46
8.31	7.32	1.79	1.80	0.46
8.32	7.38	1.77	1.78	0.46
8.33	7.45	1.75	1.76	0.47
8.34	7.51	1.74	1.74	0.47
8.35	7.58	1.72	1.73	0.47
8.36	7.65	1.70	1.71	0.48
8.37	7.71	1.69	1.69	0.48
8.38	7.78	1.67	1.68	0.48
8.39	7.85	1.66	1.66	0.49
8.40	7.93	1.64	1.65	0.49
8.41	8.00	1.63	1.63	0.49
8.42	8.07	1.61	1.62	0.50
8.43	8.15	1.60	1.60	0.50
8.44	8.22	1.58	1.59	0.51
8.45	8.30	1.57	1.58	0.51
8.46	8.38	1.56	1.56	0.51
8.47	8.46	1.55	1.55	0.52
8.48	8.54	1.53	1.54	0.52
8.49	8.62	1.52	1.53	0.52
8.50	8.70	1.51	1.51	0.53
8.51	8.78	1.50	1.50	0.53
8.52	8.87	1.49	1.49	0.54
8.53	8.96	1.48	1.48	0.54
8.54	9.04	1.46	1.47	0.54
8.55	9.13	1.45	1.46	0.55
8.56	9.22	1.44	1.45	0.55
8.57	9.31	1.43	1.44	0.56
8.58	9.41	1.42	1.43	0.56
8.59	9.50	1.41	1.42	0.56
8.60	9.60	1.40	1.41	0.57
8.61	9.69	1.40	1.40	0.57
8.62	9.79	1.39	1.39	0.58
8.63	9.89	1.38	1.38	0.58
8.64	9.99	1.37	1.37	0.58
8.65	10.09	1.36	1.36	0.59
8.66	10.20	1.35	1.36	0.59
8.67	10.30	1.34	1.35	0.60
8.68	10.41	1.34	1.34	0.60
8.69	10.51	1.33	1.33	0.60

8.70	10.62	1.32	1.32	0.61
8.71	10.73	1.31	1.32	0.61
8.72	10.84	1.31	1.31	0.62
8.73	10.96	1.30	1.30	0.62
8.74	11.07	1.29	1.30	0.62
8.75	11.19	1.29	1.29	0.63
8.76	11.30	1.28	1.28	0.63
8.77	11.42	1.27	1.28	0.64
8.78	11.54	1.27	1.27	0.64
8.79	11.66	1.26	1.26	0.65
8.80	11.79	1.26	1.26	0.65
8.81	11.91	1.25	1.25	0.65
8.82	12.04	1.24	1.25	0.66
8.83	12.16	1.24	1.24	0.66
8.84	12.29	1.23	1.24	0.67
8.85	12.42	1.23	1.23	0.67
8.86	12.55	1.22	1.22	0.67
8.87	12.68	1.22	1.22	0.68
8.88	12.82	1.21	1.21	0.68
8.89	12.95	1.21	1.21	0.69
8.90	13.09	1.20	1.20	0.69
8.91	13.23	1.20	1.20	0.69
8.92	13.37	1.19	1.20	0.70
8.93	13.51	1.19	1.19	0.70
8.94	13.65	1.19	1.19	0.71
8.95	13.79	1.18	1.18	0.71
8.96	13.94	1.18	1.18	0.72
8.97	14.08	1.17	1.17	0.72
8.98	14.23	1.17	1.17	0.72
8.99	14.38	1.17	1.17	0.73
9.00	14.53	1.16	1.16	0.73
9.01	14.68	1.16	1.16	0.73
9.02	14.83	1.15	1.16	0.74
9.03	14.98	1.15	1.15	0.74
9.04	15.14	1.15	1.15	0.75
9.05	15.29	1.14	1.15	0.75
9.06	15.45	1.14	1.14	0.75
9.07	15.60	1.14	1.14	0.76
9.08	15.76	1.13	1.14	0.76
9.09	15.92	1.13	1.13	0.76
9.10	16.08	1.13	1.13	0.77
9.11	16.24	1.13	1.13	0.77
9.12	16.41	1.12	1.12	0.78
9.13	16.57	1.12	1.12	0.78
9.14	16.73	1.12	1.12	0.78
9.15	16.90	1.11	1.12	0.79
9.16	17.06	1.11	1.11	0.79
9.17	17.23	1.11	1.11	0.79
9.18	17.40	1.11	1.11	0.80

9.19	17.57	1.10	1.11	0.80
9.20	17.74	1.10	1.10	0.80
9.21	17.90	1.10	1.10	0.81
9.22	18.07	1.10	1.10	0.81
9.23	18.24	1.10	1.10	0.81
9.24	18.42	1.09	1.09	0.82
9.25	18.59	1.09	1.09	0.82
9.26	18.76	1.09	1.09	0.82
9.27	18.93	1.09	1.09	0.83
9.28	19.10	1.08	1.09	0.83
9.29	19.28	1.08	1.08	0.83
9.30	19.45	1.08	1.08	0.83
9.31	19.62	1.08	1.08	0.84
9.32	19.80	1.08	1.08	0.84
9.33	19.97	1.08	1.08	0.84
9.34	20.14	1.07	1.07	0.85
9.35	20.32	1.07	1.07	0.85
9.36	20.49	1.07	1.07	0.85
9.37	20.66	1.07	1.07	0.85
9.38	20.84	1.07	1.07	0.86
9.39	21.01	1.07	1.07	0.86
9.40	21.18	1.06	1.06	0.86
9.41	21.36	1.06	1.06	0.86
9.42	21.53	1.06	1.06	0.87
9.43	21.70	1.06	1.06	0.87
9.44	21.88	1.06	1.06	0.87
9.45	22.05	1.06	1.06	0.87
9.46	22.22	1.06	1.06	0.88
9.47	22.39	1.05	1.06	0.88
9.48	22.56	1.05	1.05	0.88
9.49	22.73	1.05	1.05	0.88
9.50	22.90	1.05	1.05	0.89
9.51	23.07	1.05	1.05	0.89

Table S4 Soil physical and chemical properties

Soil	Depth	pH		Sand	Silt	Clay	Total C
	/ cm	pH_{elec}	pH_{spec}		/ %		/ %
Monarto	0–10	7.87	7.97	84.6	7.1	8.3	1.0
Arboretum	0–10	6.24	6.37	50.0	35.0	15.0	2.9
Lock siliceous	0–10	7.95	7.93	95.0	0	5.0	1.6
Gillman	20–80	3.01	3.16	91.2	8.0	0.8	1.2
Ngarkat	0–10	6.81	6.94	95.8	1.0	3.2	0.67
ock Horizon	0–10	8.53	8.44	97.5	2.5	0	3.7
Mt Compass	0–10	4.93	5.06	97.2	1.7	1.1	0.5
Long Flat	140–210	2.86	3.21	11.4	31.6	57.0	1.5
Long Flat	190–240	4.00	4.12	7.6	31.8	60.6	1.3
Mobilong	85–100	4.65	4.80	0	7.7	92.3	1.5

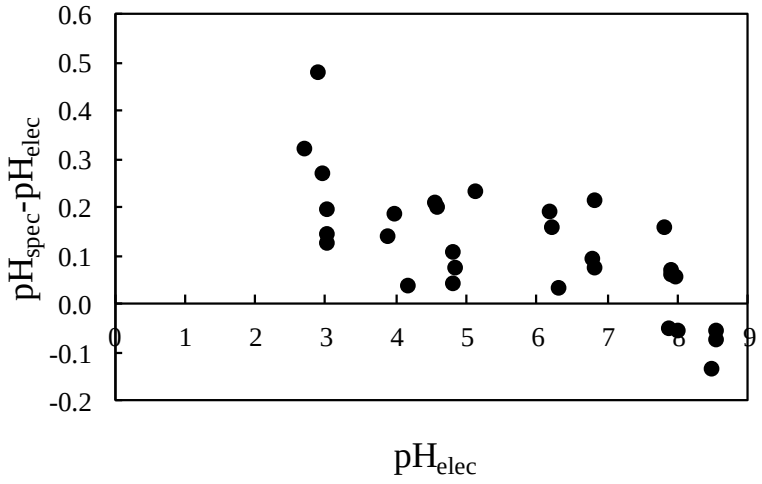

Figure S1 pH difference between the spectrophotometric and glass electrode methods plotted against electrode pH values.

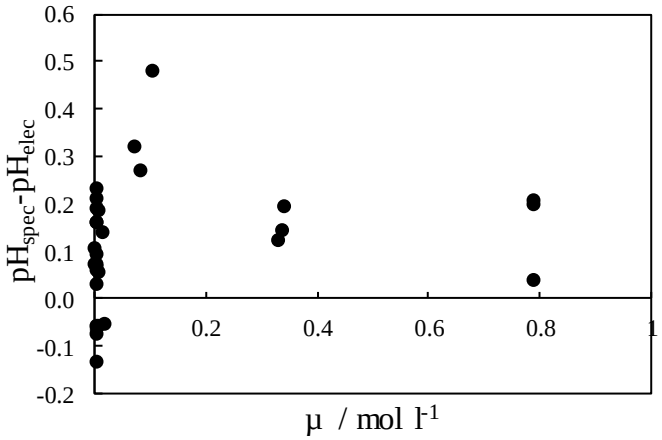

Figure S2 pH difference between the spectrophotometric and glass electrode methods plotted against ionic strength (μ).

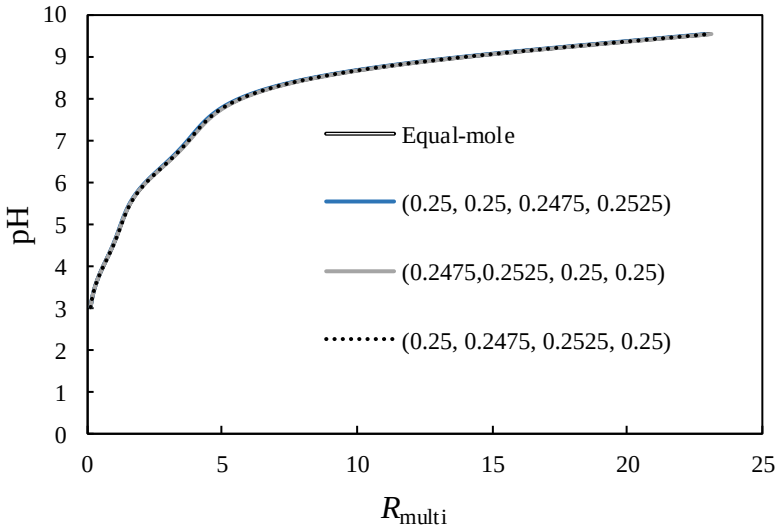

Figure S3 Effect of changing mole fractions of four-dye mixture (mCP- BCP-BPB-TB) on R_{multi} as a function of pH.

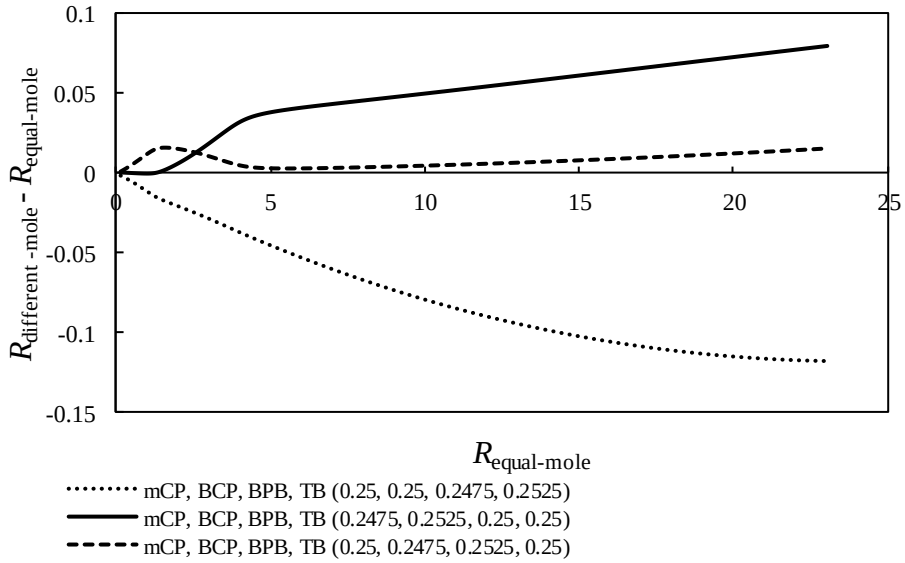

Figure S4 The residual plot for R_{multi} calculated for the equal and different mole fractions against $R_{equl\text{-}mole.}$

CHAPTER 5

Assessment of the internal consistency of the soil inorganic carbon system

Sima Bargrizan[a], Ronald J. Smernik[a], and Luke M. Mosley[b]

[a] The School of Agriculture, Food and Wine, The University of Adelaide, South Australia

[b] Acid Sulfate Soils Centre, School of Biological Sciences, The University of Adelaide, South Australia

Statement of Authorship

Title of Paper	Assessment of the internal consistency of the soil inorganic carbon system.
Publication Status	☐ Published ☐ Accepted for Publication ☐ Submitted for Publication ☑ Unpublished and Unsubmitted w ork w ritten in manuscript style
Publication Details	

Principal Author

Name of Principal Author (Candidate)	Sima Bargrizan		
Contribution to the Paper	Accomplished experiment, data collection, data analysis and interpretation, wrote manuscript		
Overall percentage (%)	70%		
Certification:	This paper reports on original research I conducted during the period of my Higher Degree by Research candidature and is not subject to any obligations or contractual agreements with a third party that would constrain its inclusion in this thesis. I am the primary author of this paper.		
Signature		Date	21.01.2019

Co-Author Contributions

By signing the Statement of Authorship, each author certifies that:

i. the candidate's stated contribution to the publication is accurate (as detailed above);

ii. permission is granted for the candidate in include the publication in the thesis; and

iii. the sum of all co-author contributions is equal to 100% less the candidate's stated contribution.

Name of Co-Author	Luke Mosley		
Contribution to the Paper	Supervised development of work, data interpretation and manuscript evaluation and correction, and acted as corresponding author .		
Signature		Date	21.01.2019

Name of Co-Author	Ron Smernik		
Contribution to the Paper	Supervised development of work, data interpretation, manuscript evaluation and correction		
Signature		Date	21.01.2019

Assessment of the internal consistency of the soil inorganic carbon system

Sima Bargrizan[a], Ron Smernik[a], Luke Mosley[b],

[a]The School of Agriculture, Food and Wine, The University of Adelaide, South Australia

[b]Acid Sulfate Soils Centre, School of Biological Sciences, The University of Adelaide, South Australia

Abstract

Carbonate system can be distinguished by measuring at least two of the four components ((partial pressure (pCO_2), total alkalinity (TA), pH and dissolved inorganic carbon (DIC)). In this study, the internal consistency of the soil carbonate system was examined using the carbonate model introduce by Stumm and Morgan (1996). For this purpose, laboratory measurements of pCO_2 through equilibrating the soil solution with air with a known pCO_2 and TA through alkalinity titration was used to calculate pH (pH_{CO2}). Then pH_{CO2} was compared with pH measured using spectrophotometric and glass electrode methods ($pH_{spec\ and}$ pH_{elec}). The results demonstrated the internal consistency of the soil carbonate system with a precision of ±0.03 pH units. Discrepancy between measured and calculated pH was within 0.00-

0.1 pH unit for most samples. However, more deviation was observed for those sample with low alkalinity (≤ 0.5 meq L^{-1}). This is likely attributable to the concentration of dissolved organic carbon (DOC)which was not considered in the thermodynamic carbonate model calculations. However, further research is required to resolve this problem. Furthermore, the potential of the carbonate model to assess the consequences of climate change such as increasing soil pCO_2 and soil carbonate dissolution was explored.

5.1 Introduction

Concentrations of atmospheric carbon dioxide (CO_2) has elevated by 40%, from 280 ppm in 1750 to 400 ppm in 2014 (MacFarling Meure et al. 2006). This increase has been caused by anthropogenic activities, especially burning of fossil fuels which has been distinguished by atmospheric global warming (Pierre Marrec 2014). Soil inorganic carbon is one of the largest sinks of atmospheric CO_2 and the global C cycle (Lal 2001) is vulnerable to these anthropogenic perturbations (Lal and Kimble 2000). Increasing soil CO_2 partial pressure (pCO_2) as a consequence of the increasing concentrations of atmospheric carbon dioxide (Andrews and Schlesinger 2001; King et al. 2001) has demonstrated the evidence of the participation of soil inorganic carbon systems regarding global soil-atmospheric CO_2 fluxes.

Under increased soil pCO_2, soil acidification occurs through carbonic acid formation followed by weak acid dissociation (Simunek et al. 1993). In arid and semi-arid areas, Ca^{2+} combines with carbonate to form calcite ($CaCO_3$) which often comprises a major part of the calcareous soil system (Strawn et al. 2015). The weathering (dissolution) of calcite in soils arises from either carbonic acid at pH > 6 or strong acids at lower pH. Dissolution of solid calcium carbonate at pH > 6.5, (provided that the weatherable

calcite is not finished) (Kilham 1982; Perrin et al. 2008; Raymond and Hamilton 2018)provides a buffer via an increase in HCO_3^- alkalinity against the pH changes in soil (Reardon et al. 1979) caused by acidification processes (Bargrizan et al. 2018, see Chapter 3). The assessment of the degree of calcium carbonate saturation is crucial for agricultural management due to its influence on chemical and physical soil characteristics such as CEC, porosity, conductivity, and pH (Peverill et al. 2001). The outcome of decreasing pH (soil acidification) as a result of climate change, would be a decrease in calcium carbonate saturation states resulting in calcite dissolution (Berner 1997; Bormann et al. 1998; Berg and Banwart 2000) and a decrease in the buffer capacity it provides. In addition to the soil acidification, the CO_2 flux from soil to the atmosphere has also been affected by elevated soil pCO_2 which lead to negative response to the atmospheric CO_2 level (De Jong and Schappert 1972).

In order to improve our understanding of the soil carbon cycle, in particular our confidence in projections of the effect of CO_2 release on climate and the consequences of soil acidification, accurate characterization of the soil inorganic carbon system (Wanninkhof et al. 1999), is essential. This requires measurement of inorganic system variables such total alkalinity (TA), pH, pCO_2 and dissolved inorganic carbon (DIC) (Karberg et al. 2005). By measuring accurately at least two of these inorganic carbon system parameters it is possible to calculate the remaining parameters using knowledge of the carbonate equilibrium constants (Dickson et al. 2007). If a third carbonate system parameter is measured this enables rigorous checking of the internal consistency of the equilibrium constants of the system and accuracy of measurements (Marion et al. 2011).

The internal consistency assists in checking if the same outcomes can be obtained through different independent carbonate system measurements (Reimer 2017). The internal consistency of different sets of marine carbonate system measurements and equilibrium constants has previously been demonstrated (Clayton et al. 1995; Zhang et al. 1996; Wanninkhof et al. 1999; Lueker et al. 2000; Patsavas et al. 2015). However, this internal consistency has not been demonstrated yet for the soil carbonate system, and this introduces major uncertainties in our ability to understand acidification risks and response to rising atmospheric CO_2 levels. Highly precise analytical measurements of carbonate parameters are a prerequisite for evaluation of internal consistency of this system (Millero et al. 1993; Lee et al. 2000; Koeve and Oschlies 2012; Hoppe et al. 2012; Salt et al. 2016). This was one of the drivers for our recent developments in spectrophotometric pH measurements methods for soils (Bargrizan et al. 2017, 2018) which had previously been proved in terms of high precision (> 0.01 pH units) in the marine chemistry field (Robert-Baldo Byrne et al. 1985; Byrne 1988; Clayton and Byrne 1993; Yao and Byrne 2001; Ohlin et al. 2007; Lai et al. 2016).

The objective of this study was to develop a model for evaluation of the consistency of thermodynamics of the soil carbonate system by calculation of a third parameter from two other parameters; Using a controlled laboratory experiment, we calculated pH of soil solutions equilibrated with a fixed pCO_2 and measured total alkalinity (TA) and then compared the results with pH measured through spectrophotometric and glass electrode methods. This study is also unique in terms of the investigation of internal consistency of soil carbonate system through the incorporation of spectrophotometric method for pH measurement. A further aim of this study was to assess the accuracy of spectrophotometric soil pH measurements against electrode method using the same

approach. A modelling approach was then explored as a potential tool for prediction of increasing soil pCO_2 and soil carbonate dissolution as a result of climate change.

5.2 Material and Methods

5.2.1 Theory

5.2.1.1 Soil pH determination using acid-base equilibria of CO_2

The pH and carbonate equilibria in the soil solution can in theory be determined using Henry's Law constant for CO_2 (K_H), the first and second dissociation constants of carbonic acid (H_2CO_3*) resulting in bicarbonate and carbonate ions, respectively, and the water ionization constant (K_w) (Stumm and Morgan 1996):

$$CO_2 + H_2O \rightleftharpoons H_2CO_3^* \qquad K_H = \frac{[H_2CO_3^*]}{pCO_2} = 10^{-1.47} \qquad [1a]$$

$$H_2CO_3^* \rightleftharpoons H^+ + HCO_3^- \qquad K_1 = \frac{[H^+][HCO_3^-]}{[H_2CO_3^*]} = 10^{-6.35} \qquad [1b]$$

$$HCO_3^- \rightleftharpoons H^+ + CO_3^{2-} \qquad K_2 = \frac{[H^+][CO_3^{2-}]}{[HCO_3^-]} = 10^{-10.33} \qquad [1c]$$

$$H_2O \rightleftharpoons H^+ + OH^- \qquad K_W = [H^+][OH^-] = 10^{-14} \qquad [1d]$$

The net negative charge arising from the dissociation of dissolved carbonic acid and other weak acids such as water (i.e. HCO_3^-, CO_3^{2-}, OH^-) has to balance exactly the net positive charge from the strong mineral bases (Na^+, K^+, Ca^{2+}, Mg^{2+}) and can be expressed as a charge balance or electroneutrality equation:

$$C_B + [H^+] = [HCO_3^-] + 2[CO_3^{2-}] + [OH^-] - C_A \qquad [2a]$$

Where C_B and C_A are the amounts of base and acid that are present in the system, respectively. Because it is usually impractical to measure the amounts of acid and base that have been added, a new quantity, alkalinity, is defined as the acid neutralizing capacity of the system. In carbonate-alkalinity dominated systems, the individual ions contributing to alkalinity may be expressed as:

$$\text{Alkalinity} = C_B - C_A = [HCO_3^-] + 2[CO_3^{2-}] + [OH^-] - [H^+] \quad [2b]$$

In actual soil-water systems, other anions (e.g. sulfate) and organic bases may also provide alkalinity (Breemen et al. 1983).

In an open system in close contact with the atmosphere (e.g. surface soil), the carbonic acid activity in a soil solution is governed by the partial pressure of $CO_2(g)$ (pCO_2) in the gas phase. Therefore, the concentration of carbonate ions based on mass balance can be defined as (Stumm and Morgan 1996):

$$[H_2CO_3^*] = C_T \alpha_0 = K_H \, pCO_2 \quad [3a]$$

Therefore

$$C_T = \frac{K_{HpCO_2}}{\alpha_0}$$

$$[HCO_3^-] = C_T \alpha_1 \quad [3b]$$

$$[CO_3^{2-}] = C_T \alpha_2 \quad [3c]$$

Where, according to carbonate dissociation constants:

$$\alpha_0 = \frac{1}{1 + \frac{K_1'}{\{H^+\}} + \frac{K_1' K_2'}{\{H^+\}^2}} \quad [4a]$$

$$\alpha_1 = \frac{1}{\frac{\{H^+\}}{K_1'} + 1 + \frac{K_2'}{\{H^+\}}} \quad [4b]$$

$$\alpha_2 = \frac{1}{\frac{\{H^+\}^2}{K_1' K_2'} + \frac{\{H^+\}}{K_2'} + 1} \quad [4c]$$

K'_H, $K'_{\alpha 1}$ and $K'_{\alpha 2}$ can be recalculated considering the effect of ionic strength on activity coefficients using the Davies equation (Stumm and Morgan 1996). (Refer to equation 1 for value of K_H, K_1 and K_2 at zero ionic strength).

Substitution into the charge balance equation [2a] and combining equation [3a] for C_T, [3b] and [3c] results in (Stumm and Morgan 1996):

$$\text{Alkalinity} = C_B - C_A = \frac{K_{HpCO_2}}{\alpha_0}(a_1 + 2a_2) + \frac{K_w}{[H^+]} - [H^+] \quad [5]$$

This equation implies experimentally measured alkalinity (acid neutralizing capacity) relative to a weak electrolyte since it corresponds to the concentration of strong acid required to titrate the solution to the endpoint of bicarbonate. pH can be determined using equation [5] provided that the amounts of acid or base added to the system and pCO_2 are known. Equation [5] can be solved iteratively by the bisection method until the left-hand side (alkalinity) equals the right-hand side or via numerical methods.

5.2.2 Soil solution preparation

Nine soils with pH range of 6-8 (Table 1) with three replicates of each soil solution (1:1 soil:water) were used in the study for pH measurements. (refer to Bargrizan et al. 2017 for details).

Table 1: Soil physical and chemical properties.

	Depth	Sand	Silt	Clay	Major cations and anions						
					Cl^-	NO_3^-	SO_4^{2-}	Ca^{2+}	K^+	Mg^{2+}	Na^+
			%		meq L^{-1}						
Monarto 1*	0-10	84.6	7.10	8.30	0.65	0.44	0.13	2.62	0.46	0.56	0.69
Lock siliceous	0-10	95	0	5	0.38	2.35	0.09	3.59	0.78	0.44	0.35
Karoonda	0-10	97.4	0.2	2.40	0.24	0.24	0.11	0.39	0.25	0.21	0.20
Ngarkat	0-10	95.80	1.0	3.20	0.18	0.04	0.05	0.25	0.11	0.17	0.21
Lock Horizon	0-10	97.50	2.50	0	0.20	0.34	0.14	1.40	0.11	0.54	0.60
Modra	0-10	65	5	30	3.36	5.70	0.31	5.72	1.34	1.39	1.34
Monarto 2*	0-10	93.6	1.1	3.8	0.31	0.24	0.19	0.50	0.39	0.30	0.25
Cowirra	0-10	41.50	18.80	39.70	4.57	0.02	35.6	25.46	1.14	14.36	9.17
Black point	10-20	72.70	9.20	18.10	2.21	0.28	0.37	2.23	0.27	0.55	2.46

*Monarto 1 and Monarto 2 were selected form two locations (Highland and Highway respectively).

5.2.3 Laboratory experimental set up

A laboratory experiment was conducted in which ca. 25 mL of soil extract was introduced into a custom-made equilibration flask (Figure 1) which was connected via tubing to a flow-through cell on a double-beam spectrophotometer (GBC UV/VIS 916).

The flask was placed on a temperature-controlled water bath adjusted to 25˚C. The temperature in the spectrophotometric cell holder was also kept constant at 25˚C using an installed water thermostat. A pH electrode (Orion SureFlow) was inserted into the flask that had been pre-calibrated with commercially manufactured (Australian Chemical Reagents) standard high ionic strength pH 7 and pH 4 buffers ($m \approx 0.1$ mol L^{-1}) at 25°C.

The soil extracts were equilibrated with a fixed pCO_2 via a gas tube connected to a pure air cylinder (BOC gases) inserted into the top of the equilibration cell (Figure 1). The pCO_2 in the gas stream was measured using a calibrated LICOR 840a infra-red gas analyser. The air was circulated through the soil solution using slow bubbling for approx. 30 min per sample until the spectra of solution and the electrode pH measurement were stable.

Then for spectrophotometric pH measurement, a sulfonephthalein indicator depending on the sample pH range (determined by the electrode) was selected and injected into the soil solution. The absorbance spectrum with dye was recorded for the circulating soil extract solution. The absorbance of indicator was corrected against baseline through subtracting of soil solution without indicator dye (as a reference) from the measurement spectra of soil extract with the dye (refer to Bargrizan et al. 2017 for details).

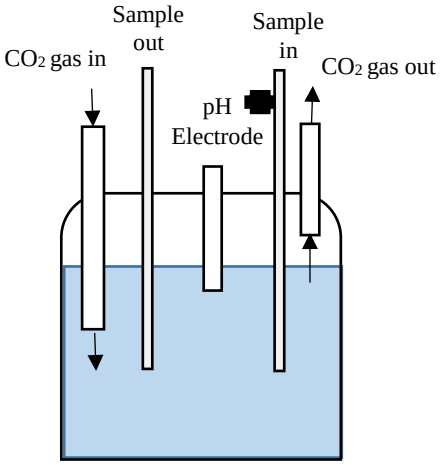

Figure 1: Diagram of soil carbonate equilibrium cell.

5.2.4 Alkalinity measurement

After pH measurement, a measured volume of soil solution and indicator dye was transferred into a separate beaker for alkalinity measurement. Great attention was taken to avoid solution loss by getting the remaining amount of solution out of the flow-through cell and connecting tubes. The solution was stirred gently, and initial pH was recorded when a stable reading was obtained, and then titration was conducted using an autotitrator to deliver increments of 0.16 N H_2SO_4 and continued to the end point at pH $\leq$ 3.5. pH was measured using a glass electrode after each acid addition. Adequate titration points were recorded, ensuring high accuracy. A gran linear extrapolation function was utilized to determine alkalinity for low ionic strength samples (Rounds 2001).

5.2.5 Laboratory analytical measurements

A stock solution of bromocresol purple (BCP) and phenol red (PR) at a total concentration of 3×10^{-3} mol L^{-1} was used. The absorbance maxima (Abs) of acid and base forms of PR were read at 433 nm, 558 nm (λ_1 and λ_2) and BCP at 432 nm, 589 nm (λ_1 and λ_2), respectively, using Cintral software and used for R (= λ_2Abs./λ_1Abs) calculation (see Bargrizan et al. 2017). The value for molar absorbance ratios (e_1-e_3) and pK_2 of indicators used in this study (PR and BCP) are those of Yao and Byrne (2001).

The ionic strength of each soil extract was determined via electrical conductivity (EC, mS cm 1) measurement using a calibrated conductivity electrode (TPS Glass K = 1.0 Cond Sensor) using the equation μ= EC x 0.0127 (Griffin and Jurinak 1973; Gillman and Bell 1978, Bargrizan et al. 2017).

DOC concentration of filtered soil solutions was also estimated using a spectrophotometer at an absorbance of 250 nm (Baldwin 1999) using the regression equation [DOC] = 33.99 A_{250} + 8.16 (Baldwin 1999; O'Connell et al. 2000; Whitworth et al. 2014).

Concentrations of major cations were measured by inductively coupled plasma optical emission spectroscopy (ICPOES) (APHA method 3120) and concentrations of anions were determined by ion chromatography using a Dionex ICS-2500 system (APHA method 4110) (Table 1).

5.2.6 Geochemical modelling calculations

To assess the internal consistency of the soil carbonate system, we compared the soil solution pH (n=27, pH range of appx. 6-8) calculated from pCO_2 (pH_{CO2}) to the pH

measurements using both spectrophotometric (pH_{spec}) and glass electrode (pH_{elec}) methods. pH_{CO2} was calculated from known pCO_2 (433ppm) and alkalinity measurements using equation (5). Carbonate system calculations were based on equilibrium constants reported by Stumm and Morgan (1996) at μ=0 and 25˚C.

The geochemical speciation program PHREEQC (USGS 2002) was also used to calculate carbonate calcium saturation (calcite) from the fixed pCO_2 and measured alkalinity, measured major ions and also at a range of pCO_2 values (to assess the effect of climate change on saturation status) and spectrophotometrically measured pH.

5.3 Results

5.3.1 Internal consistency of soil carbonate system

The pH values calculated using the carbonate model (pH_{CO2}) and pH obtained using electrode and spectrophotometric methods (pH_{elec} and pH_{spec}) is shown in Table 2. An average precision of ca. 0.03 pH units was obtained for three independent pH measurements of the carbonate system which was similar to those of measured pH_{spec} and pH_{elec} values (0.05 pH units) (Table 2).

As shown in figure 2a, the residual plot pH (CO_2 - spec/elec) for different samples, calculated pH (pH_{CO2}) was in general higher than the measured pH values (pH_{elec} and pH_{spec}). There was a good agreement between measured and calculated pH for soil extracts with pH > 7 (Table 2, Figure 2a) with the average differences of approx.0.1 pH units. These results showed that soil carbonate system model using the constants of Stumm and Morgan (1996) was internally consistent with measurements in pH > 7 solutions. However, there was larger deviation of 0.3-0.8 pH units for those samples with pH ≤ 7 (Table 2, Figure 2a), which mainly corresponded to soil extracts with low

alkalinity of < 0.5 meq L^{-1} (Figure 2b). Inconsistencies in the pH-DIC-pCO_2 relationship have been previously explained with regards to the difference between DIC and TA concentrations (Patsavas et al. 2015). Measured TA constitutes the contribution of both organic bases (Kim and Lee 2009; Hoppe et al. 2012; Patsavas et al. 2015; Salt et al. 2016) and carbonate species. Conversely, calculation of TA via the thermodynamic carbonate model used in this study does not include the contribution of organic bases. In an attempt to determine the source of total alkalinity surplus relative to calculated carbonate, dissolved organic carbon (DOC) for all samples was estimated via spectrophotometric measurements in the UV-range (Table 3). Not much difference was observed between samples' DOC which was within approx. 70 mg L^{-1}.

Table 2: Mean and standard deviation (SD) of calculated pH (pH_{CO2}), measured pH_{spec} and pH_{elec}.

Soil	pH_{CO2} ±SD	pH_{spec}	pH_{elec}
1. Lock Siliceous	7.98 (0.01)	8.00 (0.09)	7.91 (0.03)
2. Ngarkat	7.08 (0.01)	7.03 (0.04)	6.79 (0.03)
3. Monarto 1	8.06 (0.01)	8.06 (0.03)	8.11 (0.04)
4. Modra	7.60 (0.04)	7.67 (0.04)	7.63 (0.02)
5. Lock Horizon	8.17 (0.03)	8.12 (0.04)	8.10 (0.04)
6. Karoonda	7.05 (0.06)	6.47 (0.08)	6.24 (0.14)
7. Monarto 2	7.17 (0.12)	6.75 (0.06)	6.63 (0.06)
8. Cowirra	7.79 (0.01)	7.74 (0.05)	7.72 (0.02)
9. Black point	7.94 (0.01)	8.04 (0.03)	8.04 (0.01)
Average SD	0.03	0.05	0.05

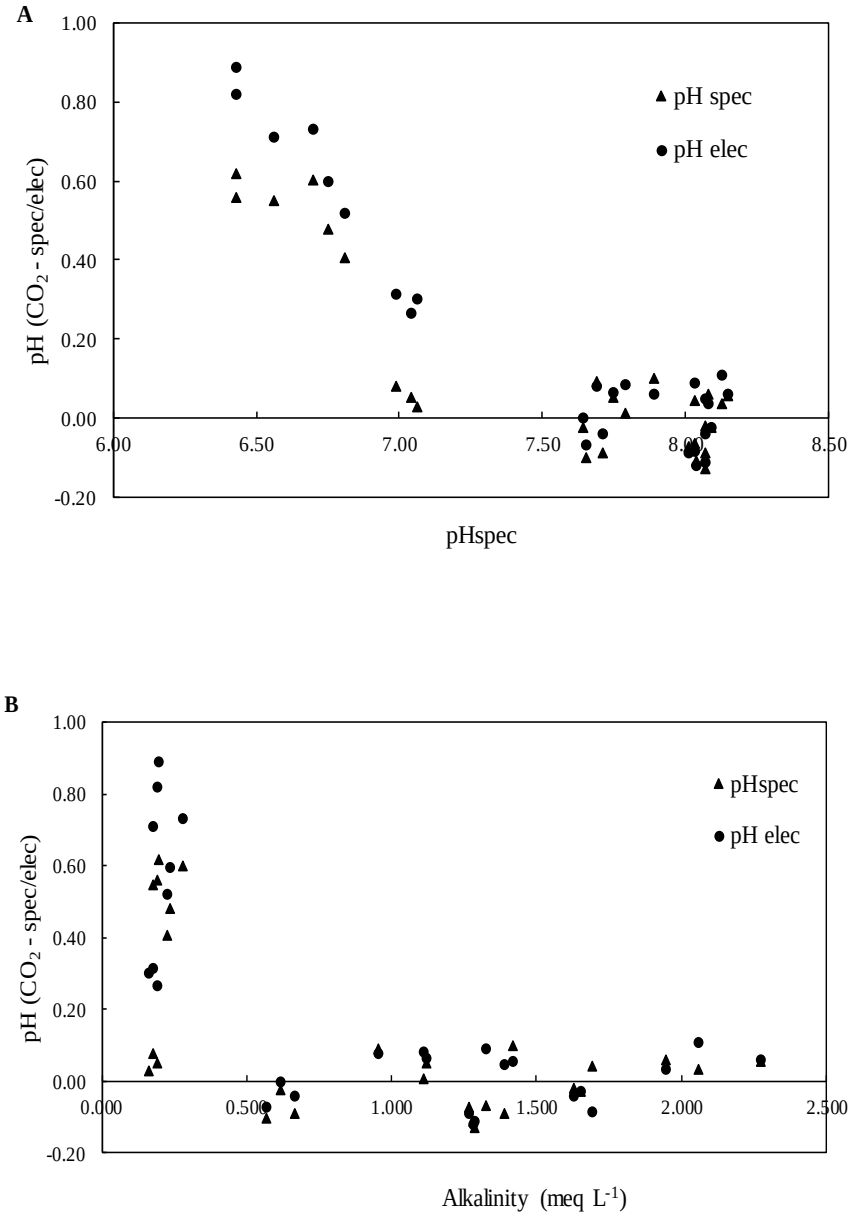

Figure 2: (A): Difference between pH calculated using carbonate systems and spectrophotometric and electrode pH measurements for different soils against spectrophotometric pH values. (B): Difference between calculated and measured pH values as a function of total alkalinity.

Table 3: The mean value of alkalinity titration (TA_{tit}) with standard deviation (SD) in brackets and estimated dissolved organic carbon (DOC).

Samples	TA_{tit} (SD) meq L^{-1}	Estimated DOC mg L^{-1}
Lock siliceous	1.38 (0.05)	74.69
Monarto 1	1.66 (0.03)	78.14
Ngarkat	0.18 (0.01)	62.08
Modra	0.62 (0.05)	68.88
Lock B	2.9 (0.17)	33.50
Karoonda	0.19 (0.01)	70.91
Monarto 2	0.25 (0.03)	73.71
Cowirra	1.06 (0.09)	76.64
Black point	1.28 (0.01)	75.24

5.3.2 Calculation of calcite saturation states using the PHREEQC program

Calcite saturation states (mg L^{-1}) of soil samples were calculated from non-fixed pCO_2 (pH_{spec} and TA) and fixed pCO_2 (pCO_2 and TA) using PHREEQC. There was variability in calcite saturation state with some over (SI > 0 at $pH_{PHREEQC}$ > 8, suggesting mineral calcite could precipitate from solution) and some under-saturated (SI < 0 at $pH_{PHREEQC}$ < 8, suggesting calcite dissolution) (Table 4).

Table 4: Calculated pH ($pH_{PHREEQC}$) and Calcite using PHREEQC program

Soil	**pH $_{PHREEQC}$**	**SI-Calcite (pH_{spec} and TA)** (mg L^{-1})	**SI-Calcite (pCO_2 and TA)** (mg L^{-1})
Lock Siliceous	8.27	0.2879	0.5432
Monarto 1	8.36	0.3414	0.6254
Ngarkat	7.41	-2.5766	-2.2017
Modra	7.89	-0.2833	-0.0659
Lock Horizon	8.47	0.2529	0.5812
Karoonda	7.38	-2.9971	-2.0907
Monarto 2	7.51	-2.4923	-1.7399
Cowirra	8.04	0.3582	0.643

5.4 Discussion

In this study, the internal consistency of the soil CO_2 system was illustrated using a carbonate system equilibrium model (Stumm and Morgan 1996) through an assessment of the ability of pCO_2 and TA pairs to calculate soil solution pH (three replicates, a precision of ±0.03 pH units). For most soils, comparison of pH_{CO2} and

measured $pH_{spec,elec}$ indicated a small difference of approximately 0.00-0.1 pH units. However, a much larger deviation was observed for samples with low alkalinity. Such inconsistencies have also been seen in other studies and have been attributed to the presence of dissolved organic carbon (Kim and Lee 2009; Hoppe et al. 2012) which is not accounted for in the thermodynamic carbonate model. Estimated dissolved organic carbon (DOC) was quite similar between the samples and in the range 33-78 mg L^{-1} (Baldwin 1999) (Table 2). For those samples with ($\leq$ 0.5 meq L^{-1}), where DIC < DOC, the discrepancy between total (Gran) and carbonate alkalinity seems likely to have occurred through the uptake of protons by organic bases (Table 2). Hence it seems preferable to not use alkalinity as a measured parameter for carbonate system calculations in soils, particularly in low alkalinity soils. Hence measuring pH and pCO_2 or TCO_2 should be preferred. Spectrophotometric carbonate measurements recently developed by Easley et al. (2013) may also enable precise values for carbonate concentration which is a parameter that can also be used in internal consistency calculations.

While the internal consistency of the seawater CO_2 system has been previously demonstrated (Millero et al. 1993; Clayton et al. 1995; Wanninkhof et al. 1999; Patsavas et al. 2015; Salt et al. 2016;), our measurements show it is possible to demonstrate this in soil solutions. This is important as it demonstrates, for the first time to our knowledge, that carbonate system equilibria can be accurately modelled in soils. According to Raupach et al. (2007), atmospheric CO_2 could increase to over 1000 ppm by the end of this century. This could even have much higher effect on CO_2 in soils, as soil pCO_2 for some soils can be 1-10 times higher than CO_2 concentrations in the open atmosphere (Strawn et al. 2015). This reaction is kinetically controlled

which mainly depends on soil respiration as a major element in carbon cycle weathering processes, soil water content and temperature (Raich and Potter, 1995).

As noted above soil pCO_2 is one of the most important variables governing soil solution pH (Robbins 1986). To indicate the potential application of the proposed model to assess climate change effects, the influence of four soil pCO_2 scenarios on pH on selected soils was shown in figure 3 where soil pH decreased from 0.4 to 1 pH units as a consequence of increased pCO_2 from 1000 to 10000 µatm.

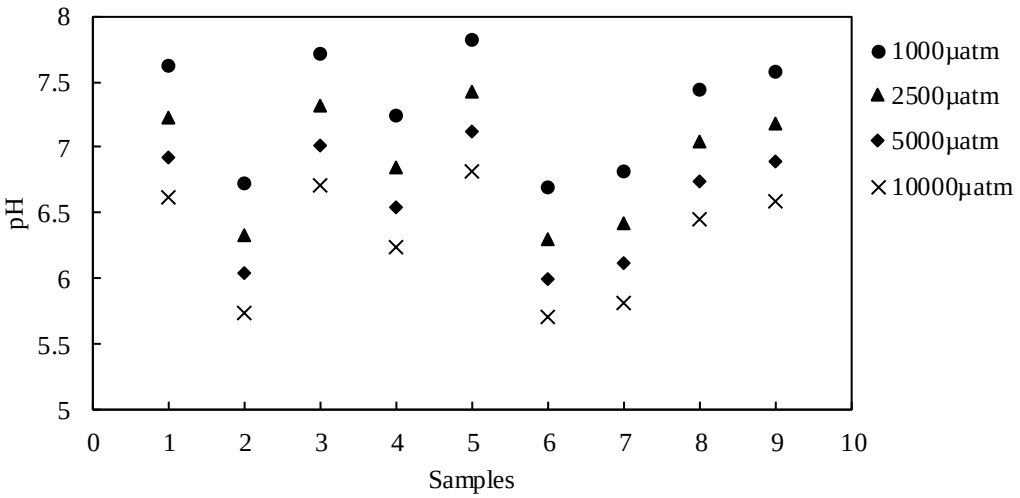

Figure 3: The mean pH calculated for the different pCO_2 (1000, 2500, 5000, 10000 uatm pCO_2) concentrations using carbonate model for 9 soil samples (1= Lock Siliceous, 2 = Ngarkat, 3= Monarto 1, 4= Modra 5= Lock Horizon B 6= Karoonda 7= Monarto 2 , 8= Cowirra 9= Black point).

Another capability of the carbonate equilibrium model is the determination of accurate $CaCO_3$ saturation states. Monitoring of calcite saturation state is important since it will provide an insight into the understanding of the impact of acidification owing to

climate change on soil ecosystems in the future. The carbonate model can help better explore this process as in previous scenario, the effect of increasing soil pCO_2 was evident in the model. The effect of varying pCO_2 on calcite saturation state (calculated using PHREEQC from pH and TA) of soil samples used in this study is illustrated in figure 4 where at higher pCO_2, calcite condition switches from supersaturated (SI > 0) to undersaturated (SI < 0). This would suggest solid calcite dissolution would occur in the soil which lowers pH buffering capacity. It is also important to note that our measurement set-up and models assumed an open system fully equilibrated with the atmosphere which likely only applies to the surface soil system. Nevertheless, the internal consistency demonstrated should also apply to a closed system.

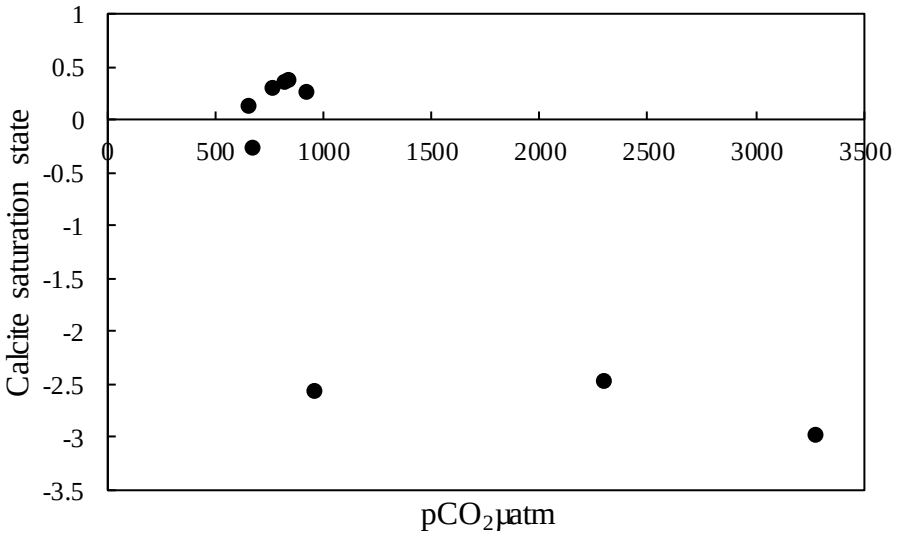

Figure 4: Relationship between calcite saturation state and soil pCO_2

The potential for higher accuracy of spectrophotometric pH determination than with a glass electrode was not proven (i.e. accuracy was very similar) using the carbonate equilibria which may be due to our very careful pH electrode measurement protocols (e.g., temperature control, electrodes with free-flowing junctions designed for soil).

Spectrophotometrically measured pH along with another carbonate system parameter has been the most common approach to calculate oceanic pCO_2 (Clayton et al. 1995; Patsavas et al. 2015). The soil carbonate modelling conducted in this study would be the first step in developing an approach for indirect measurement of soil pCO_2 in situ and better understanding risks of calcium carbonate dissolution. Consequently, it would be important to see if such internal consistency can be demonstrated in situ. Also, the contribution of spectrophotometric pH measurement method in characterization of CO_2 system is reassessed. For this purpose, field experiments are now suggested accompanied by both spectrophotometric and electrode soil pH measurement methods. Soil respiration changes pCO_2 and pH which needs to be considered in the design of field measurements. Widespread global measurement of soil pH and calcium carbonate states using these methods would appear beneficial to assess risks of the soil system to climate change.

Acknowledgements

We would like to thank Colin Rivers who provided some of the soils utilized in this research. This study was supported by the assistance of the Australian Commonwealth Government through an Australian Research Council Discovery Project Grant DP170104541 for RF and LM. Sima Bargrizan would also like to acknowledge the University of Adelaide postgraduate scholarship.

References

Andrews, J.A, Schlesinger, W.H., 2001. Soil CO_2 dynamics, acidification, and chemical weathering in a temperate forest with experimental CO_2 enrichment. Global Biogeochemal Cycles 15(1), 149-162.

Baldwin, D.S., 1999. Dissolved organic matter and phosphorus leached from fresh and `terrestrially' aged river red gum leaves: implications for assessing river-floodplain interactions. Freshwater Biology 41, 675-685.

Bargrizan, S., Smernik, R.J., Mosley, L.M., 2017. Development of a spectrophotometric method for determining pH of soil extracts and comparison with glass electrode measurements. Soil Science Society of America Journal 81, 1350-1358.

Bargrizan, S., Smernik, R.J., Mosley, L.M., 2018. The application of a spectrophotometric method to determine pH in acidic (pH < 5) soils. Talanta 186, 421-426.

Berg, A., Banwart, S.A., 2000. Carbon dioxide mediated dissolution of Ca-feldspar: implications for silicate weathering. Chemical Geology 163, 25-42.

Berner, R.A., 1997. The rise of plants and their effect on weathering and atmospheric CO_2 Science 276, 544-546.

Bormann, B.T., Wang, D., Bormann, F.H., Benoit, G., April, R., Snyder, R., 1998. Rapid plant-induced weathering in an aggrading experimental ecosystem. Biogeochemistry 43, 129-155.

Breemen, N.V., Mulder, J., Driscoll, C.T., 1983. Acidification and alkalinization of soils. Plant and Soil, Vol 75. pp. 283-308.

Byrne, R.H., Robert-Baldo, G., Thompson S.W., Chen, C.T.A., 1988. Seawater pH measurements: an at-sea comparison of spectrometric and potentiometric methods. Deep-Sea Research Part A 35, 1405-1410.

Clayton, T.D., Byrne, R.H., 1993. Spectrophotometric seawater pH measurements: Total hydrogen ion concentration scale calibration of m-cresol purple and at-sea results. Deep-Sea Research Part I, Vol 40(10). pp. 2115-2129.

Clayton, T.D., Byrne, R.H., Breland, J.A., Feely, R.A., Millero, F.J., Campbell, D.M., Murphy,P.P., Lamb, M.F., 1995. The role of pH measurements in modern oceanic CO_2-system characterizations: Precision and thermodynamic consistency. Deep-Sea Research II, Vol. 42, No. 2-3. pp. 41 l-429.

De Jong, E., Schappert, H.J. V., 1972. Calculation of soil respiration and activity from CO_2 profiles in the soil. Soil Science 119, 328-333.

Dickson, A.G., Sabine, C.L., Christian, J.R., 2007. Guide to Best Practices for Ocean CO_2 Measurements. PICES Special Publication 3, No 8. IOCCP Report.

Easley, R.A., Patsavas, M. C., Byrne, R.H., Liu, X., Feely, R. A., Mathis, J.T., 2013. Spectrophotometric Measurement of Calcium Carbonate Saturation States in Seawater. Environmental Science & Technology 47, 1468-1477.

Gillman, G.P., Bell, L.C., 1978. Soil Solution Studies on Weathered Soils from tropical North Queensland. Australian Journal of Soil Research 16, 67-77.

Griffin, B., Jurinak, J.J., 1973. Estimation of activity coefficients from the electrical conductivity of natural aquatic systems and soil extracts. Soil Science 116, 26-30.

Hoppe, C.J.M., Langer, G., Rokitta, S.D., Wolf-Gladrow, D.A., Rost, B., 2012. Implications of observed inconsistencies in carbonate chemistry measurements for ocean acidification studies. Biogeosciences 9, 2401-2405.

Karberg, N. J., Pregitzer, K. S., King, J. S., Friend, A. L., Wood, J. R., 2005. Soil carbon dioxide partial pressure and dissolved inorganic carbonate chemistry under elevated carbon dioxide and ozone. Oecologia 142, 296-306.

Kilham, P., 1982. Acid precipitation: Its role in the alkalization of a lake in Michigan. Limnology and Oceanography 27, 856-867.

Kim, H. C., Lee, K., 2009. Significant contribution of dissolved organic matter to seawater alkalinity. Geophysical Research Letters 36, L20603.

King, J.S., Pregitzer, K.S., Zak, D.R., Sober, J., Isebrands, J.G., Dickson, R.E., Hendrey, G.R., Karnsoky, D.F., 2001. Fine-root biomass and fluxes of carbon in young stands of paper birch and trembling aspen as affected by elevated atmospheric CO_2 and tropospheric O_3. Oecologia 128, 237-250.

Koeve, W., Oschlies, A., 2012. Potential impact of DOC accumulation on fCO_2 and carbonateion computations in ocean acidification experiments. Biogeosciences 9, 3787-3798.

Lai, C.Z., DeGrandpre, M.D., Wasser, B.D., Brandon, T.A., Clucas, D.S., Jaqueth, E.J., Benson, Z.D., Beatty, C.M., Spaulding, R.S., 2016. Spectrophotometric measurement of freshwater pH with purified meta-cresol purple and phenol red. Limnology &. Oceanography: Methods 14, 864-873.

Lal, R., Kimble, J.M., 2000. Pedogenic carbonates and the global carbon cycle. In: Lal, R., Kimble, J.M., Eswaran, H., Stewart, B.A. (Eds.), Global Climate Change and Pedogenic Carbonates. CRC Press, Boca Raton, FL, USA, pp. 1-14.

Lal, R., 2001. World cropland soils as a source or sink for atmospheric carbon. Advances in Agronomy 71, 145-191.

Lee, C., Wakeham, S.G., Hedges, J.I., 2000. Composition and flux of particulate amino acids and chloropigments in equatorial Pacific seawater and sediments. Deep-Sea Research I: Oceanographic Research Papers 47, 1535-1568. http://dx.doi.org/10.1016/s0967-0637(99)00116-8.

Lueker, T.J., Dickson, A.G., Keeling, C.D., 2000. Ocean pCO_2 calculated from dissolved inorganic carbon, alkalinity, and equations for K_1 and K_2: validation based on laboratory measurements of CO_2 in gas and seawater at equilibrium. Marine Chemistry 70, 105-119.

MacFarling Meure, C., Etheridge, D., Trudinger, C., Steele, P., Langenfelds, R., van Ommen, T., Smith, A., Elkins, J., 2006. Law Dome CO_2, CH_4 and N_2O ice core records extended to 2000 years BP. Geophysical Research Letters 33, L14810.

Marion, G.M., Millero, F.J., Camões, M.F., Spitzer, P., Feistel, R., Chen, C.T.A., 2011. pH of Seawater. Marine Chemistry 126, 89-96.

Millero, F.J., Byrne, R.H., Feely, R.W.R, Clayton,T., Murphy,F., Marilyn, F., Lamb, d., 1993. The internal consistency of CO_2 measurements in the equatorial Pacific. Marine Chemistry 44, 269-280.

O'Connell, M., Baldwin, D. S., Robertson, A. I., and Rees, G., 2000. Release and bioavailability of dissolved organic matter from floodplain litter: Influence of origin and oxygen levels. Freshwater Biology 45, 333-342.

Ohline, S.M., Reid, M.R., Husheer, S.L., Currie, K.I. & Hunter, K.A., 2007. Spectrophotometric determination of pH in seawater off Taiaroa Head, Otago, New Zealand: full-spectrum modelling and prediction of pCO_2 levels. Marine Chemistry 107, 143-155.

Patsavas, M.C., Byrne, R.H., Yang, B., Easley, R.A., Wanninkhof, R., Liu, X., 2015. Procedures for direct spectrophotometric determination of carbonate ion concentrations: measurements in the US Gulf of Mexico and East Coast Waters. Marine Chemistry 168, 80-85.

Perrin, A.S., Probst, A. Probst, J.L., 2008. Impact of nitrogenous fertilizers on carbonate dissolution in small agricultural catchments: Implications for weathering CO_2 uptake at regional and global scales. Geochimica et Cosmochimica Acta 72, 3105-3123.

Peverill, K.I., Sparrow, L.A., Reuter, D.J. (Eds.), 2001. Soil Analysis an Interpretation Manual. Commonwealth Scientific and Industrial Research Organisation Publishing, Melbourne, Australia.

Pierre M., 2014. Dynamics of the carbonate system and air-sea CO_2 fluxes in western European shelf waters: a multi-scale approach. Oceanography. Pierre and Marie Curie University.

Raich, J.W., Potter, C.S., 1995. Global patterns of carbon dioxide emissions from soils. Global Biogeochemical Cycles 9 (1), 23-36.

Raupach, M. R., Marland, G., Ciais, P., Le Qu´er´e, C., Canadell, J. G., Klepper, G., and Field, C. B., 2007. Global and regional drivers of accelerating CO_2 emissions. Proceedings of the National Academy of Sciences of the USA 104, 10288-10293.

Raymond, P.A., Hamilton, S.K., 2018. Anthropogenic influences on riverine fluxes of dissolved inorganic carbon to the oceans. Limnology and Oceanography Letters 3, 143-155.

Reardon, E.J., Allison, G.B., Fritz, P., 1979. Seasonal chemical and isotopic variations of soil CO_2 at Trout Creek. Ontario Journal of Hydrology 43(1), 355-371.

Reimer, j.j., Cai, W.J., Xue, L., Vargas, R., Noakese, S., Hu, X., Signorini, S.R., Mathis, J.T., Feely, R.A., Sutton, A.J., Sabine, C., Musielewicz, S., Chen, B., Wanninkhof, R., 2017. Time series pCO_2 at a coastal mooring: Internal consistency, seasonal cycles, and interannual variability. Continental Shelf Research 145, 95-108.

Robbins, C.W., 1986. Carbon Dioxide Partial Pressure in Lysimeter Soils. Agronomy Journal 78, 151-158.

Robert-Baldo, G.L., Morris, M.J., Byrne, R.H., 1985. Spectrophotometric determination of seawater pH using phenol red. Analytical Chemistry 57, 2564-2567.

Rounds, 2001. Alkalinity and acid neutralizing capacity. US Geological Survey TWRI Book.

Salt, L.A., Thomas, H., Bozec,Y., Alberto, V., Borges, A.V., de Baar, H.J.W., 2016. The internal consistency of the North Sea carbonate system. Journal of Marine Systems 157, 52-64.

Simunek, J., and Suarez, D.L., 1993. Modeling of Carbon Dioxide Transport and Production in Soil 1. Model Development. Water Resources Research 29, 487-497.

Strawn, D., Bohn, H.L., O'Connor, G., 2015. Soil chemistry 4th Edition.Wiley-Blackwell.

Stumm, W., Morgan, J., 1996. Aquatic chemistry: Chemical equilibria and rates in natural waters 3rd Edition.Wiley Interscience, New York.

USGS: van der Helm, A.W.C., Rietveld, L. C., 2002. Modelling of drinking water treatment processes within the Stimela environment. Water.Science & Technology 2, 87-93.

Wanninkhof, R., Lewis, E., Feely, R.A., and Millero, F.J., 1999. The optimal carbonate dissociation constants for determining surface water pCO_2 from alkalinity and total inorganic carbon, Marine Chemistry 65, 291-301.

Whitworth, K.L., Baldwin, D.S., Kerr, J.L., 2014. The effect of temperature on leaching and subsequent decomposition of dissolved carbon from inundated floodplain litter: implications for the generation of hypoxic blackwater in lowland floodplain rivers. Chemistry and Ecology 30, 491-500.

Yao, W., Byrne, R.H., 2001. Spectrophotometric determination of freshwater pH using bromocresol purple and phenol red. Environmental Science & Technology 35, 1197-1201.

Zhang, H., Byrne, R.H., 1996. Spectrophotometric pH measurements of surface seawater at in-situ conditions: absorbance and protonation behavior of thymol blue. Marine Chemistry 52, 17-25.

CHAPTER 6

CONCLUSIONS AND FUTURE RESEARCH

1 Conclusion:

This thesis describes the development of spectrophotometric methods, using sulfonephthalein indicator dyes, for the determination of pH of soils. The high precision and accuracy of this method compared to the conventional methods using a glass electrode has previously been demonstrated for the determination of pH of marine waters (Robert-Baldo et al. 1985; Clayton and Byrne 1993; Yao and Byrne 2001). However, the much larger range of pH values encountered in soils, greater heterogeneity of the material, along with the presence of suspended soil particles (to avoid this problem, soil solution was centrifuged for 30 mins -1 h and then soil extract supernatant was carefully pipetted into a clean tube, refer to chapter 2, 3 and 4), represented a significant challenge in adapting the method. Spectrophotometric pH measurements rely on knowledge of the molecular light absorption properties of indicator dyes and involve measurement of the absorbance ratios of acid and base forms of indicators at two wavelengths (Yao and Byrne 2001). This method has advantages over the conventional glass electrode method for measuring pH, which typically needs repeated calibration and can be compromised by a range of potential problems, including liquid junction errors, and high rates of drift of the reference electrode potential (Millero 1986; Yuan and DeGrandpre 2008). Additional problems can occur in soil extracts such as clogging of the electrode by soil colloidal particles (Skoog et al. 2007) and a “suspension effect” in which higher concentrations of H^+

(and hence lower pH) are recorded due to the presence of exchange H^+ present near cation exchange sites of suspended soil particles (Essington 2015).

Although colorimetric methods have been previously developed for use in soils by Snyder (1935) and Raupach and Tucker (1959), these previous methods are based on visual assessment of colour, which limits resolution to approximately 0.5 pH units (Rayment and Lyons 2011). Many chemical equilibria in soil occur in a narrow pH range and even ±0.1 pH unit errors can lead to poor prediction of chemical reactions such as metal speciation. Therefore, the purpose of this study was to develop accurate and precise spectrophotometric methods for measuring soil pH for a wide range of soil conditions.

While spectrophotometric methods avoid several problems inherent with electrode measurement of pH, achievement of high accuracy and precision in spectrophotometric pH measurement requires a high degree of care. For all experiments, spectrophotometric and glass electrode measurements were undertaken at 25°C and the accuracy of the spectrophotometric method was tested through the analysis of a known pH standard NIST buffer solutions. The effect of ionic strength of soil extracts on the pK_a of indicator species was corrected using the Davies equation and indicator induced pH perturbation was quantified through extrapolation of absorbance ratios (R) to zero dye addition via linear regression of R against different volume of indicators added to samples (Clayton and Byrne 1993).

This study comprises four main experiments, described in Chapters 2-5. Chapter 2 describes the development of the basic spectroscopic method, which is limited to a pH range of 5.0-8.5. Chapter 3 describes the extension of the method for use with soils in the extreme acid range (down to 3.0 pH units). The methods described in Chapters 2

and 3 involve the use of a single indicator dye, for which accurate pH determination is limited to a range of approximately 1 pH either side of the pK_a of the dye. Chapter 4 describes an important extension of the approach in which the simultaneous addition of four indicator dyes extends the range of the method to a pH range of 3-9. Chapter 5 describes the development of the carbonate model for evaluation of soil inorganic carbon systems. Simultaneously, the accuracy of spectrophotometric method for soil pH measurements using an inorganic carbon equilibrium model was assessed, along with the internal consistency of this system.

Chapter 2 (published as Bargrizan et al. 2017) describes the initial development of the spectrophotometric approach for measuring soil pH, in this case restricted to a pH range of 5-8.5, which corresponds to mildly acidic to mildly alkaline soils. This basic method involved the use of one of two sulfonephthalein indicators, bromocresol purple (BCP) and phenol red (PR), whose pK_a values are different, allowing coverage of the pH range of interest. Values of pH determined via the spectrophotometric and glass electrode methods were compared for both water and $CaCl_2$ soil extracts and at different extraction ratios. A strong correlation ($r^2 > 0.95$) was found between these two methods across all soil extracts. The precision of pH measured spectrophotometrically (i.e. the standard deviation of measurement of replicate soil extracts) was between 0.02-0.08 pH units which was similar to the precision obtained using the glass electrode. The results indicated that the spectrophotometric method can give comparable results to even the most careful application of the electrode method, where associated problems such as electrode drift, clogging and need to calibrate for variable ionic strength have been controlled for. Since glass electrode method cannot be viewed as necessarily accurate or a gold standard for measuring soil pH due to its potential issues mentioned above, the spectrophotometric method could be a robust

alternative to glass electrode method in terms of high precision and accuracy and also preventing the glass electrode-associated deficiencies.

The method developed in Chapter 2 and indeed most previous spectrophotometric pH studies are limited to the determination of pH in the range 5-8.5. Whereas this is generally sufficient for freshwater and marine water samples, a substantial number of soils are more acidic than a pH of 5.0 (e.g. those that have experienced oxidation of reduced inorganic sulfur, affected by nitrogen fertiliser application, or are organic-rich). A key management issue with acidic soils is high availability of metallic elements which can cause toxicity problems. This availability is closely related to absorption isotherms for individual metals on hydrous Fe, Al and Mn oxides in soils, and these are sensitive over narrow pH ranges. Development of an accurate pH measurement method for acidic soils would enable more accurate metal speciation prediction.

Chapter 3 (published as Bargrizan et al. 2018a) describes the extension of the spectrophotometric method to measure pH of soils in the highly acidic soil pH range, from 5.3 down to around 3.0 pH units. The performance of the method was demonstrated for a 12-week aerobic incubation of an acid sulfate soil. Acid sulfate soils, given their wide range of pH variation during oxidation and reputation for association with problems of high metal availability, provide an excellent model to determine the specific role of pH in determining metal speciation and partitioning in soils.

The development of a method for this purpose required the accurate characterization of the spectral properties of bromocresol green (BCG) indicator, for which the reported pK_a was 4.416 in seawater (Byrne and Breland 1993). This value relates to conditions

of high ionic strength; the properties of BCG at low ionic strength have never been determined accurately previously. The indicator's molar absorptivities at the wavelength of peak maxima for both acid and base forms and determination of the indicator's second dissociation constant (pK_a) were determined by dissolving BCG in a phthalate buffer with known pH. This study showed the capability of BCG for spectrophotometric soil pH measurement between the pH range of 3.0-5.3. Moreover, a good correlation between spectrophotometric and electrode methods under acidic conditions indicated that there is no interaction between the dye and metal concentrations which could otherwise affect pH determination.

All of the methods described in Chapters 2 and 3 involved the use of individual dyes, for which the working pH range is limited to approximately ±1 pH unit from their pK_a (King and Kester 1990; Yao and Byrne 2001). Therefore, prior knowledge of the probable soil pH is essential when using these single indicator dye methods. This is a particular problem for soils with a wide pH range (Miller and Kissel 2010) especially in the case of application of this method *in situ* where pH could vary widely even throughout a single soil profile (the range of 3-7) (Mosley et al. 2017).

Chapter 4 (published as Bargizan et al. 2018b) describes the development of an extended pH range (3-9) spectrophotometric pH measurement that employs a four-dye mixture including bromophenol blue (BPB), bromocresol purple (BCP), m-cresol purple (*m*CP) and thymol blue (TB). The properties of the mixed indicator are directly linked to the properties in the individual dyes in the theory and calculations. This selection was made based on the understanding that the pK_a of single dyes in the mixture should be no more than 2 pH units apart and also that the wavelengths of maximum acid and base peak absorbance of individual dyes in the mixture should be

similar. The main consequence of using dyes with different wavelengths of maximum acid and peak absorbance is that sensitivity is reduced as a common wavelength near the absorbance maxima cannot be found. Based on analysis of individual dye spectra, the common wavelengths were chosen at 434 and 585 nm for the mixed dye acid and base peak measurement respectively. An accuracy of ±0-0.06 pH units for the dye mixture was achieved using standard buffer solutions across a pH range of 3-9. The multiple indicator dye spectrophotometric method was also successfully used for measuring soil pH with a high correlation ($r^2 = 0.99$) against glass electrode methods and in an alkalinity titration. Most soil pH is within the pH range of 3-9, the method developed is not suitable for soils with pH higher than 9 or less than 3. However, the addition of a different dye to the mixture to cover a higher pH range could in theory be possible if it met the selection criteria described above. This experiment was important since it obviates the restriction of a narrow working pH range inherent with all methods that use an individual indictor for soil pH measurements, and potentially measurement in other systems. In addition, more advanced techniques such hyperspectral imaging can now be explored with the multiple dye method to potentially provide high spatial resolution soil pH measurements (e.g. to study around rhizosphere).

Finally, the soil carbon cycle is susceptible to increasing anthropogenic perturbations such as climate change and soil acidification due to the magnitude of organic and inorganic carbon fluxes (Lal and Kimble 2000). To evaluate changes in the inorganic carbon system as a consequence of climate change, the internal consistency of the marine system has been widely documented through measurement of any two of four carbonate variables (total alkalinity (TA), dissolved inorganic carbon (DIC), partial pressure of CO_2 (pCO_2), and pH) (Clayton et al. 1995, Zhang et al. 1996; Wanninkhof

et al. 1999; Lueker et al. 2000; Patsavas et al. 2015). However, insufficient attention has been paid to measuring and understanding the response of the soil inorganic carbon system to increasing concentration of atmospheric CO_2.

Chapter 5 describes experiments aimed at assessing the internal consistency of the soil carbonate system using the thermodynamic carbonate model proposed by Stumm and Morgan (1996) with pH calculated from two other inter-related variables of the carbonate system (total alkalinity, pCO_2) and compared to measurements. The purpose of this experiment was to see if the soil inorganic carbon system could be reliably evaluated, with the view to allowing more confidence in the research community's ability to study the response of the soil system to climate change. Additionally, the recent developed spectrophotometric technique for soil pH measurements in this thesis were used in this inorganic carbon system assessment. Concurrently, this enabled the accuracy of the spectrophotometric method to be assessed via associated measurements of the carbonate system and comparing calculated to measured pH as has already been conducted in the marine chemistry field (Dickson and Riley 1978; Clayton et al. 1995). The pCO_2 was fixed in the experiment by equilibrating the soil solution with air with a known pCO_2. Discrepancy of calculated pH from measured pH using spectrophotometric and glass electrode methods was within 0.00-0.1 pH units when alkalinity was > 0.5 meq L^{-1}. The result of this work implied the accurate prediction of pH from other carbonate system parameters is feasible using the inorganic carbon system dissociation constants of Stumm and Morgan (1996) at 25°C. However, the organic base contribution appeared to result in errors in the calculated pH for samples with low alkalinity < 0.5 meq L^{-1}. Moreover, although a greater accuracy of spectrophotometric method compared to glass electrode using the carbonate equilibria was not confirmed in this study, that was the first time that this

method was used for the investigation of the internal consistency of soil carbonate system.

Together, the experiments described in this thesis demonstrate spectrophotometric measurement is a valid alternative to the conventional glass electrode method for the determination of pH of soil extracts across a wide pH range and avoids many issues associated with the electrode method. The lower precision for soil pH measured spectrophotometrically compared to natural water spectrophotometric pH measurements is associated with the extra steps needed for soil extract preparation such as shaking and centrifuging which could alter the sample CO_2 levels (Zabowski and Sletten 1991) resulting in progressive increase in pH of replicate samples

Future Research

In the experiments in this thesis, all our spectrophotometric measurements were laboratory based. However, in chapter 2, the potential application of spectrophotometric method for measuring soil pH *in situ* was shown in reflectance mode following the application of dye directly to 1:1 soil/water mixtures using StellarNet Black Comet spectrometer with a R600-8-visible near infrared fiber optic reflectance probe. Therefore, the method can potentially be extended to *in situ* measurement in soils for future studies to better understand the role of pH in soils and inter-related inorganic carbon system dynamics.

The *in situ* application of spectrophotometric methods could be particularly beneficial for long term observation of carbonate equilibria in soil ecosystems using the soil carbonate modelling introduced in chapter 5. Soil pH measurement using indicator dye *in situ* could be conducted faster by using syringe pump to extract soil solution connected to cuvette cell holder and spectrograph-based detection system. (figure 1,

Martz et al. 2003). By this approach, indirect measurements of soil pCO_2 *in situ* from accurate measured pH, along with the measurement of another carbonate system parameter, would be possible. Moreover, this would provide an opportunity to assess the anthropogenic perturbations such as soil acidification and calcium carbonate dissolution.

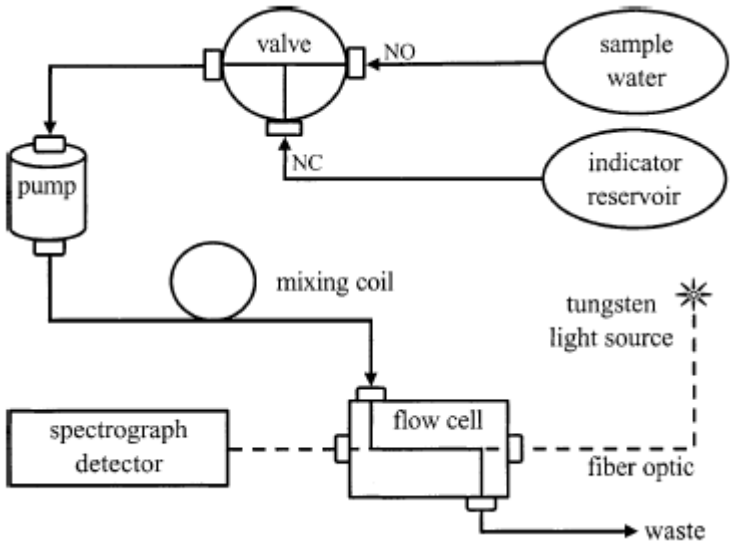

Figure 1: Diagram of the instrument for spectrophotometric pH measurements *in situ* described by Martz et al. (2003).

Additionally, based on the results obtained in Chapter 5, it would also be beneficial to quantify accurately the interference of dissolved organic carbon in low alkalinity soil solutions for accurate evaluation of soil internal consistency. Measuring DIC or carbonate instead of alkalinity may be beneficial to reduce errors in low alkalinity samples.

The development of novel technologies for use in the field is required. The next stage in the development of the spectrophotometric soil pH measurements method *in situ* could include the development of Lab-on-Chip pH sensor on platforms which has recently been used in marine system (Rerolle et al. 2018). This may allow the multidimensional study of pH at high resolution in soils which would be useful to better understanding of geochemical processes and the spatial and temporal dynamic of pH changes and carbonate system. Furthermore, the use of hyperspectral cameras and scanners is worthy of further investigation as soil pH is believed to be quite heterogeneous over mm to cm scales.

References

Bargrizan, S., Smernik, R.J., Mosley, L.M., 2017. Development of a Spectrophotometric Method for Determining pH of Soil Extracts and Comparison with Glass Electrode Measurements. Soil Science Society of America Journal 81, 1350-1358.

Bargrizan, S., Smernik, R.J., Fitzpatrick, R.W., Mosley, L.M., 2018. The application of a spectrophotometric method to determine pH in acidic (pH < 5) soils. Talanta 186, 421-426.

Bargrizan, S., Smernik, R.J., Mosley, L.M., 2018. Spectrophotometric measurement of the pH of soil extracts using a multiple indicator dye mixture. European Journal of Soil Science https://doi.org/10.1111/ejss.12745.

Byrne, R.H., Breland, J.A., 1993. Spectrophotometric procedures for determination of sea water alkalinity using bromocresol green. Deep Sea Research Part I: Oceanographic Research Papers 40, 629-641.

Clayton, T.D., Byrne, R.H., 1993. Spectrophotometric seawater pH measurements: total hydrogen ion concentration scale calibration of m-cresol purple and at-sea results. Deep Sea Research Part I: Oceanographic Research Papers 40, 2115-2129.

Clayton, T.D., Byrne, R.H., Breland, J.A., Feely, R.A., Millero, F.J., Campbell, D.M., Murphy,P.P., Lamb, M.F., 1995. The role of pH measurements in modern oceanic CO_2-system characterizations: Precision and thermodynamic consistency. Deep-Sea Research II, Vol 42. No 2-3. pp. 41, l-429.

Dickson A. G., Riley J. P., 1978. The effect of analytical error on the evaluation of the components of the aquatic carbon-dioxide system. Marine Chemistry 6, 77-85.

Essington, M.E., 2015. Soil and water chemistry: An integrative approach 2nd Edition, CRC Press, New York.

King, D.W., Kester, D.R., 1990. Spectral modeling of sulfonephthalein indicators: application to pH measurements using multiple indicators. Applied Spectroscopy 44, 722-727.

Lal, R., Kimble, J.M., 2000. Pedogenic carbonates and the global carbon cycle. In: Lal, R., Kimble, J.M., Eswaran, H., Stewart, B.A. (Eds.), Global Climate Change and Pedogenic Carbonates. CRC Press, Boca Raton, FL, USA, pp. 1-14.

Lueker, T.J., Dickson, A.G., Keeling, C.D., 2000. Ocean pCO_2 calculated from dissolved inorganic carbon, alkalinity, and equations for K_1 and K_2: validation based on laboratory measurements of CO in gas and seawater at equilibrium. Marine Chemistry 70,105-119.

Martz, T.R., Carr, J.J., French, C.R., DeGrandpre, M.D., 2003. A submersible autonomous sensor for spectrophotometric pH measurements of natural waters. Analytical Chemistry 75, 1844-1850.

Miller, R.O., Kissel, D.E., 2010. Comparison of soil pH methods on soils of North America. Soil Science Society of America Journal 74, 310-316.

Millero, F.J., 1986. The pH of estuarine waters. Limnology and Oceanography31, 839-847.

Mosley, L.M., Biswas, T.K., Cook, F.J., Marschner, P., Palmer, D., Shand, P., Yuan, C., Fitzpatrick, R.W., 2017. Prolonged recovery of acid sulfate soils with sulfuric materials following severe drought: causes and implications. Geoderma 308, 312-320.

Patsavas, M.C., Byrne, R.H., Yang, B., Easley, R.A., Wanninkhof, R., Liu, X., 2015. Procedures for direct spectrophotometric determination of carbonate ion concentrations: measurements in the US Gulf of Mexico and East Coast Waters. Marine Chemistry 168, 80-85.

Raupach, M., Tucker, B., 1959. The field determination of soil reaction. Journal of the Australian Institute of Agricultural Science 25, 129-133.

Rayment, G.E., Lyons, D.J., 2011. Soil chemical methods. CSIRO publishing, Victoria, Australia.

Rérolle, V.M.C., Achterberg, E.P., Ribas-Ribas, M., Kitidis, V., Brown, I., Bakker, D.C.E., Lee, G.A., Mowlem, M.C., 2018. High Resolution pH Measurements Using a Lab-on-Chip Sensor in Surface Waters of Northwest European Shelf Seas. Sensors Vol.18(8), p.2622

Robert-Baldo, G.L., Morris, M.J., Byrne, R.H., 1985. Spectrophotometric determination of seawater pH using phenol red. Analytical Chemistry 57, 2564-2567.

Skoog, D.A., Holler, F.J., Crouch, S.R., 2007. Principles of instrumental analysis. Cengage Learning (Inc.), Belmont, CA.

Snyder, E.F., 1935. Methods for determining the hydrogen ion concentration of soils. USDA Circular. No 56. US Department of Agriculture Washington, DC.

Stumm, W., Morgan, J., 1996. Aquatic Chemistry: Chemical Equilibria and Rates in Natural Waters 3rd Edition, Wiley Interscience, New York.

Wanninkhof, R., Lewis, E., Feely, R.A., and Millero, F.J., 1999. The optimal carbonate dissociation constants for determining surface water pCO_2 from alkalinity and total inorganic carbon. Marine Chemistry 65, 291-301.

Yao, W., and Byrne, R.H., 2001. Spectrophotometric determination of freshwater pH using bromocresol purple and phenol red. Environmental Science and Technology 35, 1197-1201.

Yuan, S., and DeGrandpre, M.D., 2008. Evaluation of indicator-based pH measurements for freshwater over a wide range of buffer intensities. Environmental Science and Technology 42, 6092-6099.

Zabowski, D., Sletten, R.S., 1991. Carbon dioxide degassing effects on the pH of spodosol soil solutions. Soil Science Society of America Journal 55, 1456-1461.

Zhang, H., Byrne, R.H., 1996. Spectrophotometric pH measurements of surface seawater at in-situ conditions: absorbance and protonation behaviour of thymol blue. Marine Chemistry 52, 17-25.

Appendix:

CHAPTER 2

Mixed dye in discussion section has also been referred to (Chapter 4, Bargrizan et al. 2018), (King and Kester 1989) and (King and Kester 1990).

References

Bargrizan, S., Smernik, R.J., Mosley, L.M., 2018. Spectrophotometric measurement of the pH of soil extracts using a multiple indicator dye mixture. European Journal of Soil Science https://doi.org/10.1111/ejss.12745

King, D.W., Kester, D.R., 1989. Determination of seawater pH from 1.5 to 8.5 using colorimetric indicators. Marine Chemistry 26, 5-20.

King, D.W., Kester, D.R., 1990. Spectral modeling of sulfonephthalein indicators: application to pH measurements using multiple indicators. Applied Spectroscopy 44, 722-727.

CHAPTER 4

Please note that in Figure 1, for the dye spectra presented, they were all measured at the same dye concentration (0.002 mol l^{-1}).